VOLUME 12 (1959) No. 2

NUCLEAR PHYSICS

JOURNAL DEVOTED TO THE EXPERIMENTAL AND THEORETICAL STUDY OF THE FUNDAMENTAL CONSTITUENTS OF MATTER AND THEIR INTERACTIONS

EDITOR: L. ROSENFELD - COPENHAGEN

A. N. MITRA, Pion-baryon interactions and "closed loop" phenomena 133

A. ARIMA and S. YOSHIDA, Analysis of a rotational state in terms of the shell model states 139

J. OLKOWSKY, I. GRATOT, M. LE PAPE et L. COHEN, Un nouvel isotope du terbium de masse 152, émetteur alpha 159

G. A. JONES, Energy dependence of the (p, n) reaction near $A = 70$ 167

R. D. EDGE, The altitude dependence of atmospheric cosmic-ray neutrons and the slow neutron density below a water surface 182

A. A. KOMAR and M. A. MARKOV, An example of a field theory with indefinite metric in Hilbert space II 190

R. K. GIRGIS and R. VAN LIESHOUT, The level scheme of ^{136}Ba 204

News Items 218

Book Reviews 219

NORTH-HOLLAND PUBLISHING COMPANY - AMSTERDAM

July (1) 1959

EDITORIAL BOARD

AUSTRALIA & NEW ZEALAND: H. Messel (Sydney), M. L. Oliphant (Canberra)
AUSTRIA: B. Karlik, (Vienna), H. Thirring (Vienna)
BELGIUM: M. de Hemptinne (Louvain), J. Verhaeghe (Ghent)
CANADA: G. Volkoff (Vancouver)
DENMARK: C. Møller (Copenhagen), S. Rozental (Copenhagen)
FINLAND: L. Simons (Helsinki)
FRANCE: A. Berthelot (Paris), S. Gorodetzky (Strasbourg)
GERMANY (DEM. REP.): G. Hertz (Leipzig)
GERMANY (FED. REP.): W. Gentner (Freiburg i. B.), J. H. D. Jensen (Heidelberg)
GREAT BRITAIN: S. Devons (Manchester), T. H. R. Skyrme (Harwell)
HUNGARY: L. Janossy (Budapest)
INDIA: H. Bhabha (Bombay), R. Ramanna (Trombay)
IRISH REPUBLIC: J. McConnell (Maynooth)
ISRAEL: G. Racah (Jerusalem)
ITALY: E. Amaldi (Rome)
JAPAN: S. Kikuchi (Tokyo), S. Tomonaga (Tokyo)
MEXICO: M. Moshinsky (Mexico)
NETHERLANDS: H. Brinkman (Groningen), S. R. de Groot (Leiden)
NORWAY: E. Hylleraas (Oslo), A. Lundbv (Oslo), H. Wergeland (Trondheim)
POLAND: L. Infeld (Warsaw)
PORTUGAL: J. M. Araújo (Porto), J. R. de Almeida Santos (Coimbra)
SOUTH AMERICA: G. Beck (Saõ Paulo), J. Leite Lopes (Rio de Janeiro)
SPAIN: J. M. Otero (Madrid), C. Sanchez del Rio (Madrid)
SWEDEN: O. Klein (Stockholm), K. Siegbahn (Uppsala), I. Waller (Uppsala)
SWITZERLAND: P. Huber (Basel), P. Scherrer (Zürich)
U.A.R. & ARAB COUNTRIES: F. El Bedewi (Alexandria), M. G. Nooh (Cairo)
U.S.A.: H. H. Barschall (Madison, Wisconsin), V. Weisskopf (Cambridge, Mass.)
U.S.S.R.: M. A. Markov (Moscow), I. S. Shapiro (Moscow), D. V. Skobeltzyn (Moscow)
YUGOSLAVIA: I. Supek (Zagreb)

CONTRIBUTIONS may be sent to the Editor, Professor L. Rosenfeld, NORDITA, Blegdamsvej 17, Copenhagen Ø, either directly, or preferably through the intermediary of one of the members of the Editorial Board of the country or region in which the author is working. They may be written in English, French or German.

NUCLEAR PHYSICS is published in monthly issues. The subscription price a volume of 700 pages is fl 57.00; 114s; $ 15.00. Postfree.

SUBSCRIPTIONS should be sent to the publishers, NORTH-HOLLAND PUBLISHING COMPANY, P.O.Box 103, Amsterdam or to any subscription-agent.

BOOKS FOR REVIEW should be sent to Professor Rosenfeld.

No part of this issue may be reproduced in any form, by print, photoprint, microfilm or any other means without written permission from the publisher. Reprints, photoprints or microfilms are obtainable at cost from the publisher.

Printed in the Netherlands

8.B Nuclear Physics 12 (1959) 133—138; © North-Holland Publishing Co., Amsterdam

Not to be reproduced by photoprint or microfilm without written permission from the publisher

PION-BARYON INTERACTIONS AND "CLOSED LOOP" PHENOMENA

A. N. MITRA

Department of Physics, Muslim University, Aligarh, U. P., India

Received 23 March 1959

Abstract: The effect of strong pion-hyperon interactions on $\pi^0 \rightarrow 2\gamma$ decay and $\pi-\pi$ interaction, both of which are "closed loop" processes, is examined. It is found that while the interaction of pions with hyperons helps to reduce the decay rate of π^0, it leads to an unreasonably strong $\pi-\pi$ attraction. To reduce the attraction it is suggested that either the meson-meson divergence should not be renormalized or $\pi-$K interactions of the Yukawa type should be invoked.

1. Introduction

During recent times the problem of fundamental interactions involving strange particles has received attention from several quarters. These interactions have been broadly classified as very strong, of intermediate strength and weak. Regarding very strong and intermediate interactions significant contributions have been made by d'Espagnat and Prentki ¹), Gell-Mann ²) and Schwinger ³). It is now generally believed that pions have very strong interactions not only with nucleons but with other baryons (viz., hyperons) as well. In particular, the hypothesis of "global symmetry" for very strong interactions has been favourably received. Elementary interactions of pions with K-mesons, on the other hand, are not yet regarded as a basic necessity.

The ultimate test of the validity of the different types of elementary interactions proposed must of course be provided from comparison with experimental facts which are numerous and diverse. Thus, Lichtenberg and Ross ⁴) found that the hypothesis of a very strong interaction of K-mesons with baryons and intermediate interaction of pions with hyperons was incompatible with the correct spin-dependence of the baryon-baryon forces which would lead to hyperfragment binding. We propose, in this note, to consider the working of the pion-baryon interactions with reference to two phenomena, viz. the 2γ-decay of a π^0 and the π—π interaction. These processes have one feature in common, viz., both involve closed baryon loops. From the experimental point of view, however, they are on different footings, since the former is directly measurable while the latter is not.

July (1) 1959

2. $\pi^0 \rightarrow 2\gamma$ Decay

This process was first calculated by Steinberger [5]) using pseudoscalar coupling for pseudoscalar mesons in the lowest order perturbation approximation. The "triangle diagram" in this case does not give rise to any divergence, so that no subtraction is necessary. The calculated life-time for decay with a π—N coupling constant $G^2/4\pi \approx 15.5$ was found to be about 100 times smaller than the observed one of nearly 5×10^{-15} sec. This discrepancy was generally attributed to the failure of perturbation theory for strong interactions. A few years later, Kinoshita [6]) made the important suggestion that, apart from the failure of perturbation theory, the effects of possible strong interactions of pions with hyperons should also be considered in this context. Indeed, he showed that if pions were coupled to nucleons and V^+-particles with equal and opposite strengths (not all the presently known hyperons had been discovered then), the decay rate would be reduced by the factor $(M_V - M_N)^2/M_V^2$, where M_V is the mass of the V-particle. Taking $M_V \approx 2200m$, which makes this factor 0.027, he was thus able to increase the value of $G^2/4\pi$ deduced from the observed decay rate, from 0.14 to 5.0. The remaining discrepancy in $G^2/4\pi$ could reasonably be attributed to the failure of perturbation theory.

More recently, Gell-Mann [2]) put this point on a firmer footing by showing how the cancellations would actually occur between the various matrix elements, leading to a reduction in the decay rate. Thus, the matrix elements for π^0-decay via the pairs $\bar{\Sigma}^+\Sigma^+$ and $\bar{\Sigma}^-\Sigma^-$ would cancel out exactly, since $M_{\Sigma^+} = M_{\Sigma^-}$. Only the matrix elements via the pairs $\bar{\mathrm{P}}\mathrm{P}$ and $\bar{\Xi}^-\Xi^-$ would make unequal contributions of opposite signs. More precisely, perturbation theory gives the following modification in the transition probability arising from the hyperon loops:

$$\left(\frac{g_{\pi N}}{M_N}\right)^2 \rightarrow \left[\frac{g_{\pi N}}{M_N} - \frac{g_{\pi \Xi}}{M_\Xi} + \frac{g_{\pi \Sigma}}{M_{\Sigma^+}} - \frac{g_{\pi \Sigma}}{M_{\Sigma^-}}\right]^2. \tag{1}$$

Assuming "global symmetry" and taking $M_{\Sigma^+} = M_{\Sigma^-}$, $M_\Xi \approx 2590m$, the reduction factor is now seen to be 0.085 which is able to raise the deduced value of $g_{\pi N}^2/4\pi$ to only 1.6, as against Kinoshita's 5.0. This represents a discrepancy of roughly a factor of ten from the generally accepted value 15.5 of the coupling constant. It would thus appear that even a cancellation of the matrix elements does not improve matters significantly if all the coupling constants are taken to be the same. Unless, therefore, it is contended that a non-perturbation treatment alone would account for as much as a factor of 10, the above figures would seem to indicate deviations from global symmetry. A crude estimate of this deviation could be made in the framework of perturbation calculations by requiring that the expression on the right of (1) should be about 1 % of the quantity on the left. This gives

$$g_{\pi\Xi}/g_{\pi\mathrm{N}} \approx 0.9(M_{\Xi}/M_{\mathrm{N}}) \approx 1.27. \tag{2}$$

That the magnitude of $g_{\pi\Sigma}$ does not enter eq. (2) is a result of the equality of $M_{\Sigma^\pm}$ and the highly plausible assumption that pions interact with equal and opposite strengths with $\Sigma^\pm$. This fact is strictly independent of any perturbation calculation. As for the estimate (2), a more rigorous treatment would no doubt change it, possibly to a lower value, if it is contended that a non-perturbation calculation alone should account substantially for the discrepancy between theory and experiment. It is, however, interesting to note that a value of $g_{\pi\Xi}$ larger than $g_{\pi\mathrm{N}}$, as indicated by (2), is in line with a model of strong interactions recently proposed by Hu [7]), according to which the pion-baryon interaction is not universal and hence accounts for the mass differences among the various baryons. On the other hand, the idea of global symmetry of very strong interactions is so attractive that much more evidence of this type would be needed to disprove it.

3. The π—π Interaction

We now turn to the $\pi-\pi$ interaction. The formulation of this problem was recently given by Mitra and Saxena [8]). (This paper is referred to as A in what follows.) Since the hyperons are also regarded as Dirac particles (of spin $\frac{1}{2}$) in ordinary space, the results of A can be quantitatively adapted to the consideration of π—π interactions via hyperon loops as well. The only point of difference that can arise is in connection with the isobaric spin dependence of the pion-hyperon interactions. For Ξ-particles, which are also spinors in isobaric spin space, the treatment is in fact identical with A. A slight modification is necessary for Σ- and Λ-particles which are respectively vector and scalar in isobaric spin space.

For our present purposes we take the pion interaction with baryons in the form given by Hu [7]). In the latter's notation we have

$$\begin{aligned} H_1 = {} & f_1\bar{\psi}^{(1)}i\gamma_5(\boldsymbol{\tau}\cdot\boldsymbol{\pi})\psi^{(1)}+f_2\bar{\psi}^{(2)}i\gamma_5(\boldsymbol{\tau}\cdot\boldsymbol{\pi})\psi^{(2)} \\ & +(f_3-f'_3)[\bar{\Lambda}i\gamma_5\boldsymbol{\pi}\cdot\boldsymbol{\Sigma}+\mathrm{h.c.}]+(f_3+f'_3)[i\boldsymbol{\Sigma}i\gamma_5\times\boldsymbol{\Sigma}]\cdot\boldsymbol{\pi}, \end{aligned} \tag{3}$$

where

$$\psi^{(1)} = \begin{pmatrix}\mathrm{N}_+\\ \mathrm{N}_0\end{pmatrix}, \qquad \psi^{(2)} = \begin{pmatrix}\Xi^0\\ \Xi^-\end{pmatrix}, \qquad \boldsymbol{\Sigma} = (\Sigma_1, \Sigma_2, \Sigma_3);$$

$$\Sigma^\pm = (2)^{-\frac{1}{2}}(\Sigma_1 \pm i\Sigma_2), \qquad \Sigma_0 = \Sigma_3.$$

By analogy with the vector $\boldsymbol{\tau}$ which expresses the isospin dependence of N and Ξ, we may introduce the vector $\mathbf{T}$ (the matrix for unit angular momentum [9])) which would represent the isospin dependence of the Σ-particles. For Λ-particles the isospin operator is just unity. At this stage our formalism can be considerably simplified if we ignore the mass difference between Λ and Σ so that these particles may be represented by the *same* spinor ϕ in ordinary space. This would allow us to write the last two terms of (3) as

$$2(f_3-f'_3)\bar{\phi}i\gamma_5(\boldsymbol{\pi}\cdot\mathbf{T})\phi-(f_3+f'_3)\bar{\phi}i\gamma_5(\boldsymbol{\pi}\cdot\mathbf{T})\phi, \tag{4}$$

where in the first term the factor two comes from the requirement of hermitian conjugation, and in the second term use has been made of the relation $\mathbf{T}\times\mathbf{T}=i\mathbf{T}$. The expression (4) finally simplifies to

$$(f_3-3f'_3)\bar{\phi}i\gamma_5(\boldsymbol{\pi}\cdot\mathbf{T})\phi. \tag{5}$$

Using the methods of A, the effective hamiltonian for π—π interaction via Σ and Λ loops can now be calculated from (5) in a straightforward manner. The only modification will occur in the isospin dependence and this will consist in the replacement of the factor D_{1234} in eq. (6) of A (and subsequent steps) by the factor

$$\mathscr{D}_{1234}=\tfrac{1}{2}\mathrm{Tr}\,(T_{\alpha_1}T_{\alpha_2}T_{\alpha_3}T_{\alpha_4})=\delta_{12}\delta_{34}. \tag{6}$$

Proceeding as in A one can then deduce the contribution to the operator $\mathscr{R}$ arising from (Σ,Λ) loops as

$$\mathscr{R}^{(\Sigma)}=\xi(\mathscr{I}_1{}^{\Sigma}+\mathscr{I}_2{}^{\Sigma})+\tfrac{1}{2}(\zeta-\eta)\mathscr{I}_3{}^{\Sigma}, \tag{7}$$

where ξ, η, ζ are isospin operators discussed in another paper by Mitra 10) (referred to as B). The integrals $\mathscr{I}^{\Sigma}$ are as given in eqs. (15) and (16) of A, with M replaced by $M_{\Sigma}\approx M_{\Lambda}$. Finally, the contributions to $\mathscr{R}$ arising from the N and Ξ loops are given, as in eq. (18) of A, by

$$\mathscr{R}^{(\mathrm{N},\Xi)}=[\xi(\mathscr{I}_1+\mathscr{I}_2-\mathscr{I}_3)+\eta(\mathscr{I}_1-\mathscr{I}_2)+\zeta\mathscr{I}_3]^{(\mathrm{N},\Xi)}, \tag{8}$$

where the superscripts (N, Ξ) indicate the particular baryon loops considered, with corresponding modifications in the masses appearing in the integrals $\mathscr{I}$. Collecting all these contributions one finally arrives, as in A, at the effective hamiltonian H_I for a π—π state of total isobaric spin I given by

$$H_I(\mathbf{s},\mathbf{q})=\frac{-i}{32\pi^5\omega_s\omega_q}\left[\frac{f_1^4}{16\pi^2}\mathscr{R}_I{}^{(\mathrm{N})}+\frac{f_2^4}{16\pi^2}\mathscr{R}_I{}^{(\Xi)}+\frac{(f_3-3f'_3)^4}{16\pi^2}\mathscr{R}_I{}^{(\Sigma)}\right]. \tag{9}$$

We are now in a position to discuss some qualitative aspects of the π—π interaction with the help of (9).

It may be seen that unlike the case of $\pi^0\rightarrow 2\gamma$ decay, where the different baryon loops were making contributions of opposite signs, the case of the π—π interaction is one in which the baryon contributions all reinforce one another, thus enhancing the interaction to a considerable degree. This result ows its origin to the respective "odd" and "even" natures of the baryon loops, and should be largely independent of any approximate treatment. Now it was found in A that while the π—π s-state of isobaric spin 2 was moderately attractive and indicated a resonance at a C.M. momentum of $\approx$ 90 MeV/c for each pion, the corresponding s-state of isobaric spin 0 showed too strong attraction to give any resonance with the conventional value 15.5 of $G^2/4\pi$ (here denoted by $f_1^2/4\pi$). In fact, some estimates made subsequently with the hamiltonian defined by eqs. (19) and (28) of A for the $I = 0$ state did indicate a *bound* state with binding energy large enough to depress the "mass" of the composite "particle" much below $2m_\pi$†. While this result need not be taken quantitatively, it at least lends strong credence to the belief that with a π—N coupling constant as large as 15.5, the π—π interaction via nucleon loops alone would be very strongly attractive, particularly in the $I = 0$ state. The hypothesis of strong pion interactions with other baryons would further enhance this attraction (since all the terms in (9) are of the same sign and order of magnitude), beyond all reasonable limits. To find a way out of such an obviously unphysical situation, one must therefore look for some source of repulsion which should be strong enough to counteract largely the effects of the unreasonable attraction provided by the baryon loops.

Before speculating about any possibility in this direction it is useful first to inquire into the mechanism which led to such an attractive π—π interaction via baryon loops. It may be recalled that in the treatment of π—π interaction in A, the so-called meson-meson divergence was encountered and had to be subtracted out in the spirit of renormalization. Further, this divergent term was *repulsive* (see appendix of A). Off-hand, therefore, it might appear that the problem is trivial and all that is needed is that this term should be *retained*. This last in turn would involve a cut-off procedure. On the other hand, a cut-off procedure is inconsistent with renormalization theory, apart from the introduction of an arbitrary parameter into the formalism. If, therefore, we insist on renormalization, the problem of finding repulsive terms remains ††.

In the framework of renormalization theory we must look for additional pion interactions. One possibility is provided by pion interactions with K-mesons which are spinors in isobaric spin space but scalars and/or pseudoscalars in ordinary space. A Yukawa-type coupling $\tilde{\mathrm{K}}\mathrm{K}\pi$ was indeed suggested by Schwinger in his earlier paper [11]). With such a coupling the isospin dependence of the interaction would be exactly the same as for the interaction via nucleon loops. Further, since K-mesons are bosons, the factor (−1) which always arises for a fermion loop according to the Feynman-Dyson rules of evaluation of matrix elements, will now be absent. This has the consequence that the *sign* of the π—π interaction will now be *opposite* to that obtained via baryon loops. Thus the π—π contribution via K-meson loops will be repulsive, as required. Unfortunately, such a coupling suffers from certain formal difficulties associated with rapid parity fluctuations of the K-field (see ref.[11])), and for this and similar reasons it did not find favour in Schwinger's later paper [3]). Instead, Schwinger [3]) † introduced a quadratic coupling $\tilde{K}K\pi\pi$. Now a π—π interaction of the desired sign can indeed be obtained through two steps of such a hamiltonian. Further, this interaction would be effective only in the states $I = 0$ and 1, since $\tilde{K}K$ cannot couple to $I = 2$. This circumstance is not unwelcome, as we have seen that it is only for $I = 0$ that a strong repulsion is badly needed. The main disadvantage of this coupling, on the other hand, is that it needs a cut-off at high momenta, which is again contrary to the spirit of renormalization.

---

† Such a particle would be strictly neutral and scalar and as such would interact rather weakly with an external system. Further, it would show no sign of decay.

†† There is of course the possibility that pion-pion interactions through baryon loops of higher orders may provide terms of the opposite sign. It may, however, be noted that our treatment already takes account of various iterations of the "square diagram" through the Bethe-Salpeter type approach.

As for the effect of π—K interactions on $\pi^0 \rightarrow 2\gamma$ decay, it is obvious that the quadratic one does not contribute to the process. Even for the Yukawa-type coupling, the only term involving π^0 is of the form $\tilde{K}^0K^0\pi^0$, which has nothing to do with the $\pi^0 \rightarrow 2\gamma$ process.

4. Conclusion

To sum up, the presence of hyperon loops tends to reduce the π^0 decay rate, but leaves enough gap between theory and experiment to warrant some misgivings about the validity of global symmetry. π—K interactions do not affect this conclusion. As for the π—π interaction, the presence of hyperon loops reinforces the attraction which is already very strong in the $I = 0$ state, at least in the framework of renormalization theory. This necessitates some compensating repulsion which may be provided by a Yukawa-type π—K coupling. A quadratic π—K coupling also provides for π—π repulsion, but it involves a cut-off procedure. Of course in a cut-off theory, repulsion is already present in the interaction via baryon loops themselves.

I am indebted to Professor P. S. Gill for his interest in this work.

---

† Such a quadratic coupling was also considered, along with some of its physical consequences, by S. Barshay (see ref.[12])).

References

1) d'Espagnat and Prentki, Nuclear Physics **1** (1956) 33
2) M. Gell-Mann, Phys. Rev. **106** (1957) 1296
3) J. Schwinger, Annals of Physics **2** (1957) 407
4) D. Lichtenberg and M. Ross, Phys. Rev. **109** (1958) 2163
5) J. Steinberger, Phys. Rev. **76** (1949) 1180
6) T. Kinoshita, Phys. Rev. **94** (1954) 1384
7) Ning Hu, Nuclear Physics **8** (1958) 85
8) A. N. Mitra and R. P. Saxena, Phys. Rev. **108** (1957) 1083
9) L. I. Schiff, Quantum Mechanics (McGraw Hill Book Co., New York, 1949) Ch. VI
10) A. N. Mitra, Phys. Rev. **103** (1956) 752
11) J. Schwinger, Phys. Rev. **104** (1956) 1164
12) S. Barshay, Phys. Rev. **109** (1958) 2160

1.D.4 *Nuclear Physics* **12** (1959) 139—158; ©*North-Holland Publishing Co., Amsterdam*

Not to be reproduced by photoprint or microfilm without written permission from the publisher

ANALYSIS OF A ROTATIONAL STATE IN TERMS OF THE SHELL MODEL STATES

A. ARIMA and S. YOSHIDA

Institute for Nuclear Study, University of Tokyo, Tanashimachi, Tokyo

Received 27 January 1959

Abstract: The wave function of a rotational state is analyzed in terms of shell model wave functions. The rotational wave function is constructed in the three dimensional model for even nuclei according to the method of the generator coordinates. For the single particle potential the deformed harmonic oscillator well is assumed, and the spin orbit coupling is neglected. The wave function of the rotational state is expressed in terms of the shell model wave functions. The distribution function of the shell model states of given excitation-energy is found to be of Poisson type. For light nuclei in lower excited states the rotational wave function is mainly composed of the degenerate lowest shell model states, Elliott's wave functions, while for heavy nuclei or light nuclei in higher excited states the main contribution comes from shell model states with excitation energy of a few $\hbar\omega_0$, where ω_0 is the angular frequency of the harmonic oscillator. The matrix element of the quadrupole transition is also calculated. Its value, taking only the Elliott states, is found to give half the correct value, while the calculation taking into account both the Elliott states and the interference terms with the states of excitation energy $2\hbar\omega$ is found to give the right answer.

1. Introduction

Nuclear spectroscopic data accumulated so far indicate the usefulness of the collective model in analyzing various phenomena in almost all nuclei [1]). Although many papers have been published on this model, it is not yet clear how the collective model may be constructed from first principles of quantum mechanics.

Recently the nuclei with mass numbers 18 and 19 were investigated by the shell model, taking into account the configuration mixing [2]), and also by the collective model [3]). Both of them were very successful in accounting for the low energy properties of those nuclei. The wave functions resulting from the shell model calculation with configuration mixing are shown to be very similar to those in the collective model based on the method of the generator coordinates [4]).

More recently, Elliott classified the nuclear states of the 2s—1d shell with the aid of group theory by introducing special quantum numbers, and the resulting energy levels were shown to have a rotational character [5]). The wave functions obtained by him were identified with the wave functions in the collective model when the deformation of the nuclear shape tends to zero [6,7]). This is a significant result, and it seems helpful for the further development and better understanding of the nature of the collective model to analyse the wave function in the latter model into shell model wave functions.

In this paper the rotational state wave functions will be expanded in terms of the shell model wave functions. For the rotational state wave function the method of the generator coordinates is employed, because it has the advantage of preserving the individual particle picture in the collective wave function [8,9]). The single particle wave functions are assumed to be solutions of the wave equation for a deformed harmonic oscillator well, and the spin-orbit interaction is neglected. This choice of the single particle potential may not be fully justified, but it makes calculations very easy and enable us to develop the theory further. At least it gives a good starting point for a more realistic approach.

In the present paper, the wave function of a rotational state is constructed in the three-dimensional model in section 2). This is an extension of the work by Yoccoz [9]) in two dimensions. In section 3 the wave function thus obtained is expanded in terms of the shell model wave functions. First, the percentage of the most dominant single Slater determinant in the rotational state is calculated. Next, the total percentage of the shell model states with the same excitation energy is investigated, and its distribution function is found to be approximately of a Poisson type. For light nuclei in the ground or lower excited states the rotational state wave function is mainly composed of the degenerate lowest states, Elliott wave functions. On the other hand, in the rotational wave function of heavy nuclei or light nuclei in higher excited states the main contribution comes from shell model states with excitation energy of a few $\hbar\omega_0$, where ω_0 is the angular frequency of the harmonic oscillator. For these nuclei the Elliott wave function represents a small portion of the whole wave function. In section 4 the matrix element of the quadrupole transition is calculated. The matrix element taking into account only the Elliott states is found to give half the correct value, while the calculation taking into account the Elliott states and the interference terms with the states of excitation energy $2\hbar\omega_0$ gives the right answer. It will be shown that this is due to the character of the quadrupole moment operator.

2. The Rotational Wave Function by the Method of the Generator Coordinates

The rotational model is often treated in two dimensions only, but the three-dimensional model will be investigated here to facilitate comparisons with the shell model. The wave function of the rotational state is written for an axially symmetric nucleus as

$$\Psi_{IM}(\varepsilon, \mathbf{r}_1 \cdots \mathbf{r}_A) = N_{IM}(\varepsilon) \int Y_{IM}(\theta\varphi)\psi_0(\mathbf{r}_1 \cdots \mathbf{r}_A; \varepsilon, \varphi\theta\psi) \sin\theta \, \mathrm{d}\theta \, \mathrm{d}\varphi \quad (2.1)$$

where I is the spin of the nucleus, M is its z-component, the component along the symmetric axis being assumed to be zero, and $N_{IM}(\varepsilon)$ is the normalization constant. The function $\psi_0(\mathbf{r}_1 \cdots \mathbf{r}_A \, \varepsilon\varphi\theta\psi)$ is the Slater determinant constructed from single particle wave functions, solutions of a spheroidal harmonic oscillator well whose deformation parameter is ε, and the orientation of the symmetry axis is characterized by Euler angles $\theta\varphi\psi$. In the following details of the Slater determinant will be given.

To describe the single particle potential it is convenient to introduce the body-fixed coordinate system x', y', z' which is obtained from the space-fixed system x, y, z by applying a rotation characterized by Euler angles φ, θ and ψ. The transformation from the x, y, z system to the x', y', z' system is given by

$$\begin{aligned} x'_i &= a_{11}x_i + a_{12}y_i + a_{13}z_i \\ y'_i &= a_{21}x_i + a_{22}y_i + a_{23}z_i \\ z'_i &= a_{31}x_i + a_{32}y_i + a_{33}z_i \end{aligned} \quad (2.2)$$

where

$$(a_{\mu\nu}) = \begin{pmatrix} \cos\varphi\cos\theta\cos\psi - \sin\varphi\sin\psi & \sin\varphi\cos\theta\cos\psi + \cos\varphi\sin\psi & -\sin\theta\cos\psi \\ -\cos\varphi\cos\theta\sin\psi - \sin\varphi\cos\psi & -\sin\varphi\cos\theta\sin\psi + \cos\varphi\cos\psi & \sin\theta\sin\psi \\ \cos\varphi\sin\theta & \sin\varphi\sin\theta & \cos\theta \end{pmatrix}. \quad (2.3)$$

The nucleus is assumed to have an axially symmetric spheroidal shape; the single-particle potential in the body-fixed system is thus given by

$$U(\mathbf{r}'; \varepsilon) = \tfrac{1}{2}m\omega_0^2(\mathrm{e}^{4\varepsilon}x'^2 + \mathrm{e}^{4\varepsilon}y'^2 + \mathrm{e}^{-8\varepsilon}z'^2) \quad (2.4)$$

where the deformation parameter ε is related to the usual parameter β by [1])

$$\varepsilon = \tfrac{1}{6}\left(\frac{45}{16\pi}\right)^{\frac{1}{2}} \beta \approx 0.1578\,\beta. \quad (2.5)$$

The single-particle wave function corresponding to the potential (2.4) takes the form

$$\phi_{lmn}(\mathbf{r}, \varepsilon, \varphi\theta\psi) \equiv \phi_{lmn}(\mathbf{r}', \varepsilon, 000) = u_l(k_x x')u_m(k_y y')u_n(k_z z') \quad (2.6)$$

where

$$u_l(kx) = N_l(k)\mathrm{e}^{-\frac{1}{2}k^2x^2} H_l(kx) \quad (2.7)$$

and the normalization constant is given by

$$N_l(k) = [k/\sqrt{\pi}\, 2^l l!]^{\frac{1}{2}}. \quad (2.8)$$

Three parameters k_x, k_y and k_z are related to ε by the following expressions:

$$k_x = k_y = \mathrm{e}^{\varepsilon} k_0, \quad k_z = \mathrm{e}^{-2\varepsilon} k_0, \quad (2.9)$$

in which

$$k_0^2 = m\omega_0/\hbar. \tag{2.10}$$

To specify a single particle state, τ-spin and ordinary spin quantum numbers should be introduced besides the quantum numbers l, m and n. However, they will not be explicitly written for simplicity unless they are needed. From these single particle wave functions the Slater determinant is constructed, which is denoted by

$$\psi_n(\mathbf{r}_1 \cdots \mathbf{r}_A;\, \varepsilon, \varphi\theta\psi) \equiv \psi_n(\mathbf{r}'_1 \cdots \mathbf{r}'_A;\, \varepsilon, 000). \tag{2.11}$$

The suffix n specifies the configuration and especially $n = 0$ is reserved for the lowest intrinsic state. The zero-th order energy of the nucleus is given by

$$E'_0 = \hbar\omega_0 \sum [\mathrm{e}^{2\varepsilon}(l+m+1)+\mathrm{e}^{-4\varepsilon}(n+\tfrac{1}{2})]. \tag{2.12}$$

Let us consider an even nucleus whose last neutron and proton shells are both less than half filled. Other cases may be treated with slight modifications. The lowest intrinsic configuration is as follows: neutrons and protons fill all levels up to

$$l+m+n \leqq \rho_\mathrm{n}, \quad l+m+n \leqq \rho_\mathrm{p} \tag{2.13}$$

respectively, and the last shells $l+m+n = \rho_\mathrm{n}+1$ and $\rho_\mathrm{p}+1$ are partly filled:

$$l+m \leqq \lambda_\mathrm{n}, \quad n \geqq \rho_\mathrm{n}+1-\lambda_\mathrm{n} \tag{2.14}$$

and

$$l+m \leqq \lambda_\mathrm{p}, \quad n \geqq \rho_\mathrm{p}+1-\lambda_\mathrm{p}. \tag{2.15}$$

For this configuration the energy (2.12) is expressed by

$$E'_0 = \hbar\omega_0[\mathrm{e}^{2\varepsilon}(s_1+s_2)+\mathrm{e}^{-4\varepsilon}s_3] \tag{2.16}$$

where

$$\begin{aligned} s_1 = s_2 = {} & \tfrac{1}{12}[(\rho_\mathrm{n}+1)(\rho_\mathrm{n}+2)^2(\rho_\mathrm{n}+3)+(\rho_\mathrm{p}+1)(\rho_\mathrm{p}+2)^2(\rho_\mathrm{p}+3)] \\ & +\tfrac{1}{6}[(\lambda_\mathrm{n}+1)(\lambda_\mathrm{n}+2)(2\lambda_\mathrm{n}+3)+(\lambda_\mathrm{p}+1)(\lambda_\mathrm{p}+2)(2\lambda_\mathrm{p}+3)], \\ s_3 = {} & \tfrac{1}{12}[(\rho_\mathrm{n}+1)(\rho_\mathrm{n}+2)^2(\rho_\mathrm{n}+3)+(\rho_\mathrm{p}+1)(\rho_\mathrm{p}+2)^2(\rho_\mathrm{p}+3)] \\ & +\tfrac{1}{6}[(\lambda_\mathrm{n}+1)(\lambda_\mathrm{n}+2)(6\rho_\mathrm{n}-4\lambda_\mathrm{n}+9)+(\lambda_\mathrm{p}+1)(\lambda_\mathrm{p}+2)(6\rho_\mathrm{p}-4\lambda_\mathrm{p}+9)]. \end{aligned} \tag{2.17}$$

It is noted that s_1, s_2 and s_3 correspond to the numbers of powers of k_x, k_y and k_z in the Slater determinant apart from the exponential factor.

The equilibrium deformation ε_eq is obtained by minimizing the energy (2.16):

$$\varepsilon_\mathrm{eq} = \tfrac{1}{6}\ln(s_3/s_1). \tag{2.18}$$

The neutron number N, proton number Z and mass number A of the nucleus with the configuration given by (2.13), (2.14) and (2.15) are expressed as

$$\begin{aligned} N &= \tfrac{1}{3}(\rho_\mathrm{n}+1)(\rho_\mathrm{n}+2)(\rho_\mathrm{n}+3)+(\lambda_\mathrm{n}+1)(\lambda_\mathrm{n}+2), \\ Z &= \tfrac{1}{3}(\rho_\mathrm{p}+1)(\rho_\mathrm{p}+2)(\rho_\mathrm{p}+3)+(\lambda_\mathrm{p}+1)(\lambda_\mathrm{p}+2), \\ A &= N+Z. \end{aligned} \tag{2.19}$$

As the method of the generator coordinates is employed in constructing the nuclear wave function in the collective model, the calculation of the overlap integral is necessary. In the following we shall give the outline of the calculation. First we consider the overlap integral

$$I_{00}(\varepsilon, \varphi\theta\psi; \varepsilon, 000) = \int \psi_0^*(\mathbf{r}_1 \cdots \mathbf{r}_A; \varepsilon, \varphi\theta\psi)\psi_0(\mathbf{r}_1 \cdots \mathbf{r}_A; \varepsilon, 000)\mathrm{d}\mathbf{r}_1 \cdots \mathrm{d}\mathbf{r}_A. \tag{2.20}$$

The argument of the exponential function in the integrand of (2.20) is

$$-k_0^2/2[\sum_i (e'_1 x_i'^2 + e'_2 y_i'^2 + e'_3 z_i'^2 + e_1 x_i^2 + e_2 y_i^2 + e_3 z_i^2)] \tag{2.21}$$

where

$$e'_1 = e'_2 = e_1 = e_2 = \mathrm{e}^{2\varepsilon}, \qquad e'_3 = e_3 = e^{-4\varepsilon}. \tag{2.22}$$

By introducing the notation

$$A_{\mu\nu} = \tfrac{1}{2}[\sum_\lambda e'_\lambda a_{\lambda\mu} a_{\lambda\nu} + e_\mu \delta_{\mu\nu}] \tag{2.23}$$

and using (2.2), the expression (2.21) is written as

$$-k_0^2 \sum_i (A_{11} x_i^2 + A_{22} y_i^2 + A_{33} z_i^2 + 2A_{12} x_i y_i + 2A_{23} y_i z_i + 2A_{31} z_i x_i). \tag{2.24}$$

By the transformation

$$\begin{aligned} x_i &= b_{11} X_i + b_{12} Y_i + b_{13} Z_i \\ y_i &= b_{21} X_i + b_{22} Y_i + b_{23} Z_i \\ z_i &= b_{31} X_i + b_{32} Y_i + b_{33} Z_i \end{aligned} \tag{2.25}$$

the bilinear form (2.24) is shown to be transformed into a quadratic form

$$-k_0^2 \sum_i (A^2 X_i^2 + B^2 Y_i^2 + C^2 Z_i^2), \tag{2.26}$$

where

$$(b_{\mu\nu}) = \begin{pmatrix} 1 & -A_{12}/A_{11} & -\dfrac{A_{13}A_{22} - A_{12}A_{23}}{A_{11}A_{22} - A_{12}^2} \\ 0 & 1 & -\dfrac{A_{11}A_{23} - A_{12}A_{13}}{A_{11}A_{22} - A_{12}^2} \\ 0 & 0 & 1 \end{pmatrix} \tag{2.27}$$

and

$$\begin{aligned} A^2 &= A_{11} \\ B^2 &= (A_{11}A_{22} - A_{12}^2)/A_{11} \\ C^2 &= \det(A_{\mu\nu})/(A_{11}A_{22} - A_{12}^2). \end{aligned} \tag{2.28}$$

For the body-fixed coordinate system the transformation (2.25) becomes

$$\begin{aligned} x'_i &= b'_{11} X_i + b'_{12} Y_i + b'_{13} Z_i \\ y'_i &= b'_{21} X_i + b'_{22} Y_i + b'_{23} Z_i \\ z'_i &= b'_{31} X_i + b'_{32} Y_i + b'_{33} Z_i \end{aligned} \tag{2.29}$$

where

$$b'_{\mu\nu} = \sum_\lambda a_{\mu\lambda} b_{\lambda\nu}. \tag{2.30}$$

This transformation may be rewritten in a more convenient form:

$$\begin{aligned} x'_i &= C'_{11}X_i + C'_{12}y_i + C'_{13}z'_i \\ y'_i &= C'_{21}X_i + C'_{22}Y_i + C'_{23}z'_i \\ z'_i &= C'_{31}X_i + C'_{32}Y_i + C'_{33}Z_i . \end{aligned} \tag{2.31}$$

The matrix elements are expressed in terms of $a_{\mu\nu}$ and $b_{\mu\nu}$ as

$$(C'_{\mu\nu}) = \begin{pmatrix} \dfrac{1}{\Sigma a_{1\mu} f_\mu} & -\dfrac{\Sigma a_{2\mu} f_\mu}{\Sigma a_{1\mu} f_\mu} & -\dfrac{\Sigma a_{3\mu} f_\mu}{\Sigma a_{1\mu} f_\mu} \\ -\dfrac{b_{11}(a_{12}b_{33} - a_{13}b_{23})}{\Sigma a_{3\mu} b_{\mu 3}} & \dfrac{\Sigma a_{1\mu} f_\mu}{\Sigma a_{3\mu} b_{\mu 3}} & \dfrac{\Sigma a_{2\mu} b_{\mu 3}}{\Sigma a_{3\mu} b_{\mu 3}} \\ \sum a_{3\mu} b_{\mu 1} & \sum a_{3\mu} b_{\mu 2} & \sum a_{3\mu} b_{\mu 3} \end{pmatrix} \tag{2.32}$$

where

$$f_1 = 1, \qquad f_2 = -b_{12}, \qquad f_3 = b_{12}b_{23} - b_{13}.$$

Applying the transformations (2.25) and (2.31) to the wave function in (2.20), the overlap integral is given as

$$\begin{aligned} I_{00}(\varepsilon, \varphi\theta\psi; \varepsilon, 000) &= \left(\frac{e^{2\varepsilon}}{AB}\right)^{2s_1} \left(\frac{e^{-2\varepsilon}}{C}\right)^{2s_3} (C'_{33})^{s_3 - s_1} \\ &= (1 + \sinh^2 3\varepsilon \sin^2 \theta)^{-s_3} (\cos \theta)^{s_3 - s_1}. \end{aligned} \tag{2.33}$$

The method of calculation is explained in ref.[9]). As the overlap integral obtained in (2.33) depends only on the angle θ between the two orientations of the symmetry axis of the nucleus, it is expressed, in general, by

$$\begin{aligned} I_{00}(\varepsilon, \varphi''\theta''\psi''; \varepsilon, \varphi'\theta'\psi') &= I_{00}(\varepsilon, \omega) \\ &= (1 + \sinh^2 3\varepsilon \sin^2 \omega)^{-s_3} (\cos \omega)^{s_3 - s_1} \end{aligned} \tag{2.34}$$

where

$$\cos \omega = \cos \theta' \cos \theta'' + \sin \theta' \sin \theta'' \cos(\varphi' - \varphi''). \tag{2.35}$$

If $s_3 \gg 1$ and $s_3 - s_1 \gg 1$, eq. (2.34) is approximated by

$$I_{00}(\varepsilon, \varphi''\theta''\psi''; \varepsilon, \varphi'\theta'\psi') \approx \exp[-S \sin^2 \omega] \tag{2.36}$$

where

$$S = s_3 \sinh^2 3\varepsilon + \tfrac{1}{2}(s_3 - s_1). \tag{2.37}$$

The normalization constant $N_{IM}(\varepsilon)$ is obtained from

$$\begin{aligned} 1 &= \int |\Psi_{IM}(\mathbf{r}_1 \cdots \mathbf{r}_A)|^2 \mathrm{d}\mathbf{r}_1 \cdots \mathrm{d}\mathbf{r}_A \\ &= (N_{IM}(\varepsilon))^2 \int Y^*_{IM}(\theta''\varphi'') I_{00}(\varepsilon, \omega) Y_{IM}(\theta'\varphi') \sin \theta' \, \mathrm{d}\theta' \, \mathrm{d}\varphi' \sin \theta'' \, \mathrm{d}\theta'' \, \mathrm{d}\varphi''. \end{aligned} \tag{2.38}$$

First, the overlap integral is expanded in terms of the Legendre polynomials:

$$I_{00}(\varepsilon, \omega) = \sum_{L=0}^{\infty} t_L(\varepsilon)(2L+1) P_L(\cos \omega), \tag{2.39}$$

where the coefficient t_L is given by

$$t_L(\varepsilon) = \int_0^{\frac{1}{2}\pi} I_{00}(\varepsilon, \omega) P_L(\cos \omega) \sin \omega \, \mathrm{d}\omega. \tag{2.40}$$

By inserting (2.39) into (2.38) and using the well-known formula

$$P_L(\cos\omega) = \frac{4\pi}{2L+1}\sum_M Y^*_{LM}(\theta'\varphi')Y_{LM}(\theta''\varphi''), \qquad (2.41)$$

the normalization constant is obtained as

$$N_{IM}(\varepsilon) = (4\pi t_I(\varepsilon))^{-\frac{1}{2}} \qquad (2.42)$$

For the special case $s_3 \gg 1$, $s_3 - s_1 \gg 1$ and $2S \gg I$, the integral (2.40) is easily calculated using (2.36) and (2.40), and becomes

$$t_I(\varepsilon) = (2S)^{-1}. \qquad (2.43)$$

3. Expansion of the Rotational State Wave Functions in Terms of the Shell Model States

We now proceed to calculate the expansion coefficients of the wave function for the rotational state in terms of the shell model wave functions. If we write

$$\Psi_{IM}(\varepsilon, \mathbf{r}_1 \cdots \mathbf{r}_A) = \sum_n C_{IM,n}\psi_n(\mathbf{r}_1 \cdots \mathbf{r}_A; 0, 000), \qquad (3.1)$$

the expansion coefficients are calculated from

$$C_{IM,n} = N_{IM}(\varepsilon)\int Y_{IM}(\theta\varphi)I_{0n}(\varepsilon, \varphi\theta\psi; 0, 000)\sin\theta\, d\theta\, d\varphi. \qquad (3.2)$$

The overlap integral

$$I_{0n}(\varepsilon, \varphi\theta\psi; 0, 000) = \int \psi_0{}^*(\mathbf{r}_1 \cdots \mathbf{r}_A; \varepsilon, \varphi\theta\psi)\psi_n(\mathbf{r}_1 \cdots \mathbf{r}_A; 0, 000)d\mathbf{r}_1 \cdots d\mathbf{r}_A \qquad (3.3)$$

may be easily calculated by applying the transformation (2.25) and (2.31). However, e_μ and e'_μ should be chosen as

$$e'_1 = e'_2 = \mathrm{e}^{2\varepsilon}, \quad e'_3 = \mathrm{e}^{-4\varepsilon}, \quad e_1 = e_2 = e_3 = 1 \qquad (3.4)$$

instead of (2.22).

It is interesting to estimate the probability for the ground state of the shell model state to be found in the rotational state. After some calculation the overlap integral is obtained as

$$I_{00}(\varepsilon, \varphi, \theta, \psi; 0, 000) = (\cosh\varepsilon)^{-2s_1}(\cosh 2\varepsilon)^{-s_3}(\cos\theta)^{s_3-s_1}. \qquad (3.5)$$

Inserting this overlap integral in (3.2), the expansion coefficient is calculated as

$$|C_{IM,0}|^2 = \exp\left[-2\varepsilon^2(s_1+2s_3)\right]\cdot\frac{(2I+1)2S}{(s_3-s_1)^2}\delta_{M,0} \qquad (3.6)$$

provided the conditions $s_3 \gg 1$, $s_3 - s_1 \gg 1$ and $2S \gg I$ are satisfied.

To obtain the order of magnitude, the following example is considered:

proton levels $\rho \leqq 3$ are all filled, and $\lambda_n = 2$
neutron levels $\rho \leqq 4$ are all filled, and $\lambda_p = 3$.

This nucleus has the mass number $A = 142$, and corresponds to a rare earth nucleus because the spin-orbit interaction is neglected in our model. From (2.17) we obtain

$$s_1 = s_2 = 199, \quad s_3 = 263. \tag{3.7}$$

By using (2.18) the equilibrium deformation $\varepsilon_{eq} = 0.04648$ ($\beta_{eq} = 0.2946$) is obtained, from which S is calculated:

$$S = 37.14.$$

Inserting these figures into (3.6),

$$|C_{I0,0}|^2 = (2I+1) \times 7.91 \times 10^{-4}.$$

This figure shows that the probability is extremely small compared to unity. However, it should be noted that the shell model wave function considered here is a Slater determinant, which is not an eigenfunction of the total angular momentum. In order to find the probability for the real shell model wave function it is necessary to calculate the expansion coefficient for the eigenfunction of the angular momentum.

When the expansion coefficients for the excited shell model states are calculated, the transformation

$$\begin{aligned} e^{\varepsilon} x_i &= g_1 \xi_i \\ \xi_i &= h_{11} A X_i + h_{12} e^{\varepsilon} y_i + h_{13} e^{2\varepsilon} z_i \end{aligned} \tag{3.8}$$

$$\begin{aligned} e^{\varepsilon} y_i &= g_2 \eta_i \\ \eta_i &= h_{22} B Y_i + h_{23} e^{-2\varepsilon} z_i \end{aligned} \tag{3.9}$$

$$e^{-2\varepsilon} z_i = g_3 C Z_i, \tag{3.10}$$

where

$$h_{11}^2 + h_{12}^2 + h_{13}^2 = 1, \quad h_{22}^2 + h_{23}^2 = 1, \tag{3.11}$$

makes it possible to apply the formulae given in the appendix. The coefficients g_i and h_{ij} should be chosen so that the resultant transformation be equivalent to the transformation (2.25).

Since the percentage of the individual shell model state in the rotational state was found to be extremely small, the shell model states with the same excitation energy will be considered together. This method of analysis is also convenient for the comparison with Elliott's model. First, the Slater wave function in the deformed well is expanded in terms of those in the spherical well:

$$\psi_0(\mathbf{r}'_1 \cdots \mathbf{r}'_A; \varepsilon, 000) = p_0 \sum_n p_{0n} \psi_n(\mathbf{r}'_1 \cdots \mathbf{r}'_A; 0, 000), \tag{3.12}$$

where the expansion coefficient is given by

$$p_0 p_{0n} = \int \psi_0^*(\mathbf{r}'_1 \cdots \mathbf{r}'_A; \varepsilon, 000)\psi_n(\mathbf{r}'_1 \cdots \mathbf{r}'_A; 0, 000)d\mathbf{r}_1 \cdots d\mathbf{r}_A. \tag{3.13}$$

Before calculating the coefficient, configurations should be specified explicitly. They are denoted by the quantum numbers of excited nucleons and those of holes: $l'_i m'_i n'_i$; $l_i m_i n_i$. Letters with primes are always used for excited nucleons.

By using the formula (A.1) the ground state wave function in the integral (3.13) may be written in terms of the wave function with arbitrary deformation parameters α, α and γ for the x, y and z directions:

$$\begin{aligned}\psi_0(\mathbf{r}_1 \cdots \mathbf{r}_A; \varepsilon, 000) = {} & e^{(\varepsilon-\alpha)(s_1+s_2)-(2\varepsilon+\gamma)s_3} \\ & \cdot \exp\left[-\tfrac{1}{2}k_0{}^2 \sum_i (e^{2\varepsilon}-e^{2\alpha})(x_i{}^2+y_i{}^2)+(e^{-4\varepsilon}-e^{2\gamma})z_i{}^2\right] \\ & \times \psi_0(\mathbf{r}_1 \cdots \mathbf{r}_A; \alpha, \alpha, \gamma; 000).\end{aligned} \tag{3.14}$$

A similar procedure may be applied to the wave functions of the excited states. By choosing the deformations α and γ as follows:

$$2e^{2\alpha} = 1+e^{2\varepsilon}, \qquad 2e^{2\gamma} = 1+e^{-4\varepsilon}, \tag{3.15}$$

one finally obtains

$$p_0 = (\cosh \varepsilon)^{-(s_1+s_2)}(\cosh 2\varepsilon)^{-s_3} \simeq \exp[-(\tfrac{1}{2}(s_1+s_2)+2s_3)\varepsilon^2], \tag{3.16}$$

$$\begin{aligned} p_{00} &= 1, \\ p_{0n} &= (-\tanh \varepsilon)^{Q_1+Q_2}(\tanh 2\varepsilon)^{Q_3} \det (C_{l'_i l_i} C_{m'_i m_i} C_{n'_i n_i}), \end{aligned} \tag{3.17}$$

where

$$\begin{aligned} Q &= Q_1+Q_2+Q_3, & Q_1 &= \tfrac{1}{2}\sum (l'_i-l_i), \\ Q_2 &= \tfrac{1}{2}\sum (m'_i-m_i), & Q_3 &= \tfrac{1}{2}\sum (n'_i-n_i) \end{aligned} \tag{3.18}$$

are related to the excitation energies. In the equation (3.17) the determinant appears because of the antisymmetric character of the wave function. It is also noted that $C_{l'_i l_i}\, C_{m'_i m_i}\, C_{n'_i n_i}$ has a non-vanishing value only for transitions between two states with the same spin, parity and τ-spin quantum numbers. For $l'_i m'_i n'_i$ and $l_i m_i n_i$ the states of the excited nucleons and holes should be taken, but sometimes it is necessary to include intermediate states. A detailed discussion will not be given, because it is not necessary for our present purpose.

The next step is to expand the Slater determinant $\psi_n(\mathbf{r}'_1 \cdots \mathbf{r}'_A; 0, 000)$ in terms of the eigenfunctions of the angular momentum:

$$\psi_n(\mathbf{r}'_1 \cdots \mathbf{r}'_A; 0, 000) = \sum_{\mu' L} q^{\mu'}_{n,L} \Phi^{\mu'}_{L0}(\mathbf{r}'_1 \cdots \mathbf{r}'_A). \tag{3.19}$$

The wave function $\Phi^{\mu'}_{L0}(\mathbf{r}'_1 \cdots \mathbf{r}'_A)$ is an eigenfunction of the total angular momentum L, and its component along the z' axis is zero. The symbol μ' denotes the configuration of the shell model wave function, and the particular symbol μ will be used for those configurations which are obtained by replacing a number of neutron states lmn in the last shell $l+m+n = \rho_n+1$ by other states $l'm'n'$ within the same shell $l'+m'+n' = \rho_n+1$, and similarly for the protons, while the nucleon states in lower shells $l+m+n \leqq \rho_n$ and ρ_p are kept unchanged.

The transformation of this wave function from the x', y', z' system to the x, y, z system may be carried out by the representation of the three dimensional rotational group

$$\Phi^{\mu'}_{L0}(\mathbf{r}'_1 \cdots \mathbf{r}'_A) = \sum_M D^L_{M0}(\theta\varphi\psi)\Phi^{\mu'}_{LM}(\mathbf{r}_1 \cdots \mathbf{r}_A). \tag{3.20}$$

By putting (3.12), (3.19) and (3.20) into (2.1) the following expansion is obtained:

$$\begin{aligned}\Psi_{IM}(\varepsilon, \mathbf{r}_1 \cdots \mathbf{r}_A) = [(2I+1)t_I(\varepsilon)]^{-\frac{1}{2}}p_0[\sum_\mu q^\mu_{0,I}\Phi^\mu_{IM}(\mathbf{r}_1 \cdots \mathbf{r}_A)&\\ +\sum_{n\mu'} p_{0n}q^{\mu'}_{n,I}\Phi^{\mu'}_{IM}(\mathbf{r}_1 \cdots \mathbf{r}_A)].&\end{aligned} \tag{3.21}$$

In the last equation $t_I(\varepsilon)$ is given by (2.40). The first sum in the brace of the right-hand side of this equation corresponds to the Elliott wave-function, apart from the normalization.

Noting that the amplitude of the state with configuration Q_1Q_2 and Q_3 in the rotational state is proportional to $(-\tanh\varepsilon)^{Q_1+Q_2}\times(\tanh 2\varepsilon)^{Q_3}$ as given by (3.17), the wave function (3.21) may be rewritten as

$$\begin{aligned}&\Psi_{IM}(\varepsilon_1\varepsilon_1\varepsilon_3; \mathbf{r}_1 \cdots \mathbf{r}_A)\\ &= (t_I(\varepsilon_1\varepsilon_1\varepsilon_3))^{-\frac{1}{2}}(\cosh\varepsilon_1)^{-2s_1}(\cosh\varepsilon_3)^{-s_3}\sum(-\tanh\varepsilon_1)^{Q_1+Q_2}(-\tanh\varepsilon_3)^{Q_3}\\ &\qquad\times\Phi_{Q_1Q_2Q_3}(\mathbf{r}_1 \cdots \mathbf{r}_A).\end{aligned} \tag{3.22}$$

The symbols ε_1, ε_3 are introduced to denote the scale parameters of the x and z directions, i.e. $\varepsilon_1 = \varepsilon$ and $\varepsilon_3 = -2\varepsilon$. The notation $t_I(\varepsilon_1\varepsilon_1\varepsilon_3)$ corresponds to $t_I(\varepsilon)$ occurring in (2.40). The wave function $\Phi_{Q_1Q_2Q_3}(\mathbf{r}_1 \cdots \mathbf{r}_A)$ is an aggregation of wave functions $\psi_n(\mathbf{r}_1 \cdots \mathbf{r}_A; 0, 000)$ with the configuration Q_1Q_2 and Q_3; it is independent of ε_1 and ε_3, but not normalized to unity.

The overlap integral of the two wave functions with different sets of deformations $\varepsilon_1\varepsilon_3$ and $\varepsilon'_1\varepsilon'_3$ is calculated using the expression (3.22) and also the original expression (2.1):

$$\begin{aligned}&\langle\Psi_{IM}(\varepsilon_1\varepsilon_1\varepsilon_3)|\Psi_{IM}(\varepsilon'_1\varepsilon'_1\varepsilon'_3)\rangle\\ &= [t_I(\varepsilon_1\varepsilon_1\varepsilon_3)t_I(\varepsilon'_1\varepsilon'_1\varepsilon'_3)]^{-\frac{1}{2}}(\cosh\varepsilon_1\cosh\varepsilon'_1)^{-2s_1}(\cosh\varepsilon_3\cosh\varepsilon'_3)^{-s_3}\\ &\quad\times\sum(-\tanh\varepsilon_1)^{Q_1+Q_2}(-\tanh\varepsilon_3)^{Q_3}(-\tanh\varepsilon'_1)^{Q'_1+Q'_2}(-\tanh\varepsilon'_3)^{Q'_3}\langle\Phi_{Q_1Q_2Q_3}|\Phi_{Q'_1Q'_2Q'_3}\rangle\\ &= N_{IM}(\varepsilon_1\varepsilon_1\varepsilon_3)N_{IM}(\varepsilon'_1\varepsilon'_1\varepsilon'_3)\\ &\qquad\times\int Y^*_{IM}(\theta\varphi)I_{00}(\varepsilon_1\varepsilon_1\varepsilon_3\varphi\theta\psi;\varepsilon_1'\varepsilon'_1\varepsilon'_3\varphi'\theta'\psi')Y_{IM}(\theta'\varphi')\sin\theta\mathrm{d}\theta\mathrm{d}\varphi\sin\theta'\mathrm{d}\theta'\mathrm{d}\varphi'\end{aligned} \tag{3.23}$$

where

$$\begin{aligned}&I_{00}(\varepsilon_1\varepsilon_1\varepsilon_3\varphi\theta\psi; \varepsilon'_1\varepsilon'_1\varepsilon'_3\varphi'\theta'\psi')\\ &= \int\psi_0(\mathbf{r}_1 \cdots \mathbf{r}_A; \varepsilon_1\varepsilon_1\varepsilon_3; \varphi\theta\psi)\psi_0(\mathbf{r}_1 \cdots \mathbf{r}_A; \varepsilon'_1\varepsilon'_1\varepsilon'_3; \varphi'\theta'\psi')\mathrm{d}\mathbf{r}_1 \cdots \mathrm{d}\mathbf{r}_A.\end{aligned} \tag{3.24}$$

From the last equation the following relation is obtained:

$$\sum (-\tanh \varepsilon_1)^{Q_1+Q_2}(-\tanh \varepsilon_3)^{Q_3}(-\tanh \varepsilon'_1)^{Q'_1+Q'_2}(-\tanh \varepsilon'_3)^{Q_3}\langle \Phi_{Q_1Q_2Q_3}|\Phi_{Q'_1Q'_2Q'_3}\rangle$$
$$= \frac{1}{4\pi}(\cosh \varepsilon_1 \cosh \varepsilon'_1)^{2s_1}(\cosh \varepsilon_3 \cosh \varepsilon'_3)^{s_3}\int Y^*_{IM}(\theta\varphi)I_{00}(\varepsilon_1\varepsilon_1\varepsilon_3\varphi\theta\psi; \tag{3.25}$$
$$\varepsilon'_1\varepsilon'_1\varepsilon'_3\varphi'\theta'\psi')Y_{IM}(\theta'\varphi')\sin\theta\,\mathrm{d}\theta\,\mathrm{d}\varphi\,\sin\theta'\,\mathrm{d}\theta'\,\mathrm{d}\varphi'.$$

The overlap integral $I_{00}(\varepsilon_1\varepsilon_1\varepsilon_3\varphi\theta\psi;\ \varepsilon'_1\varepsilon'_1\varepsilon'_3\varphi'\theta'\psi')$ may be calculated using the transformation (2.25) and (2.31) with the following choice of the parameters in (2.23):

$$e'_1 = e'_2 = \mathrm{e}^{2\varepsilon'_1}, \qquad e'_3 = \mathrm{e}^{2\varepsilon'_3}, \qquad e_1 = e_2 = \mathrm{e}^{2\varepsilon_1}, \qquad e_3 = \mathrm{e}^{2\varepsilon_3}. \tag{3.26}$$

The result is given by

$$I_{00}(\varepsilon_1\varepsilon_1\varepsilon_3\varphi\theta\psi; \varepsilon'_1\varepsilon'_1\varepsilon'_3\varphi'\theta'\psi')$$
$$= (\cosh \varepsilon_1 \cosh \varepsilon'_1)^{-2s_1}(\cosh \varepsilon_3 \cosh \varepsilon'_3)^{-s_3}u(1-v\cos^2\omega)^{-s_3}(\cos\omega)^{(s_3-s_1)} \tag{3.27}$$

where cos ω is defined by (2.35) and

$$u = (1-\tanh \varepsilon_1 \tanh \varepsilon'_1)^{s_3-2s_1}[(1-\tanh \varepsilon'_1 \tanh \varepsilon_3)(1-\tanh \varepsilon_1 \tanh \varepsilon'_3)]^{-s_3}$$
$$v = (\tanh \varepsilon'_1 - \tanh \varepsilon'_3)(\tanh \varepsilon_1 - \tanh \varepsilon_3) \tag{3.28}$$
$$\cdot\ [(1-\tanh \varepsilon'_1 \tanh \varepsilon_3)(1-\tanh \varepsilon_1 \tanh \varepsilon'_3)]^{-1}.$$

If we put (3.27) into the right hand side of (3.25) after expanding $u(1-v\cos^2\omega)^{-s_3}$ in terms of powers of $\tanh \varepsilon_1$, $\tanh \varepsilon'_1 \ldots$, the integral over Euler angles is easily carried out. Comparing the left and right hand sides of (3.25) with the same powers of $\tanh \varepsilon_1$, $\tanh \varepsilon'_1 \ldots$ we obtain

$$\sum_{\substack{Q_1+Q_2+Q_3=Q\\ Q'_1+Q'_2+Q'_3=Q'}} \langle \Phi_{Q_1Q_2Q_3}|\Phi_{Q'_1Q'_2Q'_3}\rangle = \delta_{QQ'}\sum_{\alpha pq}(-)^{Q+p+q}\binom{-s_3}{\alpha}\binom{s_3-2s_1}{Q-Q_3-Q'_3-\alpha+p+q}$$
$$\times\binom{-s_3-\alpha}{Q_3-q}\binom{-s_3-\alpha}{Q'_3-p}\binom{\alpha}{p}\binom{\alpha}{q}h_{2\alpha} \tag{3.29}$$

where

$$h_{2\alpha} = \int_0^{\frac{1}{2}\pi}(\cos\omega)^{s_3-s_1+2\alpha}P_I(\cos\omega)\sin\omega\,\mathrm{d}\omega. \tag{3.30}$$

In particular $h_0 = t_I(0)$.

Putting (3.29) into (3.23) and taking $\varepsilon_1 = \varepsilon'_1 = \varepsilon$, $\varepsilon_3 = \varepsilon'_3 = -2\varepsilon$ we can obtain the probability of the shell model states with excitation energy $2Q\hbar\omega_0$ occurring in the rotational state. Denoting this probability by P_Q

$$P_Q = \sum_{Q_3, Q'_3}\frac{1}{t_I(\varepsilon)}(\cosh\varepsilon)^{-4s_1}(\cosh 2\varepsilon)^{-2s_3}(\tanh\varepsilon)^{2Q-Q_3-Q'_3}(\tanh 2\varepsilon)^{Q_3+Q'_3} \tag{3.31}$$
$$\times\sum_{\alpha pq}(-)^{Q+p+q}\binom{-s_3}{\alpha}\binom{s_3-2s_1}{Q-Q_3-Q'_3-\alpha+p+q}\binom{-s_3-\alpha}{Q_3-q}\binom{-s_3-\alpha}{Q'_3-p}\binom{\alpha}{p}\binom{\alpha}{q}h_{2\alpha}.$$

In particular the probability of the Elliott wave function occurring in the rotational wave function is given by

$$P_0 = \frac{t_I(0)}{t_I(\varepsilon)} (\cosh \varepsilon)^{-4s_1} (\cosh 2\varepsilon)^{-2s_3} \approx \exp[-2(s_1+2s_3)\varepsilon^2] \frac{s_3-s_1+2s_3 \sinh^2 3\varepsilon}{s_3-s_1}. \tag{3.32}$$

The second expression is valid when $s_1 \gg 1$, $s_3 - s_1 \gg 1$ and $2S \gg I$.

In fig. 1 the distribution function is presented for ^{20}Ne. The bulk contribution comes from $Q = 0$ states for smaller I values, and the Elliott wave function is expected to give a good approximation to the collective model wave function. However, for larger I values the situation is a little different: the main contribution comes from $Q = 1$ states. For the $A = 142$ nucleus the distribution function is given in fig. 2. In this case the distribution functions are approximately the same for different I and the main contribution comes from $Q = 2$ and $Q = 3$ states. The Elliott wave function is, in this case, considerably different from the rotational state wave function.

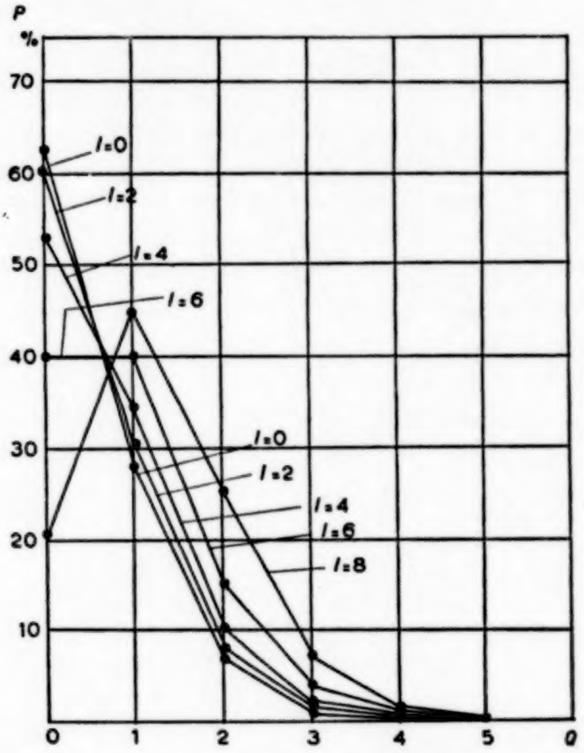

Fig. 1. The distribution function P_Q for ^{20}Ne.
The percentage P of the shell model states with excitation energy $2Q\hbar\omega_0$ occurring in the rotational states of ^{20}Ne is plotted against Q. The deformation parameter ε is taken as the equilibrium value. The spin of the rotational states is varied from 0 to 8.

When the conditions $s_3 \gg 1$ and $s_3 - s_1 \gg 1$ are satisfied the expression for P_Q becomes very simple. In this case the right hand side of (3.25) may easily be calculated by using the following approximation:

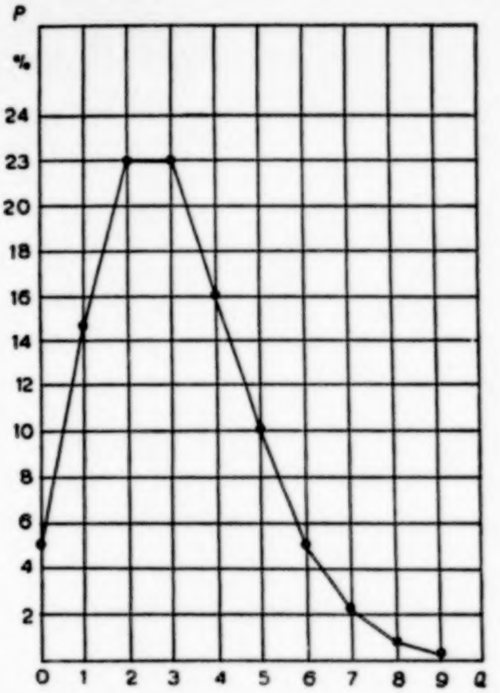

Fig. 2. The distribution function P_Q for the $A = 142$ nucleus. The percentage similar to fig. 1 is plotted for the $A = 142$ nucleus. The distribution function is approximately the same for various values of the spin.

$$\int_0^{\frac{1}{2}\pi} P_I(\cos\omega)(1-v\cos^2\omega)^{-s_3}(\cos\omega)^{s_3-s_1}\sin\omega\,\mathrm{d}\omega \approx (1-v)^{-s_3}t_I(0). \tag{3.33}$$

The right hand side of (3.25) is approximately expressed as

$$t_I(0)\mathrm{e}^z = t_I(0)\sum_{Q=0}^{\infty}\frac{z^Q}{Q!}, \tag{3.34}$$

where

$$z = 2s_1 \tanh^2\varepsilon + s_3 \tanh^2\varepsilon. \tag{3.35}$$

The approximation (3.33) also leads the following relation:

$$t_I(\varepsilon)/t_I(0) = (\cosh\varepsilon)^{-4s_1}(\cosh 2\varepsilon)^{-2s_3}\mathrm{e}^z. \tag{3.36}$$

Using (3.34) and (3.36) we obtain from (3.25)

$$P_Q = \mathrm{e}^{-z}\frac{z^Q}{Q!}. \tag{3.37}$$

This distribution function P_Q is of the Poisson type. The mean excitation energy $\langle \Delta E\rangle$ and the standard deviation $\sqrt{\langle \Delta E^2\rangle - \langle \Delta E\rangle^2}$ are easily calculated:

$$\begin{aligned}\langle \Delta E\rangle &= 2\hbar\omega_0 z,\\ \sqrt{\langle \Delta E^2\rangle-\langle \Delta E\rangle^2} &= 2\hbar\omega_0\sqrt{z}.\end{aligned} \tag{3.38}$$

In order that the Elliott wave function be a good approximation to the collective model wave function, the states with $Q = 0$ must be dominant, that is

$$z \ll 1. \tag{3.39}$$

For the case of ^{20}Ne, although the conditions $s_3 \gg 1$ and $s_3-s_1 \gg 1$ may not be satisfied,

$$z = 0.653$$

while for the nucleus $A = 142$

$$z = 3.12.$$

These results are in a good agreement with those presented in figs. 1 and 2.

Finally we should like to remind that the distribution function calculated here is for the collective model wave functions based on the formalism of generator coordinates, and not for the real rotational state wave functions. The model wave function may be different from the real wave function.

4. Quadrupole Transition Matrix Elements

Although the wave function of Elliott's model was found to be very different from that of the collective model, it is interesting to calculate expectation values of some physical quantities for the two models. As an example, the matrix element of the quadrupole transition will be considered. The operator of the quadrupole moment is

$$Q_{2m}(\mathbf{r}_1\cdots\mathbf{r}_A) = e\sum_i(1-\tau_{i3})/2\cdot r_i^2 Y_{2m}(\theta_i\varphi_i), \tag{4.1}$$

where e is charge of the proton and $\tau_{i,3}$ is the third component of the τ-spin for the i-th nucleon. The matrix element of the operator is expressed by

$$\begin{aligned}\langle I'00|Q_{20}|I00\rangle = N^*_{I'0}N_{I0}\sqrt{\frac{2I+1}{2I'+1}}\sum_m (I200|I2I'0)(I20m|I2I'm)\sqrt{\frac{4\pi}{2I'+1}}\\ \times\int Y^*_{I'm}(\theta\varphi)Q_{2m}(\varepsilon,\theta\varphi)\sin\theta\, \mathrm{d}\theta\, \mathrm{d}\varphi\end{aligned} \tag{4.2}$$

where

$$\begin{aligned}&Q_{2m}(\varepsilon,\theta\varphi)\\ &= \int\psi^*(\mathbf{r}_1\cdots\mathbf{r}_A;\varepsilon,\theta\varphi)Q_{2m}(\mathbf{r}_1\cdots\mathbf{r}_A)\psi(\mathbf{r}_1\cdots\mathbf{r}_A;\varepsilon,00)\mathrm{d}\mathbf{r}_1\cdots\mathrm{d}\mathbf{r}_A.\end{aligned} \tag{4.3}$$

In eq. (4.2) $(I200|I2I'0)$ is the Clebsch-Gordan coefficient and the matrix element is evaluated between two states, one with spin I, its z-component zero and its component along the symmetry axis zero and another with spin I' and its components zero.

The calculation of the last equation may be carried out using the transformation (2.25) and (2.31) with the parameters given by (2.22), and the result is given by

$$\begin{aligned} Q_{20}(\varepsilon, \theta\varphi) &= I_{00}(\varepsilon, \theta)\frac{e}{k_0^2}\sqrt{\frac{5}{4\pi}}\Big[-\mathrm{e}^{-2\varepsilon}s_1^{\mathrm{p}} \\ &+\frac{\mathrm{e}^{4\varepsilon}-\frac{1}{4}\mathrm{e}^{\varepsilon}\sinh 3\varepsilon(9+\mathrm{e}^{-6\varepsilon})\sin^2\theta+\frac{1}{4}\mathrm{e}^{-2\varepsilon}\sinh^2 3\varepsilon(5+\mathrm{e}^{-6\varepsilon})\sin^4\theta}{(1+\sinh^2 3\varepsilon\sin^2\theta)(1-\mathrm{e}^{-3\varepsilon}\sinh 3\varepsilon\sin^2\theta)}s_3^{\mathrm{p}}\Big] \\ Q_{2\pm1}(\varepsilon, \theta\varphi) &= I_{00}(\varepsilon, \theta)\frac{e}{k_0^2}Y_{2\pm1}(\theta\varphi)\left[\frac{\mathrm{e}^{\varepsilon}\sinh 3\varepsilon}{1+\sinh^2 3\varepsilon\sin^2\theta}s_3^{\mathrm{p}}+\frac{\mathrm{e}^{-2\varepsilon}}{2\cos^2\theta}(s_3^{\mathrm{p}}-s_1^{\mathrm{p}})\right] \\ Q_{2\pm2}(\varepsilon, \theta\varphi) &= I_{00}(\varepsilon, \theta)\frac{e}{k_0^2}Y_{2\pm2}(\theta\varphi)\frac{\mathrm{e}^{-2\varepsilon}\sinh 3\varepsilon\cosh 3\varepsilon}{1+\sinh^2 3\varepsilon\sin^2\theta}s_3^{\mathrm{p}} \end{aligned} \tag{4.4}$$

where s_1^{p} and s_3^{p} are respectively contributions from protons to s_1 and s_3, given by eq. (2.17).

It is necessary to make some approximation to calculate analytically the integral of (4.2). As $\sinh 3\varepsilon$ is small compared to the unity and the contribution from terms with higher powers of $\sin^2\theta$ is also small, the expressions on the right hand side of eq. (4.4) may be expanded in terms of $\sin^2\theta$. Neglecting terms with $\sin^4\theta$ and higher terms the integration is easily performed and the final expression is obtained;

$$\begin{aligned} \langle I'00|Q_{20}|I00\rangle &= \sqrt{\frac{5}{4\pi}}\sqrt{\frac{t_{I'}(\varepsilon)}{t_I(\varepsilon)}}\sqrt{\frac{2I+1}{2I'+1}}(I200|I2I'0)^2\frac{e}{k_0^2}\Big[\mathrm{e}^{4\varepsilon}s_3^{\mathrm{p}}-\mathrm{e}^{-2\varepsilon}s_1^{\mathrm{p}} \\ &+\tfrac{1}{2}\mathrm{e}^{-2\varepsilon}(s_3^{\mathrm{p}}-s_1^{\mathrm{p}})g'_{21}(\varepsilon)-\tfrac{1}{3}\sinh 3\varepsilon\cosh 3\varepsilon(\mathrm{e}^{4\varepsilon}+\tfrac{1}{2}\mathrm{e}^{-2\varepsilon})s_3^{\mathrm{p}}(2-g_{20}(\varepsilon)) \\ &+\mathrm{e}^{-2\varepsilon}\sinh 3\varepsilon\cosh 3\varepsilon\cdot s_3^{\mathrm{p}}\{g_{22}(\varepsilon)-\tfrac{2}{7}\sinh^2 3\varepsilon(2g_{21}(\varepsilon) \\ &-\sqrt{\tfrac{6}{5}}g_{41}(\varepsilon)+3g_{22}(\varepsilon)-\sqrt{\tfrac{3}{5}}g_{42}(\varepsilon))\}\Big], \end{aligned} \tag{4.5}$$

where

$$\begin{aligned} g_{NM}(\varepsilon) &= 2\frac{(I20M|I2I'M)}{(I200|I2I'0)}\sum_L\frac{t_L(\varepsilon)}{t_{I'}(\varepsilon)}(-)^M(I'N00|I'NL0)(I'N-M0|I'NL-M), \\ g'_{NM}(\varepsilon) &= 2\frac{(I20M|I2I'M)}{(I200|I2I'0)}\sum_L\frac{t'_L(\varepsilon)}{t_{I'}(\varepsilon)}(-)^M(I'N00|I'NL0)(I'N-M0|I'NL-M); \end{aligned} \tag{4.6}$$

$t'_L(\varepsilon)$ appearing in the last equation is defined by

$$t'_L(\varepsilon) = \int_0^{\frac{1}{2}\pi} I_{00}(\varepsilon, \theta)P_L(\cos\theta)\cdot\cos^{-2}\theta\sin\theta\,\mathrm{d}\theta. \tag{4.7}$$

The matrix element $Q^{(0)}$ of the quadrupole transition in Elliott's model is obtained by taking the limit $\varepsilon \to 0$ in eq. (4.5):

$$Q^{(0)}=\sqrt{\frac{5}{4\pi}}\sqrt{\frac{t_{I'}(0)}{t_I(0)}}\sqrt{\frac{2I+1}{2I'+1}}\,(2I00|2II'0)^2\frac{e}{k_0^{\,2}}$$
$$\cdot\,(s_3^{\,\mathrm{p}}-s_1^{\,\mathrm{p}})[1+\{\tfrac{3}{2}+\tfrac{1}{4}I'(I'+1)-\tfrac{1}{4}I(I+1)\}/(s_3-s_1)]. \tag{4.8}$$

In deriving this result the following formulae were used:

$$\begin{aligned} t_I(0) &= \frac{2^I(s_3-s_1)!(\frac{1}{2}s_3-\frac{1}{2}s_1+\frac{1}{2}I)!}{(s_3-s_1+I+1)!(\frac{1}{2}s_3-\frac{1}{2}s_1-\frac{1}{2}I)!}\\ t'_I(0) &= \frac{2^I(s_3-s_1-2)!(\frac{1}{2}s_3-\frac{1}{2}s_1+\frac{1}{2}I-1)!}{(s_3-s_1+I-1)!(\frac{1}{2}s_3-\frac{1}{2}s_1-\frac{1}{2}I-1)!}. \end{aligned} \tag{4.9}$$

When the conditions $s_3 \gg 1$, $s_3-s_1 \gg 1$ are satisfied, the approximation (2.36) is valid and

$$g_{NM}(\varepsilon) = g'_{NM}(\varepsilon) = 2\delta_{M,0}, \tag{4.10}$$

because $t_I(\varepsilon) = t'_L(\varepsilon) = t'_I(\varepsilon)$. In this case the expressions (4.5) and (4.8) are simplified as

$$\begin{aligned} \langle I'00|Q_{20}|I00\rangle &= \sqrt{\frac{5}{4\pi}}\sqrt{\frac{2I+1}{2I'+1}}\,(I200|I2I'0)^2\frac{e}{k_0^{\,2}}\,[\mathrm{e}^{4\varepsilon}s_3^{\,\mathrm{p}}-\mathrm{e}^{-2\varepsilon}s_1^{\,\mathrm{p}}],\\ Q^{(0)} &= \sqrt{\frac{5}{4\pi}}\sqrt{\frac{2I+1}{2I'+1}}\,(I200|I2I'0)^2\frac{e}{k_0^{\,2}}\,(s_3^{\,\mathrm{p}}-s_1^{\,\mathrm{p}}). \end{aligned} \tag{4.11}$$

As seen from the expression (4.11) the values of the matrix element increases approximately linearly as ε increases. This suggests that the main contribution comes from the Elliott wave function and its interference term with excited states with $Q = 1$ defined by eq. (3.18), because the mixing parameters of the latter states are proportional to ε as given by eq. (3.17). The constant proportional to ε in the matrix element, denoted by $Q^{(1)}$, is calculated from (4.11):

$$Q^{(1)} = \sqrt{\frac{5}{4\pi}}\sqrt{\frac{2I+1}{2I'+1}}\,(I200|I2I'0)^2\frac{e}{k_0^{\,2}}\,(2s_1^{\,\mathrm{p}}+4s_3^{\,\mathrm{p}}). \tag{4.12}$$

Higher order terms in ε are found to be extremely small, for usual magnitudes of ε, compared to the first two terms, $Q^{(0)}$ and $\varepsilon Q^{(1)}$. Thus, the approximation consisting in including the Elliott wave function and its interference term with $Q = 1$ states is found to be good for the calculation of the quadrupole transition rate.

So far, the deformation parameter has been treated as a free parameter. However, it should be chosen so that the zero-th order energy of the nuclear system may become a minimum. The equilibrium value of ε given by (2.18) is approximately expressed as

$$\varepsilon_{\mathrm{eq}} \approx (s_3-s_1)/6s_3. \tag{4.13}$$

On the other hand the mean square of the proton radius is expressed as

$$\tfrac{3}{5}ZR^2 = (2\mathrm{e}^{2\varepsilon} s_1^{\mathrm{p}} + \mathrm{e}^{-4\varepsilon} s_3^{\mathrm{p}})/k_0^2 \tag{4.14}$$

where Z is the atomic number of the nucleus and R is the root mean square of the proton radius. Assuming

$$s_1/s_3 = s_1^{\mathrm{p}}/s_3^{\mathrm{p}} \tag{4.15}$$

we obtain from (4.13) and (4.14)

$$s_3^{\mathrm{p}} = \tfrac{1}{5}ZR^2k_0^2(1+4\varepsilon_{\mathrm{eq}}), \qquad s_1^{\mathrm{p}} = \tfrac{1}{5}ZR^2k_0^2(1-2\varepsilon_{\mathrm{eq}}). \tag{4.16}$$

The matrix element of the quadrupole transitions (4.11) is expressed in terms of $\varepsilon_{\mathrm{eq}}$:

$$\langle I'00|Q_{20}|I00\rangle \simeq \sqrt{\frac{5}{4\pi}}\sqrt{\frac{2I+1}{2I'+1}}\,(I200|I2I'0)^2\tfrac{1}{5}eZR^2(6\varepsilon_{\mathrm{eq}}+6\varepsilon_{\mathrm{eq}}). \tag{4.17}$$

Smaller terms are all neglected. On the right hand side of the last equation, the first term is the contribution from Elliott states and the second is that from interference terms between the Elliott states and the $Q = 1$ states. So long as the approximation (4.17) is good, the Elliott model gives only half the total contribution. It is also noted that the matrix element (4.17) coincides with that obtained by Bohr and Mottelson [1]).

Now, it has become clear that the quadrupole transition matrix element is obtained in a good approximation by taking into account only the contribution from the states $Q = 0$ and the interference term with $Q = 1$ states, while both $Q = 0$ and $Q = 1$ states occupy a small portion of the whole wave function for heavy nuclei. This may look strange at first, but it will be shown in the following that the character of the quadrupole moment operator is responsible for this fact. As our interest is in heavy nuclei the condition $s_3 \gg 1$ and $s_3 - s_1 \gg 1$ are assumed to be satisfied.

To calculate contributions of the matrix element of the quadrupole moment from states with various Q, a method similar to that used in section 3 will be employed. First observing that $\sin\theta$ may be replaced by zero in the quadrupole moment kernel because of the condition $s_3 \gg 1$ and $s_3 - s_1 \gg 1$, one obtains approximately

$$\begin{aligned} &Q_{20}(\varepsilon'_1\varepsilon'_1\varepsilon'_3\varphi\theta\psi;\, \varepsilon_1\varepsilon_1\varepsilon_3 000) \\ &\quad\approx I(\varepsilon'_1\varepsilon'_1\varepsilon'_3\varphi\theta\psi;\, \varepsilon_1\varepsilon_1\varepsilon_3 000)\,\frac{e}{k_0^2}\sqrt{\frac{5}{4\pi}}\left[\frac{2}{\mathrm{e}^{2\varepsilon_3}+\mathrm{e}^{2\varepsilon'_3}}s_3^{\mathrm{p}} - \frac{2}{\mathrm{e}^{2\varepsilon_1}+\mathrm{e}^{2\varepsilon'_1}}s_1^{\mathrm{p}}\right] \end{aligned} \tag{4.18}$$

where the definition of the left hand side of the equation is apparent. As the last factor of the right hand side of eq. (4.18) may be expanded in terms of $\tanh \varepsilon_1$, $\tanh \varepsilon'_1, \ldots$, and the constant term and the linear terms give a good approximation, one can write approximately

$$Q_{20}(\varepsilon, \theta\varphi) \approx I_{00}(\varepsilon, \theta)\, \frac{e}{k_0^2} \sqrt{\frac{5}{4\pi}}\, [(s_3^{\mathrm{p}} - s_1^{\mathrm{p}}) + 2(s_3^{\mathrm{p}} \tanh 2\varepsilon + s_1^{\mathrm{p}} \tanh \varepsilon)] \tag{4.19}$$

where the deformation parameters are again replaced by the usual ε.

Putting (4.19) into (4.2) the matrix element is given by

$$\langle I'00|Q_{20}|I00\rangle = N^{*}_{I'0}(\varepsilon) N_{I0}(\varepsilon) \sqrt{\frac{4\pi}{2I'+1}} \int Y^{*}_{I'0}(\theta\varphi) I_{00}(\varepsilon, \theta) \sin\theta\, d\theta\, d\varphi \cdot (q_0 + q_1), \tag{4.20}$$

where

$$\begin{aligned} q_0 &= \sqrt{\frac{2I+1}{2I'+1}}\, (I200|I2I'0)^2 \frac{e}{k_0^2} \sqrt{\frac{5}{4\pi}}\, (s_3^{\mathrm{p}} - s_1^{\mathrm{p}}) = Q^{(0)} \\ q_1 &= \sqrt{\frac{2I+1}{2I'+1}}\, (I200|I2I'0)^2 \frac{e}{k_0^2} \sqrt{\frac{5}{4\pi}}\, 2(s_3^{\mathrm{p}} \tanh 2\varepsilon + s_1^{\mathrm{p}} \tanh \varepsilon) \approx \varepsilon Q^{(1)}. \end{aligned} \tag{4.21}$$

$Q^{(0)}$ and $Q^{(1)}$ are already given by (4.11) and (4.12). Owing to the assumption of heavy nuclei, $N_{I'0}(\varepsilon) = N_{I0}(\varepsilon)$, so that the right hand side of (4.20) apart from the last factor $(q_0 + q_1)$ is just the normalization integral and equal to unity. However, as we are interested in the contribution from states with various Q, contributions to the integral from each state should be analysed. Such a analysis was done in section 3 and the factor is expressed as $\sum_{Q=0}^{\infty} P_Q$. Then we obtain

$$\begin{aligned} \langle I'00|Q_{20}|I00\rangle &= (P_0 + P_1 + \ldots)(q_0 + q_1) \\ &= P_0 q_0 + P_0 q_1 + P_1 q_0 + P_1 q_1 + \ldots \end{aligned} \tag{4.22}$$

It is noted that the second line of the last equation is written to the order of ε for small ε. If the second line is rewritten as

$$P_0[q_0 + q_1 + (P_1/P_0) q_0 + (P_1/P_0) q_1 + \ldots],$$

the first term in the square brackets is independent of ε, the next is a linear combination of tanh ε and tanh 2ε and so on. As we have seen in section 3 the relative amplitude of the shell model state with excitation energy $2\hbar\omega_0 Q$ is proportional to ε^Q for small ε and also the quadrupole moment operator is independent of ε; then we can identify each term of the second line of (4.22) as a contribution from definite states. Thus, $P_n q_0$ is the contribution from the state $Q = n$, and $P_n q_1$, is the interference term between the states $Q = n$ and $Q = n+1$. Now, it is possible to calculate the various contributions separately. The matrix element taking into account all states with $Q \leqq n$ is given by

$$(P_0 q_0 + P_0 q_1 + \ldots + P_n q_0)/(P_0 + P_1 + \ldots + P_n), \tag{4.23}$$

while the matrix element including the interference term with $Q = n+1$ states in addition to the previous one is

$$(P_0q_0+P_0q_1+\ldots+P_nq_0+P_nq_1)/(P_0+P_1+\ldots+P_n) = q_0+q_1. \quad (4.24)$$

This is an exact result. In particular if we put $n = 0$ in (4.24) we obtain the result taking account of $Q = 0$ states and the interference term with $Q = 1$ states. It is seen from the preceding discussion that the results obtained above are based on the possibility of the decomposition of the quadrupole moment kernel into the overlapping integral and the linear term in tanh ε and tanh 2ε. In fig. 3 the value of the matrix element calculated from (4.23) is presented for the $A = 142$ nucleus. From the figure it is seen that the higher excited states are necessary to get a good result unless the interference term with the next higher excited states is included.

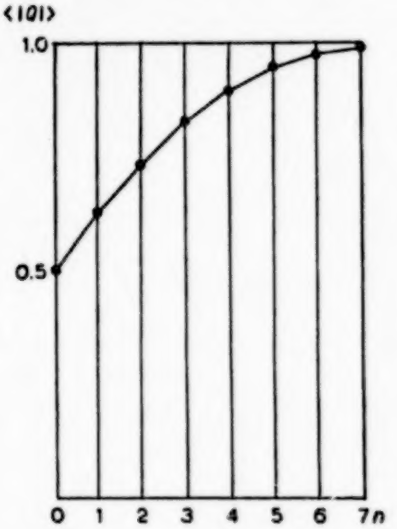

Fig. 3. The matrix element of the quadrupole transition for the $A = 142$ nucleus. The matrix element is calculated taking into account all states with configurations $Q \leq n$. However, the interference term with $Q = n+1$ states is not included. The unit is taken as the correct value. If the above-mentioned interference term is included the matrix element becomes equal to the exact value.

The authors wish to thank Prof. G. Takeda, Drs. F. Iwamoto and M. Sano for stimulating discussions.

Appendix

For the Hermite polynomial appearing in (2.7) some useful formulae are presented in the following. First,

$$N_l(\lambda k)H_l(\lambda kx) = \sum C_{ll'}\lambda^{l'+\frac{1}{2}}(1-\lambda^2)^{\frac{1}{2}(l-l')}N_{l'}(k)H_{l'}(kx) \quad (A.1)$$

where

$$\begin{aligned} C_{ll'} &= (-)^{\frac{1}{2}(l-l')}[l(l-1)\cdots(l'+1)]^{\frac{1}{2}}/(l-l')!! && \text{for } l-l'=\text{positive even number,} \\ &= 0. && \text{otherwise.} \end{aligned}$$

This is derived from the corresponding formula for the Laguerre polynomial by using the relations between these two polynomials 10).

Other useful formulae are

$$H_n(a_1x_1+a_2x_2+\ldots+a_rx_r)$$
$$= n! \sum_{m_1+m_2+\cdots+m_r=m} \frac{a_1^{m_1}}{m_1!}\frac{a_2^{m_2}}{m_2!}\cdots\frac{a_r^{m_r}}{m_r!} H_{m_1}(x_1)\cdots H_{m_r}(x_r) \quad \text{(A.2)}$$

where

$$\sum_{i=1}^{r} a_i^2 = 1,$$

and also

$$H_l(x)H_{l'}(x) = \sum_{k=0}^{\min(l,l')} 2^k k! \binom{l}{k}\binom{l'}{k} H_{l+l'-2k}(x). \quad \text{(A.3)}$$

References

1) A. Bohr and B. R. Mottelson, Mat. Fys. Medd. Dan. Vid. Selsk. **27** (1953) no. 16
2) J. P. Elliott and B. H. Flowers, Proc. Roy. Soc. A **229** (1955) 536;
M. G. Redlich, Phys. Rev. **99** (1955) 1427
3) E. B. Paul, Phil. Mag. **2** (1957) 311;
G. Rakavy, Nuclear Physics **4** (1957) 375
4) M. G. Redlich, Phys. Rev. **110** (1958) 468
5) J. P. Elliott, Proc. Roy. Soc. A **245** (1958) 128
6) J. P. Elliott, Proc. Roy. Soc. A **245** (1958) 562
7) S. A. Moszkowski, Phys. Rev. **110** (1958) 403;
T. Tamura, preprint
8) J. J. Griffin and J. A. Wheeler, Phys. Rev. **108** (1957) 311;
J. J. Griffin, Phys. Rev. **108** (1957) 328
9) R. E. Peierls and J. Yoccoz, Proc. Phys. Soc. A **70** (1957) 381;
J. Yoccoz, Proc. Phys. Soc. A **70** (1957) 388
10) H. Bateman, manuscript project, Higher Transcendental Functions II (McGraw Hill, 1953)

4.E:5

Nuclear Physics **12** (1959) 159—166; © *North-Holland Publishing Co., Amsterdam*

Not to be reproduced by photoprint or microfilm without written permission from the publisher

UN NOUVEL ISOTOPE DU TERBIUM DE MASSE 152, ÉMETTEUR ALPHA

J. OLKOWSKY, I. GRATOT, M. LE PAPE et L. COHEN

Section des réactions nucléaires à moyenne énergie, C.E.N., *Saclay, Gif sur Yvette* (S & O)

Reçu le 19 Mars 1959

Abstract: A new isotope of terbium has been produced by ^{151}Eu(α, 3n) and ^{152}Gd(p, n) reactions. Its half-life is found to be 4 ± 0.5 minutes. This isotope decays by electron-capture, β^+ and α rays. The ratio α/X_K is $\approx 2 \times 10^{-5}$. 140-keV and 235-keV γ-rays are observed. The relative proportions of the different gamma-rays detected are

X_K	140 keV	235 keV	511 keV
100	25	30	15

1. Introduction

Au cours de nos expériences sur la spallation du terbium [1]), nous avons été conduits à rechercher les isotopes inconnus de cet élément. Le présent travail porte sur la recherche et l'obtention du ^{152}Tb.

Dans le travail [2]), les auteurs lui attribuaient une période inférieure à 10 minutes ou supérieure à 5 ans.

2. Méthodes Expérimentales

2.1. IRRADIATIONS

1) ^{151}Eu séparé (sous forme d'oxyde)$+\alpha_{44\ \mathrm{MeV}}$
La composition isotopique était la suivante:

151	153
91.9	8.1

2) ^{152}Gd séparé (sous forme d'oxyde)$+\mathrm{p}_{11\ \mathrm{MeV}}$
La composition isotopique était la suivante:

152	154	155	156	157	158	160
14.96	9.75	27.26	19.32	10.08	11.67	6.97

2.2. ÉTUDE DES DIFFÉRENTS RAYONNEMENTS

Les méthodes sont les mêmes que pour le travail 1).

Rayonnement α:
pour la période: détecteur au SZn;
pour l'énergie: chambre d'ionisation à impulsions 3).

Rayonnement β:
compteur Geiger du type cloche à paroi mince (2 mg/cm^2).

Rayonnements γ, X:
cristal INa 1.5×1 pouce et photomultiplicateur EMI 6097 F.

2.3. ACTIVITÉS PARASITES

Aucune séparation chimique n'a été faite. Nous avions étudié, au préalable, les produits des réactions sur l'oxygène de la cible des faisceaux de protons et d'alpha, l'oxygène étant irradié sous forme d'oxyde d'aluminium.

Les isotopes formés sont:
avec les protons: ^{13}N(10 min), ^{17}F(1.1 min), ^{18}F (118 min);
avec les alpha: ^{17}F(1.1 min), ^{18}F(118 min).

2.4. DÉTERMINATION DU NOMBRE ATOMIQUE DE L'ISOTOPE DE PÉRIODE 4 MINUTES

Avec des alpha de 44 MeV irradiant de l'europium 151, nous ne pouvons former que ^{151}Tb et ^{152}Tb. En effet, la connaissance des fonctions d'excitation (vérifiée dans plusieurs expériences précédentes) nous permet de conclure à une réaction (α, 4n) ou (α, 3n) ou à des filiations de terbium 151 et 152. Mais ^{151}Gd est très connu (classe A), sa période est 150 d, et ^{152}Gd est stable.

Avec des protons de 11 MeV sur ^{152}Gd (et les autres isotopes du gadolinium), nous ne pouvons faire que des réactions (p, n); donc, le fait de retrouver l'isotope 4 minutes dans cette deuxième réaction ne laisse aucune ambiguité concernant le nombre atomique de l'isotope 4 minutes.

2.5. DÉTERMINATION DU NOMBRE DE MASSE

Le nombre de masse de l'isotope ^{151}Tb (19h) paraît maintenant tout à fait établi 4, 5).

Il ne reste donc plus qu'une seule possibilité de situer l'isotope trouvé: masse 152. Cette détermination est encore confirmée par l'obtention de cet isotope dans la réaction (p, n) sur ^{152}Gd.

2.6. ÉTUDE DES RAYONNEMENTS ÉMIS

Rayonnement α

La décroissance obtenue sous un détecteur au SZn est présentée sur la fig. 1. L'angle solide du détecteur est environ $\frac{2}{3}\pi$.

Le rapport α/X_K a été établi en comparant deux sources, l'une mesurée en α, l'autre en X_K. Ce rapport est $\approx 2\times 10^{-5}$.

La mesure de l'énergie alpha n'a pas été possible jusqu'à présent dans notre chambre d'ionisation [3]). Cette mesure sera reprise par d'autres méthodes dans un travail ultérieur.

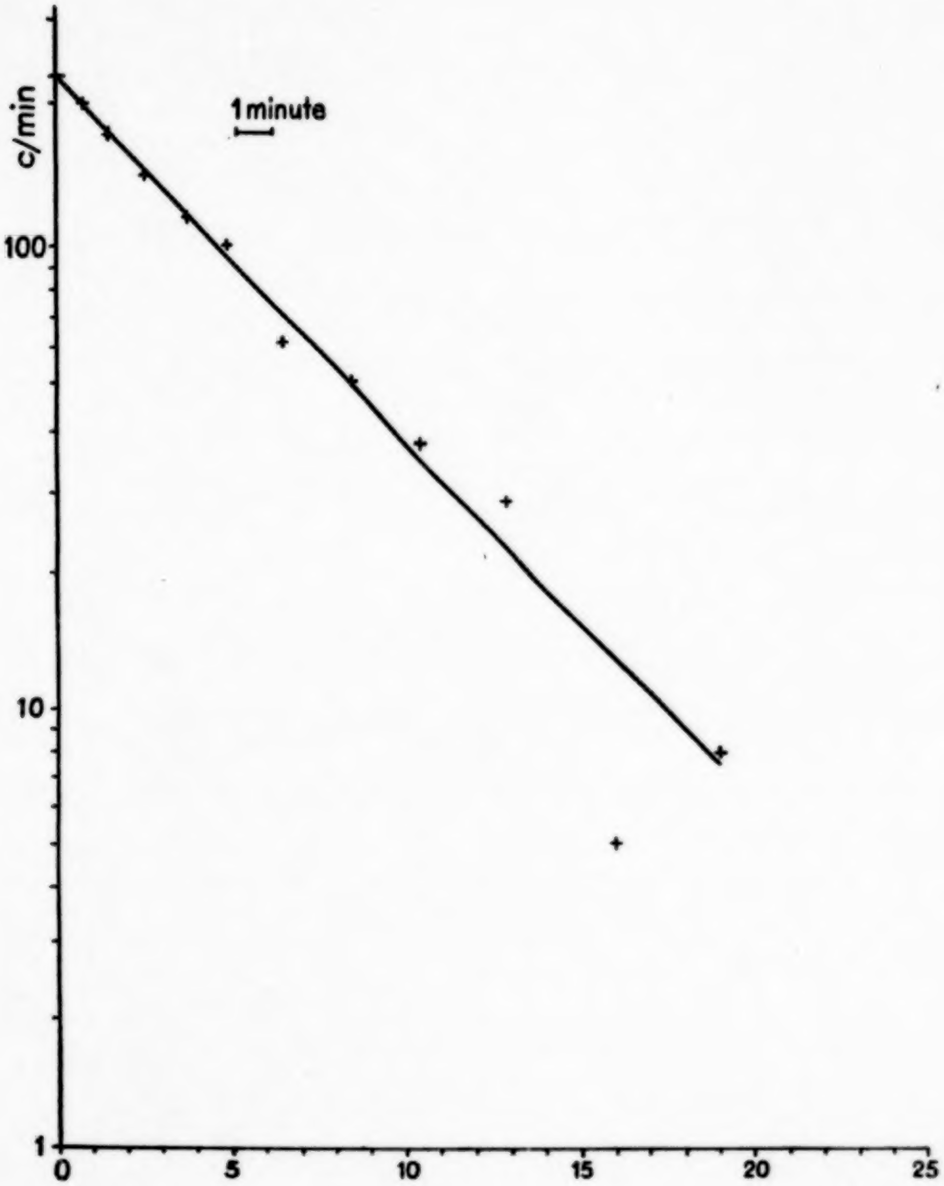

Fig. 1. Décroissance α du Tb^{152}.

Nous sommes cependant sûrs qu'il ne s'agit pas d'activité α due à l'irradiation d'impuretés contenues dans la cible.

En effet, les seuls émetteurs alpha de 4 minutes connus dans les éléments lourds sont $^{183-187}$Au et ^{197}Po et, avec les faisceaux utilisés ($\alpha_{44\ \mathrm{MeV}}$, $p_{11\ \mathrm{MeV}}$), il n'est pas possible de les former, compte tenu des isotopes stables existants.

Rayonnement β

La fig. 2 présente la décroissance des β et e sous le compteur Geiger, obtenue pour ^{151}Eu $+\alpha$. Dans la réaction ^{152}Gd+p, la proportion de ^{152}Tb est si faible qu'elle est masquée en β. On ne l'observe qu'en γ et X.

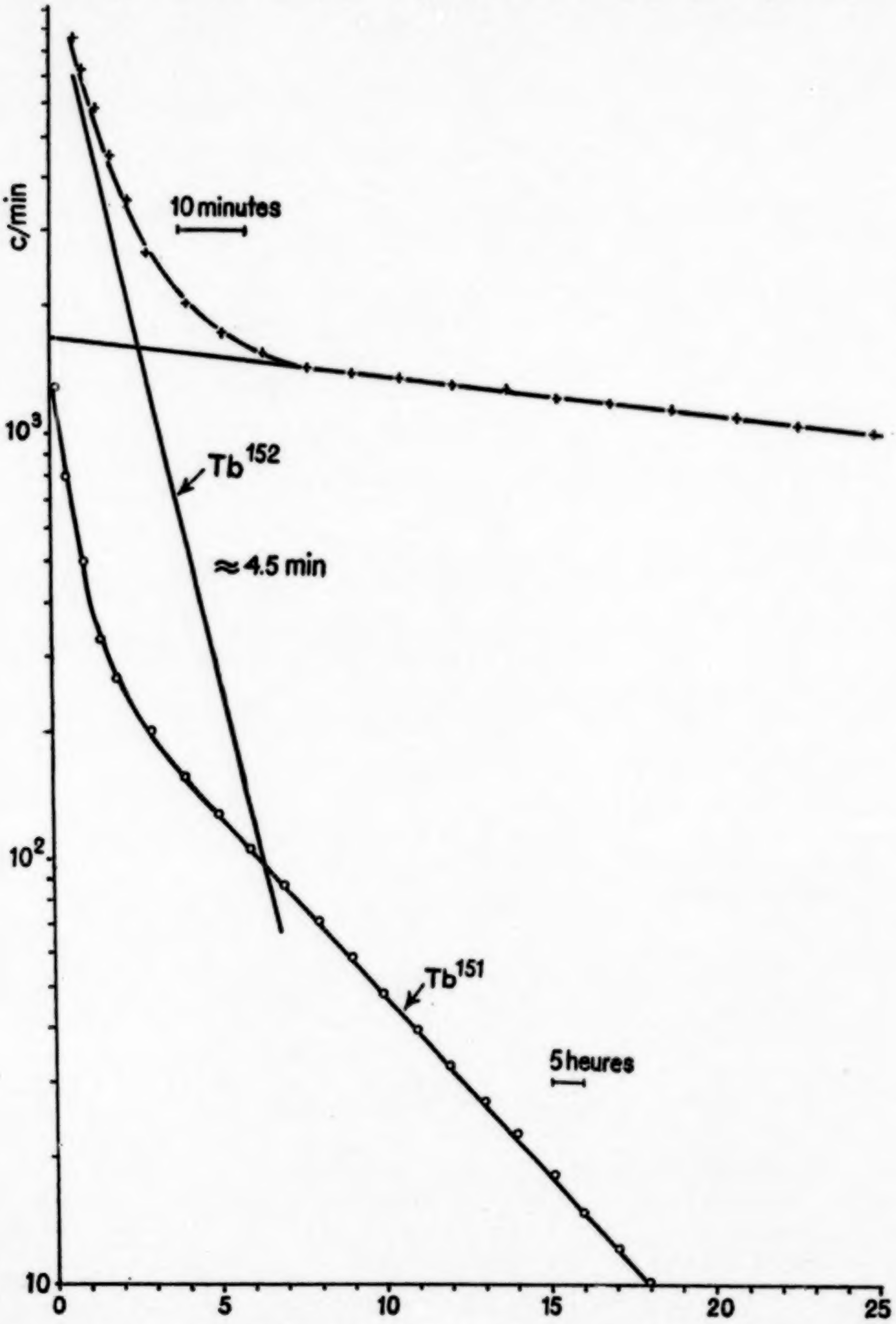

Fig. 2. Décroissance β de Eu^{151}+α(44 MeV).

Rayonnements γ et X

La fig. 3 présente les raies γ associées à la période 4 minutes. Ces raies se détachent bien du fond Compton des raies parasites.

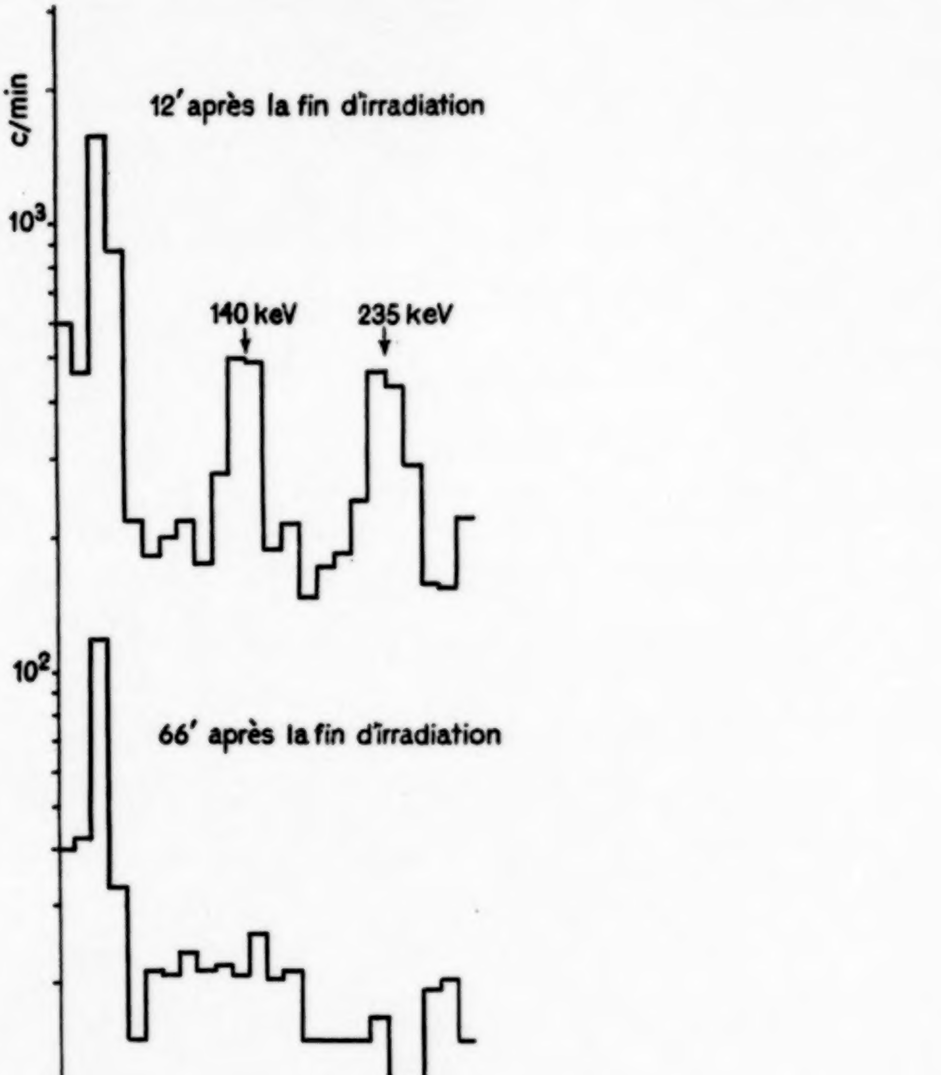

Fig. 3. $Eu^{151}+\alpha$(44 MeV).

Dans l'expérience de contrôle $^{152}Gd+p$, le terbium 152 se forme en petite quantité à cause de la composition isotopique de la cible. Nous présentons dans la fig. 4 la décroissance de la raie X_K obtenue dans cette expérience. La fig. 5 présente la raie X_K dans l'expérience $^{151}Eu+\alpha$.

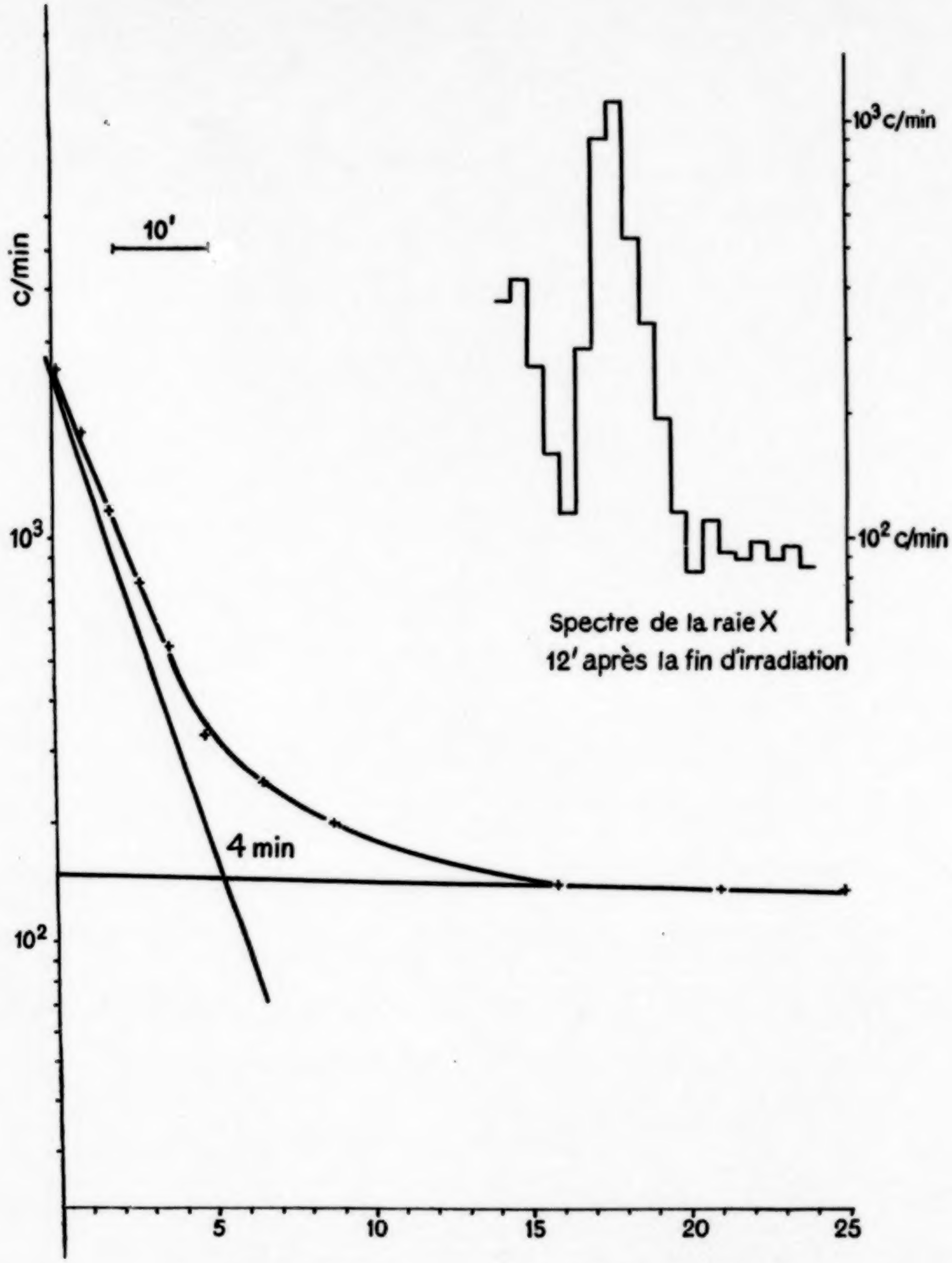

Fig. 4. Décroissance de la raie X de Gd^{152}+p(11 MeV).

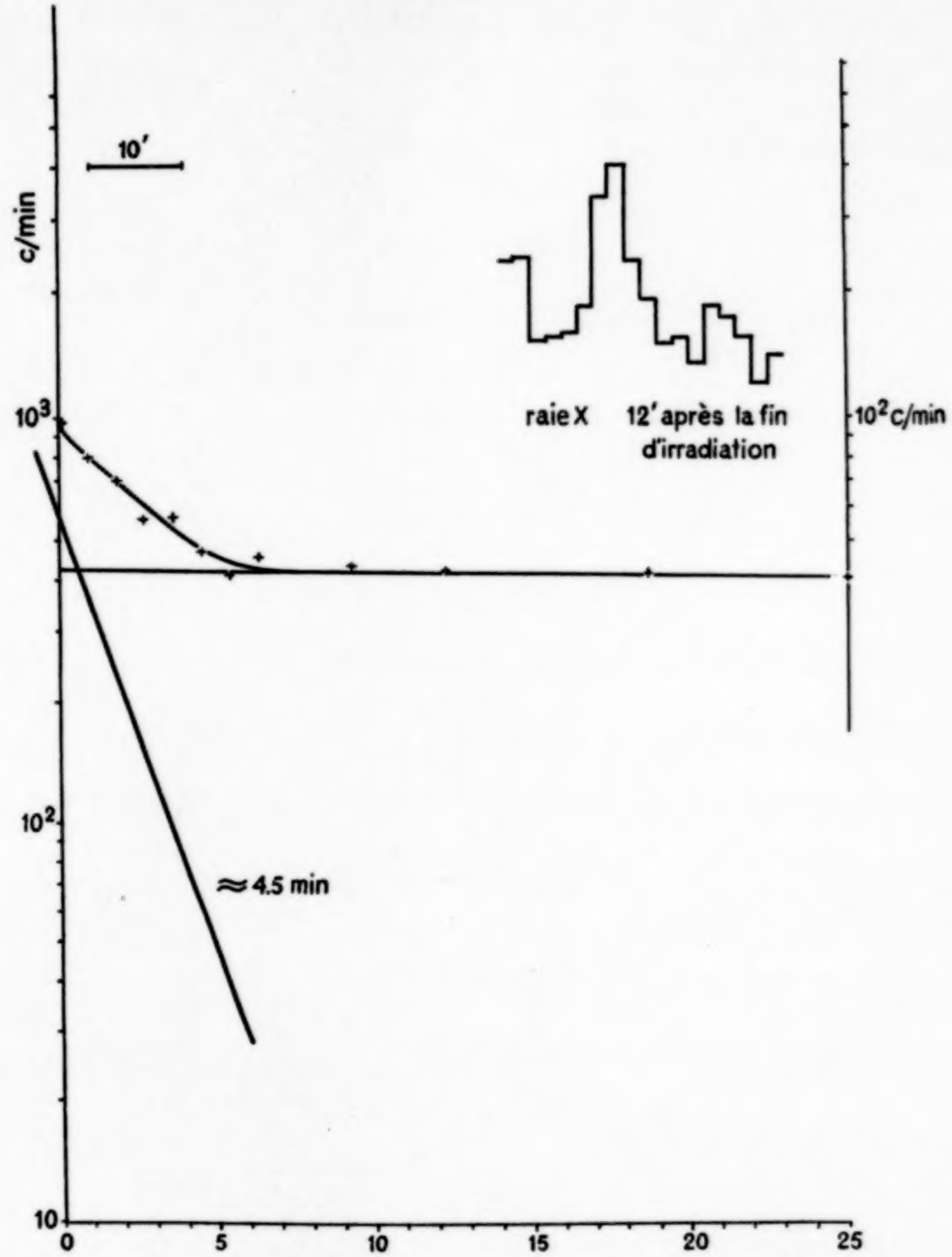

Fig. 5. Décroissance de la raie X de $Eu^{151}+\alpha$(44 MeV).

La proportion relative des raies (après correction d'efficacité de l'installation γ) est:

X_K	140 keV	235 keV	511 keV
100	25	30	15

Nous remercions l'équipe du Cyclotron de Saclay pour les nombreuses irradiations.

Bibliographie

1) J. Olkowsky, M. Le Pape, I. Gratot et L. Cohen, J. Phys. Radium (à paraître)
2) T. H. Handley et W. S. Lyon, Phys. Rev. **99** (1955) 1415
3) J. Olkowsky, G. Valladas et L. Cohen, J. Phys. Radium **17** (1956) 587
4) Baranovsky et Mourine, Izvestia Akad. Nauk SSSR **22** (1958) 7, 808
5) J. W. Mihelich, B. Harmatz et T. H. Handley, Phys. Rev. **108** (1957) 989

2.E

Nuclear Physics **12** (1958) 167—181; © *North-Holland Publishing Co., Amsterdam*

Not to be reproduced by photoprint or microfilm without written permission from the publisher

ENERGY DEPENDENCE OF THE (p, n) REACTION NEAR $A = 70$

G. A. JONES
A.E.R.E., *Harwell, Didcot, Berks.*

Received 1 February 1959

Abstract: Measurements on the energy dependence of the (p, n) reaction for elements near the size-resonance in the proton strength function have been made. It is shown that the (p, n) reaction is not always a good measure of the total reaction cross-section. The measurements made confirm that the size-resonance is for s-wave protons and that a radius $R = 1.45\, A^{\frac{1}{3}} \times 10^{-13}$ cm is suitable for computation of barrier penetrabilities; if a rounded potential well is used to represent the nuclear interaction, they limit the variation of parameters used in the description of the well.

1. Introduction

The complex potential model for nuclear reactions in the continuum region was employed by Fernbach, Serber and Taylor [1]) to describe nuclear scattering at very high energies. Feshbach, Porter and Weisskopf [2]) extended its use to the resonance region. They showed that, by making appropriate averages over many resonances, cross-sections are obtained which may be derived from a complex potential model.

Since the model considers only the incident channel it can be used to predict elastic scattering and total reaction cross-sections only. Feshbach, Porter and Weisskopf applied the model to the scattering and absorption of low energy neutrons and showed how it can be used to explain the systematic behaviour of the cross-section over a wide range of target nuclei. The model has been applied to proton scattering at comparatively large energies, e.g. 17 and 31 MeV by Melkanoff *et al.*[3]). At lower proton energies the elastic scattering is dominated by the Coulomb contribution, while the total reaction cross-section is difficult to measure if compound-elastic scattering is at all important. Under certain conditions, however, the (p, n) reaction gives a good measure of the total reaction cross-section, and Schiffer and Lee [4]) and Johnson, Galonsky and Ulrich [5]) have used this type of reaction to show that proton reaction cross-sections, when plotted against target mass number, exhibit systematic features similar to the gross features of neutron reactions. These features are somewhat obscured by the dominating effect of the Coulomb barrier upon the cross-section.

The experiments here described, upon the energy dependence of neutron yields in (p, n) reactions, have been carried out to determine whether the Coulomb effect has been correctly accounted for, whether the (p, n) reaction is in fact a good measure of the total reaction cross-section, and whether a systematic behaviour of the total cross-section with proton energy is discernible.

The average total reaction cross-section can be expressed in terms of the model wave-function in the entrance channel only — see Blatt and Weisskopf [6]) Chap. VIII. Alternatively, it can be expressed as an average over resonances; the contribution from the partial wave denoted by l is

$$\bar{\sigma}_l = 4\pi^2(2l+1)\frac{\lambdabar}{A_l^2}\cdot\langle\gamma_{Jl}^2/D_J\rangle_{\text{Av}}, \tag{1}$$

where the strength function $\langle\gamma_{Jl}^2/D_J\rangle_{\text{Av}}$ is the average ratio of reduced width to level spacing of levels of given J formed by partial wave l. Statistical assumptions have been made in deriving this expression, not the least important of which is that the strength function does not vary with J.

Equating the two expressions for the cross-section gives the strength function as

$$\langle\gamma_{Jl}^2/D_J\rangle_{\text{Av}} = \frac{R}{\pi}\,\frac{-\text{Im}(f_l)}{\{\text{Re}(f_l)-\Delta_l\}^2+\{\text{Im}(f_l)-s_l\}^2}, \tag{2}$$

where f_l is R times the logarithmic derivative at R, the nuclear radius, of the model wave function in the incident channel, having real and imaginary components $\text{Re}(f_l)$ and $\text{Im}(f_l)$ respectively, and Δ_l and s_l are the real and imaginary components of R times the logarithmic derivative at R of an outgoing wave only.

As defined, s_l is necessarily a positive quantity while $\text{Im}(f_l)$ must be negative to correspond to an ingoing wave plus an outgoing wave of smaller intensity. Δ_l and s_l can be expressed in terms of the regular and irregular solutions of the wave equation (F_l and G_l) in the external region thus:

$$\Delta_l = \frac{R}{2A_l}\frac{\mathrm{d}}{\mathrm{d}r}(A_l^2), \qquad s_l = \frac{kR}{A_l^2}, \qquad \text{where } A_l^2 = F_l^2+G_l^2.$$

Feshbach, Peaslee and Weisskopf [7]) approximated to strong absorption of neutrons by putting $\text{Re}(f_l) = 0$, $\text{Im}(f_l) = -iK_0R$ which, just inside the nuclear surface, makes the wave-function look like an ingoing undamped wave with wave-number K_0. This "black nucleus" strength function reduces roughly to $(\pi K_0)^{-1}$ and for conventional well-depths has the value † 2×10^{-14} cm. The complex potential model produces absorption by means of a complex wave-number, which we write as $K+i\alpha$. For large enough values of α, the neutron wave-function will look like an ingoing, exponentially-damped wave just inside the nuclear surface with $\mathrm{Re}(f_l) = \alpha R$ and $\mathrm{Im}(f_l) = -iK$. Strictly, these values should refer only to $l = 0$, but for strong absorption they should be suitable for other partial waves having $l \ll KR$ ($KR \approx 8$ for $A = 60$ and $V = 40-50$ MeV). Substituting into eq. (2) gives a strength function very little different from the black nucleus value when αR ranges between say 1 to 3. If the complex potential is $V+iW$, then $K \approx \hbar^{-1}\{2m(E+V)\}^{\frac{1}{2}}$ and $\alpha/K \approx \frac{1}{2}W/(E+V)$; thus, this range of αR in a nucleus of $A > 60$ corresponds to W/V of order $\frac{1}{4}$ to $\frac{3}{4}$. These considerations also apply in the region of strong absorption to proton reactions below the barrier as stated in the footnote.

---

† Terms in s_l and Δ_l have been neglected in the denominator of eq. (3) in deriving the above value; this approximation is good for slow neutrons and protons well below the barrier.

Proton scattering [1, 3]) and neutron scattering and absorption [2, 8]) indicate a value of W/V much less than the above range appropriate to a black nucleus, especially for incident particles of low energy [2]). The energy dependence of the complex potential is given by Lane and Wandel [9]). At low values of αR, $\mathrm{Re}(f_0) \approx KR \cot KR$, $\mathrm{Im}(f_0) \approx -KR\alpha R \operatorname{cosec}^2 KR$ (and similar expressions obtain for other l-values), and thus, resonances occur, even in the average cross-section, when the real part is equal to Δ_l.

Let $KR = (n+\frac{1}{2})\pi + x$. Since x is usually small near resonance, $f_0 \approx -KRx - iKR\alpha R$ and

$$\langle \gamma_{J0}^2 / D_J \rangle_{\mathrm{Av}} \approx \frac{1}{\pi K} \frac{\alpha R}{(x - x_{\mathrm{res}})^2 + (\alpha R + kRA_0{}^{-2})^2}, \tag{3}$$

where $x_{\mathrm{res}} = \Delta_0 / KR$. The resonance is therefore located by the condition $KR = (n+\frac{1}{2})\pi + x_{\mathrm{res}}$; the last term is known as the "resonance shift" and is dependent upon the l-wave † and the charge on the incident particle. The yield at resonance is roughly $(\alpha R)^{-1}$ times the black nucleus value and falls to half this maximum value when KR is off resonance by the amount αR, i.e. by a fractional change in KR of α/K or approximately $\frac{1}{2}W/(E+V)$.

For s-wave neutrons size-resonances are shown to occur [2]) at $A \approx 51$ and 160 corresponding to $n = 2$ and 3 in the expression for the phase KR. A square well at $R = 1.45\, A^{\frac{1}{3}} \times 10^{-13}$ cm requires the potential $V+iW$ to be $(45+2i)$MeV, while for a diffuse potential more recent analysis gives a somewhat larger imaginary component to offset the reduced reflection obtained by smoothing out the potential discontinuity [10]).

By measuring the (p, n) cross-section for a number of elements Schiffer and Lee [4]) and Johnson *et al.* [5]) have shown that the proton strength function also undergoes size-resonance. The s-wave resonance for $n = 2$ is clearly located near $A = 70$, the difference between neutron and proton locations being attributed to resonance shift and to the effect of the Coulomb potential on K — see for example Margolis and Weisskopf [11]). There are also indications of a possible d-wave size-resonance at $A \approx 55$ agreeing with the position estimated by Johnson *et al.* [5]). The position is obscured by the fact that the total yield from a (p, n) reaction gives a measure of the proton strength function averaged over all l-values with a weight factor $(2l+1)/A_l^2$. This can be seen by summing eq. (1) over all l-values.

---

† Equation (3) refers to *s*-wave resonance; again the general features will be much the same for $l \ll KR$, but KR will be modified by the centrifugal term in the potential and for charged particles a Coulomb term also arises [11]).

In the experiments here described the neutron yield has been measured over a large range of proton energy — from the neutron threshold to about 4.7 MeV, often a range of 3 MeV. Over this range the thick target yield increases by a factor of order 10^6, chiefly arising from the term $1/A_l^2$ and this variation provides an internal check on the choice of nuclear radius for calculating barrier penetrabilities. In addition the size-resonant term in the strength function has a slow dependence on energy; as previously stated, the resonance yield drops to half its value for a fractional change in KR of $\frac{1}{2}W/(E+V)$, i.e. about 2 % change, which can be achieved by 2 MeV change of proton energy provided that V is not dependent upon proton energy †. The shape of the size-resonance as given by Schiffer and Lee [4]) gives a factor of two for the ratio of strength function on resonance to off resonance (contributions from other l-values), and one could therefore expect for a favourable nucleus 30 % change in the strength function over the available energy range. To detect such a small change a high degree of confidence in the assessment of barrier penetrability is needed. This is discussed in more detail later.

2. Experimental Procedure

Protons from the Harwell electrostatic generator were analysed by a 90° bending magnet and passed through tantalum apertures to a target, which together with its tube formed a Faraday collector for measuring the beam. The target projected into the centre of a 4π-detector of neutrons which was essentially a conventional "long" counter used in an unconventional way. The defining aperture nearest the target was $\frac{1}{8}''$ in diameter and about 1 metre away from the latter; since the beam had previously traversed 5 metres from the bending magnet and had been brought to focus by an electrostatic quadrupole system, this rather remote aperture was sufficient to define the beam safely upon a target of diameter about $\frac{3}{8}''$. Between the aperture and target, tantalum liners ensured that scattered beam (or possibly, "penumbra" from the focusing system) could not impinge upon the brass tubing of the target assembly. Near the target a liquid air trap reduced the rate of deposition of relatively volatile impurities usually encountered in vacuum systems. With this arrangement measurements on tantalum and gold targets indicated that, in most of the results taken, background effects, which arise chiefly from the defining aperture, could be neglected.

---

† There is evidence that V is in fact velocity dependent, but so also is the "effective nucleon mass", leading to a cancellation of effects [12]).

The neutron detector consisted of a cylinder of paraffin wax of length 17" and diameter 15" with a concentric hole 3" dia. into which projected the target tube. Six 1" dia. enriched BF_3 counters symmetrically situated on a circle dia. 9" detected the degraded neutrons. Since the beam had been taken through a concrete wall 1 metre thick into a room with walls and ceiling of such thickness, no protecting layer of borated wax was needed.

The detector was calibrated with three neutron sources, described by Richmond [13]), a Th-γ-D_2O source of 200 keV neutrons, a Pu^{240} source of fission neutrons (of mean energy about $1\frac{1}{2}$ MeV — see for example Nereson[14]) for a typical spectrum of fission neutrons) and a Ra-α-Be source of neutrons of 3 MeV and upwards to about 12 MeV. In addition, the energy sensitivity of the detector was checked, up to a neutron energy of 1.5 MeV, by comparing the neutron count from the reaction $Fe^{57}(pn)Co^{57}$ with the activity of the target after irradiation. Co^{57} decays by K capture with a half-life of 270 days to a level in Fe^{57} at an excitation of 137 keV which then decays chiefly by γ-emission to ground [15]). This reaction, with its inconveniently long half-life, was chosen because the first excited state in the product nucleus Co^{57} is so high (1.38 MeV); a thin target at proton energies below the threshold for this level will therefore give effectively mono-energetic neutrons. Over the range $E_n = 200$ to 1500 keV it was found that the ratio of neutron count to activity was constant to within 10 %. Since, in general, the product nucleus will have a number of levels available in such an energy range, the efficiency of detection should not vary with maximum energy available to the neutrons to an accuracy of a few percent.

To obtain the absolute detection efficiency it was found more convenient to use the above neutron sources rather than to extend the above measurements by an absolute count of the activity. The γ-D source gave the efficiency as 2.80 %, the fission source 2.66 % and the α-Be source 1.92 %, confirming the previous conclusion that the efficiency depends little on energy up to $1\frac{1}{2}$ MeV but indicating a rapid fall-off at high neutron energy. This seems reasonable when it is realised that neutrons below 2–3 MeV are strongly degraded before reaching the counter ring, whereas above 5 MeV there is a strong probability that the first collision may not take place before reaching the counter ring, and escape is therefore more likely. When used conventionally, the long counter is not so dependent on energy [16]), since the radiation falls uniformly on one end; therefore less distinction is made between inside and outside of the counter ring.

The targets used were, where possible, thick discs of the spec-pure metal, the bombarding surface having been polished with carborundum paper, a procedure which, by tests on heavier metals, was shown to produce no spurious results from light elements adhering to the surface. The targets for Ga and Ge were semi-thick oxide targets, the former being sufficiently thick to ignore corrections but the latter, being isotopic materials, were somewhat thinner. The oxides were laid down on tantalum by moistening with water containing a little nitric acid, drying fairly slowly and then baking. The Ga_2O_3 targets were stronger and stood up to bombardment better than GeO_2 targets for which the results may be somewhat suspect.

3. Results

To determine the variation of the proton strength function with energy it is necessary effectively to differentiate the thick target excitation function,

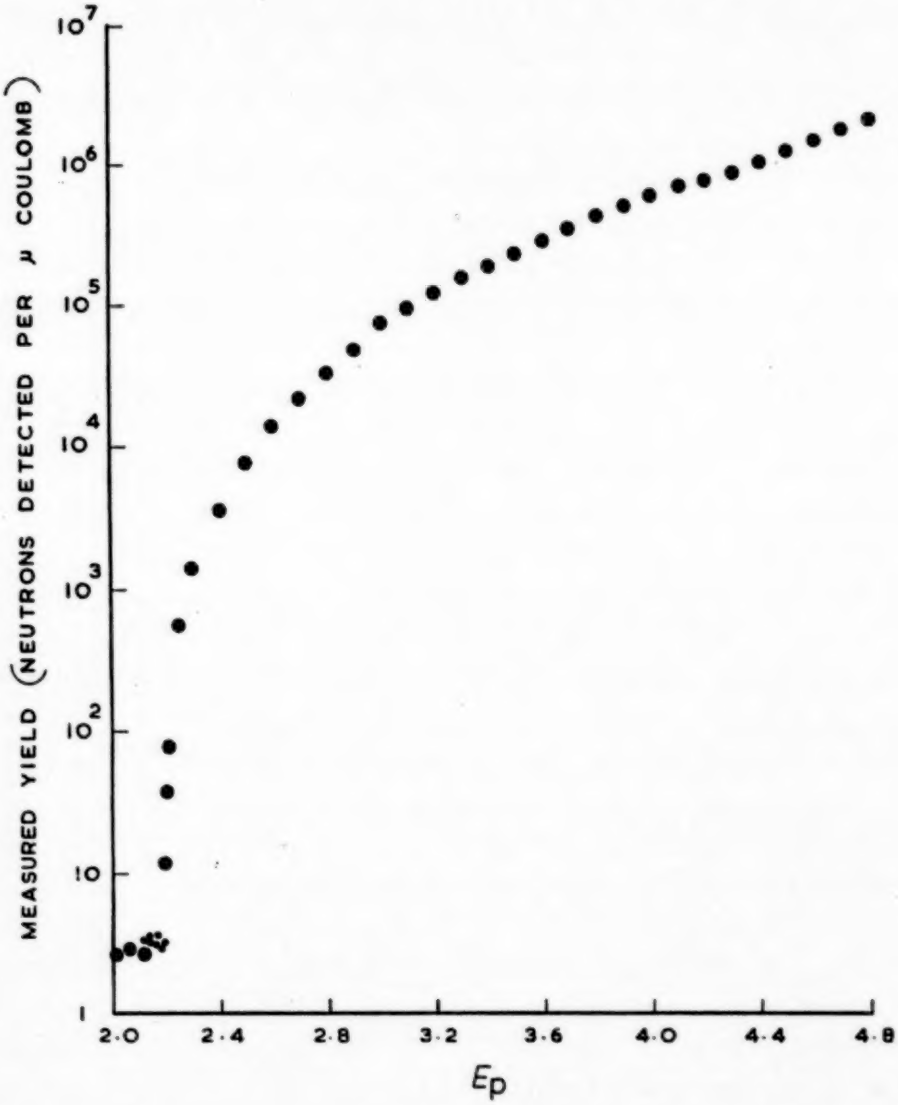

Fig. 1. Typical yield curve: measured yield of neutrons per μCb of beam of protons on thick copper target, against proton energy in MeV.

usually measured in 100 keV steps, or closer when just above thresholds. Since the variation with energy is great (a typical yield curve is given in fig. 1), it is more convenient to plot the yield on a logarithmic scale and to differentiate this latter curve, from which the required derivative is obtained using the identity $f'(E) = f(E)(\mathrm{d}/\mathrm{d}E) \log f(E)$. This separates out the derivative into two terms: $f(E)$ which may change by a factor 10^6 over the range of E_p available, and the logarithmic derivative which may change by merely a factor 10 over the same range. The differential of the logarithmic plot was made visually by drawing tangents to the curve.

A function $\bar{S}$ is defined by the equation

$$\bar{S} = f'(E_\mathrm{p}) \frac{\sigma_\mathrm{s}}{\varepsilon} \frac{1}{4\pi^2 \sum_l (2l+1) \dfrac{\lambda}{A_l^2}},$$

where ε is the efficiency of the detector, and σ_s is the stopping cross-section of the target for protons of energy E_p. When the yield from the (p, n) reaction is a good measure of the total reaction yield, the function $\bar{S}$ is a value of the proton strength function averaged over all the proton l-waves with weight factor $(2l+1)/A_l^2$. For the case in which the strength function is independent of l, $\bar{S}$ will be identical with it.

Since the method of extracting the derivative depends upon the observer's judgement, it is important to ensure that systematic errors are not introduced. A check was provided by reconstructing the thick target yield curve from the derivatives and comparing it with the original. Also, as a further check, the strength junction was deduced from the increase in yield over finite energy steps (usually of 300 keV) and comparing with a numerical integration of $(2l+1)\lambda/\sigma_\mathrm{s} A_l^2$ over the same energy range. Schiffer and Lee express their equations in terms of a finite thickness of target to emphasise the point that an average over a large number of levels in the compound nucleus is required; since our measured points are widely separated the above method of differentiating the thick target yield reproduces the same average and expresses it as an effective cross section at the particular energy.

The functions A_l^2 have been obtained chiefly from Breit *et al.*[17]) by dint of rather laborious interpolation. More recently, the Argonne National Laboratory have provided more closely tabulated functions [18]) and these tables have been very convenient to use. To present the data, and to compare with previous measurements a radius $R = 1.45\ A^{\frac{1}{3}} \times 10^{-13}$ cm has been used in deriving the averaged strength function $\bar{S}$.

The yield curves, expressed in arbitrary units proportional to $\bar{S}$ and to the isotopic abundances are given in fig. 2 in which thresholds for transitions to different states in the final nuclei are also shown. The shapes of these curves are discussed in more detail later. Adopted values of $\bar{S}$ for the elements

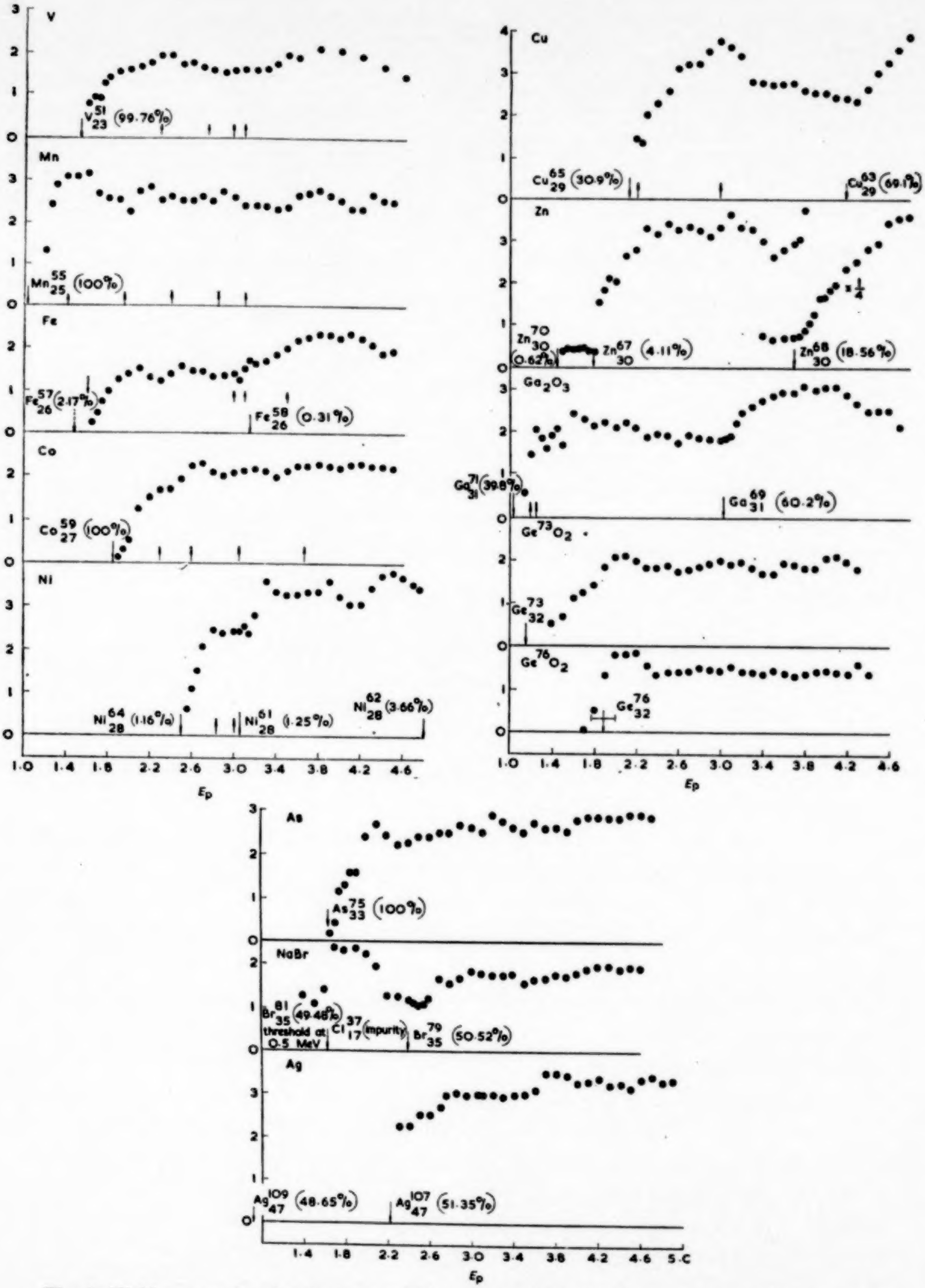

Fig. 2. Yield curves, for the elements stated, measured in arbitrary units proportional to the black nucleus strength function (i.e. barrier penetrability removed — see text) and to the atomic abundance of the isotope.

Downward pointing arrows denote thresholds to ground, upward pointing to excited states (where known) of the final nucleus. The atomic abundance of the target isotope is also given.

concerned are given in table 1; they depend, of course, upon the stopping cross-sections for protons in the various targets. These cross-sections have been obtained chiefly from Allison and Warshaw [19]) after interpolation in $Z^{\frac{1}{2}}$. The strength functions are plotted against A in fig. 3 which also includes the curve representing Schiffer and Lee's results.

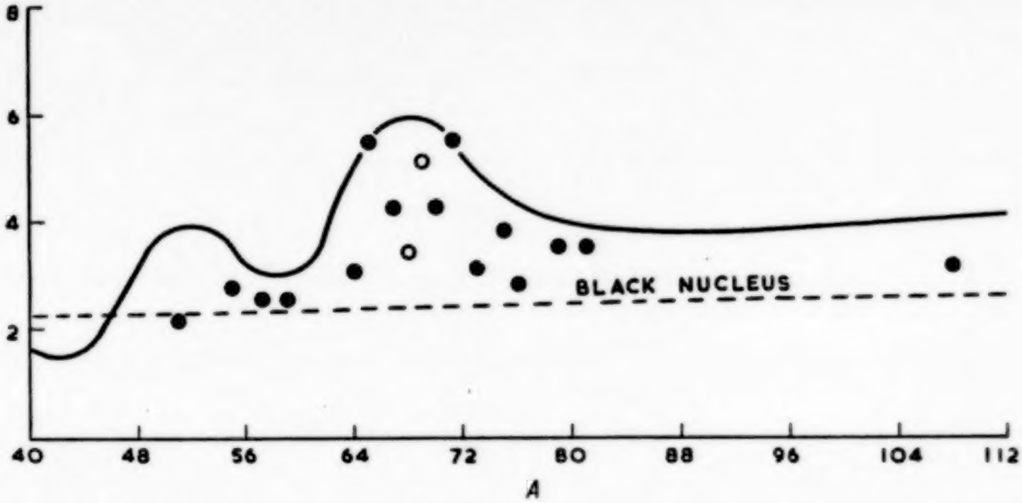

Fig. 3. Plot of $\bar{S}$ against atomic number. $\bar{S}$ is an averaged proton strength function — see text. The full line is reproduced from Schiffer and Lee [7]); the spread of their experimental points is much the same as of those measured here ($\approx \pm 20$ %). The two open points are cases in which the excitation functions indicate that neutron yields are obviously less than true reaction yields; this may also be the case for neighbouring nucleides.

TABLE 1

Averaged strength function $\bar{S}$ in units of 10^{-14} cm for the elements studied. Bracketed values are under-estimates — see text

Nucleide	V^{51}_{23}	Mn^{55}_{25}	Fe^{57}_{26}	Co^{59}_{27}	Ni^{61}_{28}	Ni^{64}_{28}	Cu^{65}_{29}	Zn^{67}_{30}	Zn^{68}_{30}	Zn^{70}_{30}
$\bar{S}$	2.15	2.75	2.5	2.5	(—)	3.05	5.4	4.2	(3.4)	4.2
Nucleide	Ga^{68}_{31}	Ga^{71}_{31}	Ge^{73}_{32}	Ge^{76}_{32}	As^{75}_{33}	Br^{79}_{35}	Br^{81}_{35}	$Ag^{107 \text{ and } 109}_{47}$		
$\bar{S}$	(5.1)	5.5	3.1	2.8	3.8	3.5	3.5	3.1		All $\pm 20\%$

4. Discussion

Roughly speaking, the excitation functions, expressed as $\bar{S}$ against E_p, are similar from element to element, consisting of a rapid rise above threshold, in which region competition between n- and γ-emission takes place, followed by a region over which $\bar{S}$ is roughly constant and in which it is expected that the neutron yield is a true measure of the reaction cross-section; at high energies S, for some targets, decreases sharply, and this is attributed to increasing importance of the elastic and inelastic scattering channels. In some of the elements more than one isotope may contribute to the yield and a superposition of such functions based on different thresholds is obtained. Measurements just above threshold have been made by Johnson *et al.* [5]), who analyse their results in terms of calculated ratios of Γ_γ/Γ_n based on level density estimates by Newton [20]) and Cameron [21]). Here we concern ourselves only with the region where $\Gamma_n \approx \Gamma_{tot}$.

The general constancy of these latter regions over all the elements studied indicates that the square well picture of the nucleus with a radius given by $R = 1.45\, A^{\frac{1}{3}} \times 10^{-13}$ cm provides an adequate scheme for calculating barrier penetrabilities. Looked at in more detail, however, the irregular fluctuations and regular trends are larger than the variations which one would accept as not significantly greater than experimental error. Manganese is a very good example in which $\bar{S}$ has no regular trend but has large fluctuations; that these fluctuations seem to be less for the heavier elements studied affords a natural explanation of them along the lines of Egelstaff's treatment [22]) of fluctuations in neutron cross sections [†].

Most of the regular trends can be explained in terms of competition. In the case of vanadium competition between neutron emission and proton emission (both elastic and inelastic) could lead to the diminished yield at $E_p = 3$ MeV, especially if the additional neutron channels opened up at 2.3 and 2.75 MeV lead to states of unfavourable spin (i.e. low ingoing l_p-values lead to high outgoing l_n-values — at $E_n = 500$ keV, $l_n = 2$ would be considered high). The subsequent rise would then be attributed to the incidence of more suitable neutron channels opening at $E_p = 3.0$ and 3.1 MeV; at higher energies $\bar{S}$ decreases when the proton-widths, even for inelastic channels, are not much reduced by the barrier. The other monoisotopic elements cobalt and arsenic have low thresholds, and $\bar{S}$ is therefore constant over a long range of E_p. There is no tendency for $\bar{S}$ to decrease at higher proton energies (nor indeed in the case of manganese) and this is partly because of the increased effect of the barrier and partly because more levels are available in the final nuclei. In the absence of definite information on the spins and parities of the final states it is not possible to discuss competition quantitatively.

At first sight iron appears to be typical of the elements with more than one contributing isotope. The rise above 3.2 MeV is, however, much too great to be attributed merely to the yield from Fe^{58}, which should bring about an increase of 15 %. We have here an extreme example of competition based on the facts that (1) there is a large spin difference between the initial and final nuclei, (2) the first excited state of the final nucleus is high (1.38 MeV) and (3) two other levels appear in the initial nucleus at 0.013 and 0.14 MeV with spins intermediate between that of the initial and final nucleus, ensuring that at least one favourable channel is available to the outgoing proton. Even at $E_p = 2.6$ MeV (corresponding to $E_n = 1$ MeV) where $A_0{}^2$ for the proton is about 50, a rough calculation based on the method of Hauser and Feshbach [23]) leads one to expect the neutron yield to be only about half the reaction cross section. Since the transmission coefficients for the neutron for the high l-values involved are changing as rapidly as the proton penetrabilities, the situation is not much changed at lower energies; at energies near to threshold competition by radiation will dominate. Above its threshold Fe^{58} begins to contribute and at about the same energy the excited states in Co^{57} influence competition in the Fe^{57} reaction in favour of neutron emission; this region has been taken for determining the strength function to plot in fig. 3. Finally, at high energies the overall scarcity of low-lying levels in Co^{57} is invoked to explain the decrease in $\bar{S}$.

[†] In the present case the effective sampling width is determined by the rapid fall in yield (dependent on barrier penetrability) as the proton loses energy inside the thick target; this effective target thickness is of the order of 200 keV at low E_p for the elements of interest, rapidly increasing with increasing E_p, to about 500 keV at $E_p = 4.5$ MeV, and such thicknesses will allow fluctuations of ± 10 to 15 % for the lighter elements used.

The measurements on Br (as NaBr) show the effect of a light element impurity (almost certainly Cl as NaCl). Just above the threshold for Cl^{37}_{17} the much greater barrier penetrability for the lighter element more than offsets the disparity in concentrations of impurity and target material; at high energies, the yield from the impurity rapidly becomes insignificant. The concentration of NaCl in the target is estimated to be less than 1 %. The presence of light element impurity in this case, while inconvenient since it prevents independent measurements on Br^{79}_{35} and Br^{81}_{35}, is reassuring in that it shows that the result in other cases is likely to be self-evident.

Concerning the elements with isotopes near the peak of the size resonance when plotted against A, it is apparent on examining the yield functions that proton re-emission is playing a large part in determining the neutron cross-section even at low energies; for example, the yield above the threshold of Zn^{68} rises very slowly as the s-wave neutron transmission factor increases ($\propto\sqrt{E}$) and again at an even lower threshold, namely that of Ga^{69}, the slow rise to a maximum much smaller than expected from the isotopic abundances is a clear indication that proton re-emission is having considerable influence down to at least $E_p = 3$ MeV. Even below $E_p = 3$ MeV, a clear trend is observed in Ga^{71}, Zn^{67} and Cu^{65}, but this is largely due to the method of presenting the data. As previously stated, the yield functions are divided by the sum of the barrier penetrabilities weighted by the factor $(2l+1)$; for a black nucleus this should give a result independent of E_p for the correct choice of nuclear radius. The weighted sum has an energy dependence very similar to that of a pure p-wave proton, while the true yield is not changing so rapidly indicating the the s-wave contribution is dominant. Off resonance, on either side, $\bar{S}$ is reasonably constant, indicating that conditions have changed rather rapidly and the s-wave contribution is no longer so important. In the resonance region, then, it is expected that the values given for the strength function which correspond to maximal measurements are all lower limits; for isotopes having high thresholds the true value may be very much higher than indicated and even for those with low threshold the error may be considerable.

The conclusions to be drawn from these results are:

(1) The (p, n) reaction does not always provide a reliable measure of the proton reaction cross section; because of this it has not been possible to determine the energy dependence of the size-resonance.

(2) Even qualitative considerations are sufficient to prove that the resonance occurs in the s-wave component of the proton beam.

(3) Our measured values seem, on the whole, to be lower than those of Schiffer and Lee and in addition the d-wave resonance seems less marked chiefly because the point for Fe^{57}, which defines the minimum between the two resonances on Schiffer and Lee's plot, has here been raised for the reasons given.

(4) The value of nuclear radius adopted for computing barrier penetrabilities, viz. $R = 1.45\ A^{\frac{1}{3}} \times 10^{-13}$ cm, leads to proton strength-functions not very dependent upon energy, and must therefore be a reasonable approximation to the effective nuclear radius.

It is of interest to enquire what set of parameters of a diffuse potential model can lead to an effective radius of this value — or at any rate can reproduce an effective strength function not very dependent upon energy. The problem of transmission of both neutrons and protons through a diffuse potential has been considered by Scott [24]) and Kikuchi [25]). Scott gives an analytical solution for s-wave neutrons and two types of diffuse potential, one of which corresponds to the form popularised by Saxon and Woods [26]). He shows that K can be replaced by an effective value $K_{\text{eff}} = [\tanh(\pi Ka)]/\pi a$, where a is the conventional diffuseness parameter; in the limit $a \to 0$, $K_{\text{eff}} \to K$, but for moderately large values of Ka, $K_{\text{eff}} \to (\pi a)^{-1}$. In dealing with protons Scott calculates the value of an effective radius such that the W.K.B. integral for the diffuse potential plus Coulomb term is equal to the integral for the Coulomb term only down to this effective radius; the effective radius is then used in conjunction with the Coulomb wave functions to obtain the value of A_l^2, thereby eliminating the errors inherent in the W.K.B approximation at least in the limit $a \to 0$. He solves the problem only for s-waves, giving in this case the solution $r_{\text{eff}} = r_{\text{em}} + 0.62a$, where r_{em} is the radius at which the proton "emerges" into positive kinetic energy; it is therefore a function of E_{p}. Neither he nor Kikuchi calculate the reflection at this inner boundary, but it cannot be very different from the case of low energy neutrons when the particle has penetrated well into the surface layer: indeed, if one assumes that $V_{\mathrm{Coul}} = \text{constant} = V_{\mathrm{C}}$ for $r < r_{\mathrm{em}}$, the problem is identical with that for a bound neutron in this region, the binding energy being $V_{\mathrm{C}} - E_{\mathrm{p}}$. One is tempted to assume that the effect of the diffuseness upon the reflection at the inner boundary is again to replace K by $K_{\mathrm{eff}} = (\pi a)^{-1}$ and this may be the basis of the universal $K = 1 \times 10^{13}$ commonly employed in computing transmission coefficients for all types of particles (cf. e.g. Blatt and Weisskopf [6]) pp. 355—357).

TABLE 2.

Effective radii (10^{-13} cm) and correction factors to be applied to s-wave penetrabilities for two schemes of diffuse potential. In addition, heights of the smoothed barriers (MeV) are given and, for comparison, radii and "sharp surface" barrier heights based upon $R = 1.45\,A^{\frac{1}{3}} \times 10^{-13}$ cm are given.

		Sharp potential		Scheme I $R = 1\frac{1}{3}A^{\frac{1}{3}}$, $a = 0.5$ $V = 50$			Scheme II $R = 1.2A^{\frac{1}{3}}$, $a = 0.5$ $V = 60$		
Nucleide	E_{p}	$1.45\,A^{\frac{1}{3}}$	E_{B}	$E_{\mathrm{B}}(\mathrm{I})$	$R_{\mathrm{eff}}(\mathrm{I})$	Correction factor (I)	$E_{\mathrm{B}}(\mathrm{II})$	$R_{\mathrm{eff}}(\mathrm{II})$	Correction factor (II)
Mn^{55}_{25}		5.51	6.7	4.15			4.4		
	1.99				6.62	2.3		6.18	1.7
	2.95				6.90	2.0		6.36	1.65
	3.92				6.15	1.9		6.70	1.6
As^{75}_{33}		6.115	7.7	5.5			5.95		
	2.225				7.05	2.4		6.54	1.3
	2.74				7.12	2.2		6.62	1.45
	3.49				7.24	2.1		6.75	1.50
	4.33				7.42	1.9		6.92	1.55
Ag^{108}_{47}		7.115	9.5	7.85			7.4		
	3.49				7.72	1.8		7.05	0.95

Energies in MeV, lengths in units of 10^{-13} cm.

In table 2, R_{eff}, E_{B} and the correction factors to be multiplied into s-wave transmission coefficients are given for different elements and for two schemes for the Saxon-Woods potential. The effective radius is smaller for p-wave than for s-wave, but the penetrability is a stronger function of radius for the higher l-wave, tending to produce the same correction factor. In fact a rough calculation of the correction factor for p-wave protons for one element (Ge^{73}) has confirmed this; therefore the correction factor may be applied directly to the weighted sum of the transmissions. This correction, as previously stated, is for the effect of the barrier only; if the estimated correction for reflection on the inner surface is included, the corrections should be increased by a further factor of order 2.

The conclusion to be drawn from table 2 is that the introduction of a diffuse potential has a much greater effect upon the absolute yield than on the energy dependence of the yield. (The overall increase of radius tends to make the penetrability less dependent upon energy, but the slight increase of radius with energy compensates for this). In addition scheme I shows little dependence upon A for the range of A under discussion; scheme II shows more change with A, but only at large A, and not enough to affect the qualitative conclusion that both these schemes can be incorporated into fig. 3 by merely a change of scale of ordinate; and to a lesser degree the same can be said for fig. 2. The changes of scale involved are, however, very large: for scheme I the scale factor is about $\frac{1}{2}$ (or $\frac{1}{4}$ with the added correction for reflection) and for scheme II about $\frac{2}{3}$ (or $\frac{1}{3}$ after correcting for reflection). The dotted line representing the black nucleus must of course be moved upward in inverse ratio to retain the same absolute value. For either scheme, therefore, most of the measured values will fall short of the black nucleus, but, as a compensating factor, the correction to be made for proton re-emission becomes larger. The fact that the measurements near the resonance even at low proton energies are strongly influenced by proton re-emission is evidence in favour of a rounding off of the barrier; on the other hand, to increase these few relative to the rest will result in a resonance too narrow to be acceptable, since one would not expect very much difference in the complex part of the potential for protons and neutrons for which the resonance widths are known [10]).

Of the two schemes considered, scheme I corresponds with the optimum values given by Melkanoff *et al.* [3]), while scheme II corresponds to a decrease in radius, using the information that the theoretical fit to the scattering experiments from which these values are derived depends roughly on VR^2. The same reduction in radius without the corresponding increase in V would probably lead to a more acceptable scaling factor, but it is not possible to be definite about this until the problem of transmission through a rounded barrier has been treated quantitatively. It is interesting to note that measurements involving charged particles below the barrier give information on V, R and a, which supplements scattering data at higher energies.

References

1) S. Fernbach, R. Serber and T. B. Taylor, Phys. Rev. **75** (1949) 1352
2) H. Feshbach, C. E. Porter and V. F. Weisskopf, Phys. Rev. **96** (1954) 448
3) M. A. Melkanoff, J. S. Nodvik, D. S. Saxon and R. D. Woods, Phys. Rev. **106** (1957) 793
4) J. P. Schiffer and L. L. Lee, Jr., Phys. Rev. **107** (1957) 640; **109** (1958) 2098
5) C. H. Johnson, A. Galonsky and J. P. Ulrich, Phys. Rev. **109** (1958) 1243

6) J. M. Blatt and V. F. Weisskopf, Theoretical Nuclear Physics (John Wiley, New York, 1952).
7) H. Feshbach, D. C. Peaslee and V. F. Weisskopf, Phys. Rev. **71** (1947) 145
8) M. Walt and J. R. Beyster, Phys. Rev. **98** (1955) 677
9) A. M. Lane and C. F. Wandel, Phys. Rev. **98** (1955) 1524
10) D. J. Hughes, Gatlinburg Conference, November 1956, ORNL 2309 (1957) 48
11) B. Margolis and V. F. Weisskopf, Phys. Rev. **107** (1957) 641
12) A. M. Lane, Private communication
13) R. Richmond, A.E.R.E. RP/M 79 (1956) and Prog. Nucl. Energy, Series 1, Phys. and Maths. Vol. 2 (1958) Ch. 4
14) N. Nereson, Phys. Rev. **88** (1952) 823
15) K. Way, R. W. King, C. L. McGinnis and R. van Lieshout, U.S.A.E.C. Report TID-5300 (1955)
16) W. D. Allen and A. T. G. Ferguson, Proc. Phys. Soc. A **70** (1957) 639
17) I. Bloch, M. M. Hull, Jr., A. A. Broyles, W. G. Bouricius, B. E. Freeman and G. Briet, Revs. Mod. Phys. **23** (1951) 147
18) J. P. Schiffer, Argonne National Laboratory Report ANL-5739 (1957)
19) S. K. Allison and S. D. Warshaw, Revs. Mod. Phys. **25** (1953) 779
20) T. D. Newton, Can. J. Phys. **34** (1956) 804
21) A. G. W. Cameron, Can. J. Phys. **35** (1957) 666
22) P. A. Egelstaff, Gatlinburg Conference, November 1956, ORNL 2309 (1957) 124
23) W. Hauser and H. Feshbach, Phys. Rev. **87** (1952) 366
24) J. M. C. Scott, Phil. Mag. **45** (1954) 441
25) K. Kikuchi, Prog. Theor. Phys. **17** (1957) 643
26) R. D. Woods and D. S. Saxon, Phys. Rev. **95** (1954) 577

9.A *Nuclear Physics* **12** (1959) 182—189; © *North-Holland Publishing Co., Amsterdam*

Not to be reproduced by photoprint or microfilm without written permission from the publisher

THE ALTITUDE DEPENDENCE OF ATMOSPHERIC COSMIC-RAY NEUTRONS AND THE SLOW NEUTRON DENSITY BELOW A WATER SURFACE

R. D. EDGE

Research School of Physical Sciences, Australian National University, Canberra

Received 29 December 1958

Abstract: The altitude dependence of atmospheric cosmic-ray neutrons over Canberra has been found to be exp $[-x/160]$ where x is the atmospheric depth in g/cm^2. The Szilard-Chalmers reaction in a sodium permanganate solution was employed as the neutron detector, and its advantages for the absolute measurement of the cosmic-ray neutron flux are discussed. A similar technique was used to determine the slow neutron flux just below a water surface.

1. Introduction

The results of absolute measurements of cosmic-ray neutron production rates in the atmosphere over the last twenty years are shown in fig. 1. After corrections have been made for the differences in altitude and latitude of the different experiments, discrepancies of a factor of 100 still remain between certain of these results. Most of these experiments were made using only two types of detector — namely, boron trifluoride-filled counters and boron-loaded nuclear emulsions. At least part of the discrepancy in results is due to the characteristics of the detectors and therefore it seemed profitable to develop a new and accurate method, employing the Szilard-Chalmers reaction, which had previously been used for only very approximate experiments [1]).

Another cause of error in the results for the neutron production rate lies in the assumptions made concerning the mode of production and the energy spectrum of the neutrons produced. Since no neutron detector is equally sensitive to neutrons of all energy ranges, any alteration made to the assumed cosmic-ray neutron spectrum will lead to a different answer for the production rate. The short half-life of the neutron (11.7 minutes) implies that the neutron component of cosmic rays must be produced in the vicinity of the earth — few neutrons could come from outside the earth's atmosphere.

Investigations with nuclear emulsions have shown that approximately 90 % of the particles entering the top of the earth's atmosphere are high-energy protons, the remainder being largely alpha particles, with a few heavier nuclei. These particles produce spallation reactions with air molecules, in which a number of high-energy protons and neutrons are produced, and some low-energy particles. The high-energy particles produce more spallation reactions, and the energy continues to degrade until it can no longer be lost by nuclear reactions or ionisation. This occurs at very low energies for protons, but for neutrons the lowest energy level through which a nuclear reaction may be induced is above 1 MeV. Below this level the neutron density becomes very large, since relatively little energy is lost at each collision, and it does not fall until the non-resonant N^{14}(n, p) reaction becomes effective, which takes place below 5 eV. The range between 5 MeV and thermal energies is of most importance in these experiments since the main body of neutrons lies here, and the spectrum must be found accurately

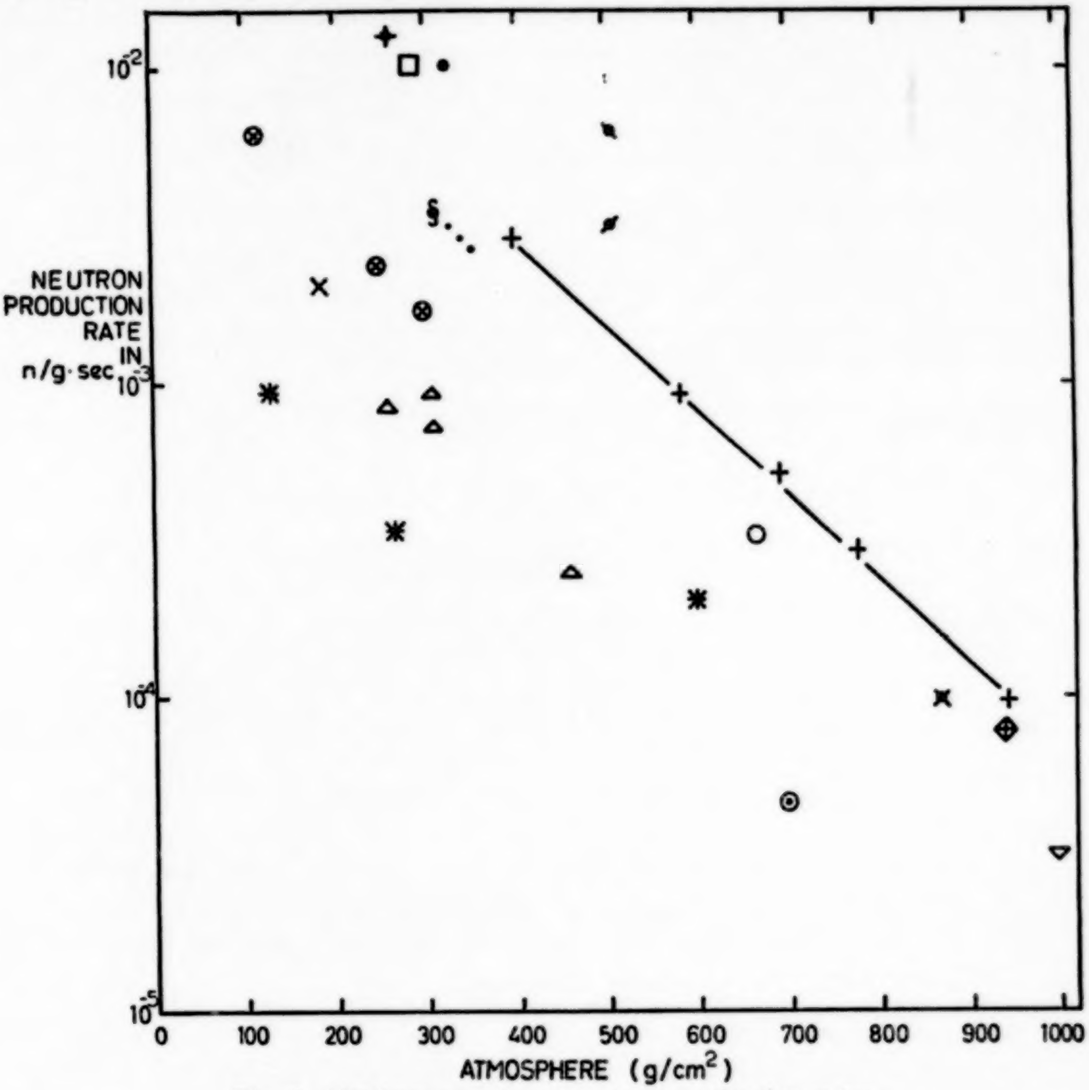

Fig. 1. Absolute cosmic-ray neutron production rates.

□ v. Halban [1]) ▲ Agnew [18]) ✱ Korff [19]) × Korff [20]) • Korff [3]) ⊗ Davis [21])
••• Yuan [22]) ✦ Yuan [14]) ○ Lattimore [23]) ⧸ Galli [22]), slow ⧹ Galli [22]), fast
✖ Montgomery [25]) ⊙ Swetnick [14]), for water § Simpson [12]) ▽ Tobey (for wax)
+ Edge ⊕ Edge (water experiment)

in this range. The slowing-down mechanism in air, and the N^{14} capture process, have been examined experimentally [2]). However, the spectrum of neutrons generated by spallation and other nuclear processes occurring in the air, and before the slowing-down process takes over, has not been adequately investigated experimentally. Bethe [3]) assumed that most cosmic-ray neutrons were produced at the lowest excitable level in N^{14} — then thought to be 4 MeV. On the Bohr model, the neutrons should presumably be evaporated from the nucleus with a Maxwell distribution corresponding to a nuclear temperature considerably less than 4 MeV [4]). For these experiments it has been assumed that the neutrons are generated with a temperature of 2 MeV, this being the best figure obtained from other sources since there are no direct experiments [5]). The neutrons are assumed to be moderated until they are captured by N^{14} through the (n, p) reaction, and this leads to the spectrum shown in fig. 2.

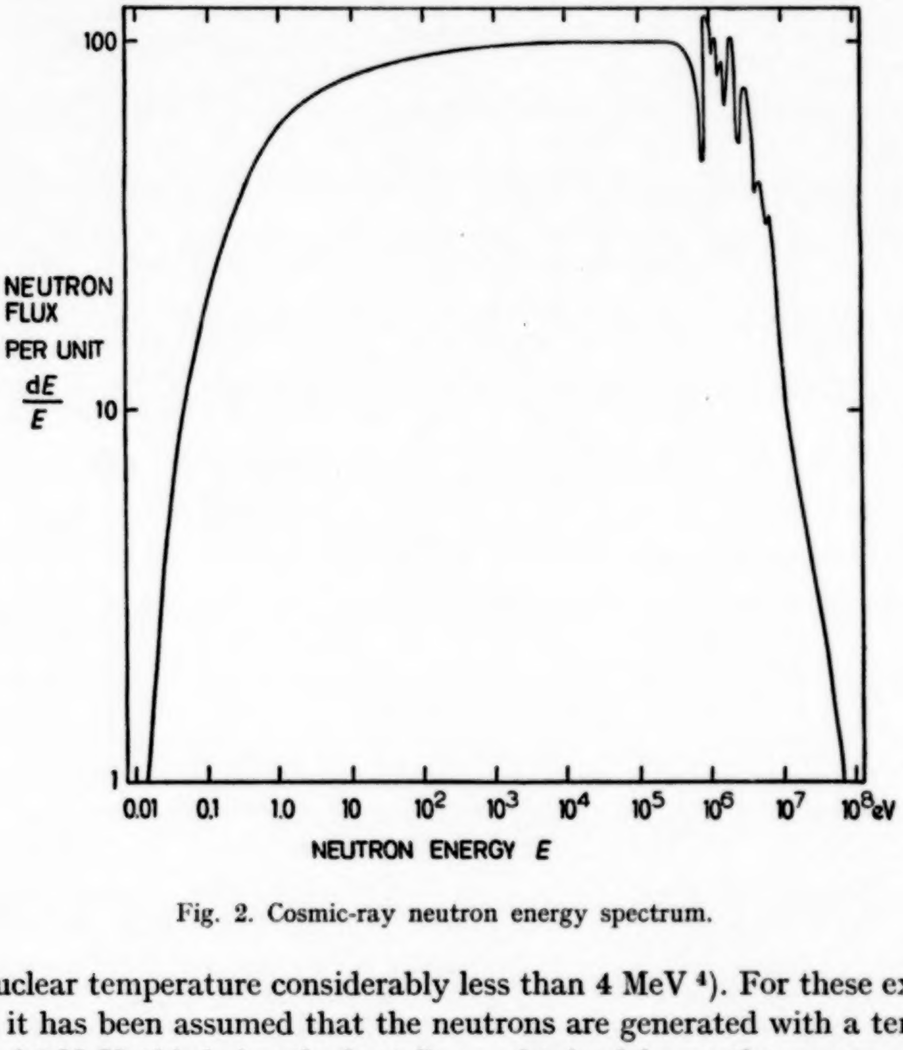

Fig. 2. Cosmic-ray neutron energy spectrum.

2. Method

When a neutron is captured by a manganese atom in the $Mn^{55}O_4^-$ complex, the recoil produced by the prompt gamma rays emitted by the Mn^{56} so formed disrupts the complex and the Mn^{56} is precipitated as $Mn^{56}O_2$. This can be filtered off, and its 2.6 h beta activity counted [6]). In order to obtain sufficient sensitivity, a concentrated aqueous solution of sodium permanganate of approximately 560 g/l was used. For the altitude determination, the solution was contained in a 3-gallon aluminium beer keg, which was pressurised to force the solution through a 7 cm filter paper, held by a perforated aluminium support, into a second keg. The kegs were contained in a light wooden box, surrounded by a layer of "lagging" which kept the temperature of the solution constant to within 2°C. The solution was filtered on the ground prior to take-off, loaded onto a DC3 aircraft, flown as quickly as possible to the required altitude and held there for a period of $2\frac{1}{2}$ hours. (The altitude was determined by a measurement of the atmospheric pressure.) After $2\frac{1}{2}$ hours the solution was filtered rapidly during descent and, on landing, the filter paper was washed, dried, placed between two cellophane sheets and the sandwich wrapped around a thin-walled glass Geiger counter which was then encased in a lead castle. It was found that a long-period background existed in addition to the 2.6 h activity [6]) and, in order to determine the background accurately, counts were recorded for up to ten hours after each flight. Runs were performed at a number of altitudes up to 28 000 ft, repeat runs being performed to check reproducibility.

A standard 5 mC Ra-Be mixed source was used to calibrate the detector. The source was placed a fixed distance from the tank of solution, and after a suitable irradiation time the solution was processed and the activity counted as above. In order to obtain the absolute cosmic-ray neutron flux from the Ra-Be calibration and the runs performed using cosmic rays, the calculations of Wallace and Le Caine [7]) were used to make allowance for the difference in sensitivity of the detector to these two neutron sources. The Ra-Be source was arranged so that minimum scattering occurred from the walls of the room. The detector was placed as far as possible from the wing fuel tanks when used in the aircraft, again to reduce scattering. An experiment was performed in which two cosmic-ray runs were made to 15 000 ft. In one run only, the detector was placed under a plate of aluminium 1" thick. The results of this experiment indicated that the effect of the aluminium shell of the aircraft in producing and scattering neutrons was less than 1 %. The results of Geiger [8]) and Ortel [9]) were used to correct for local production in the solution itself, which amounted to 17 % of the total counts. The flux of cosmic-ray neutrons through the atmosphere is subject to large fluctuations following a solar flare [10]). To ensure that such effects did not occur during our measurements, a monitor BF_3 counter was kept running at ground level.

3. Results

The altitude dependence of cosmic-ray neutrons was found to be proportional to $\exp[-x/(160\pm3)]$ where x is the atmospheric depth in g/cm^2. The error is due largely to non-reproducibility of the extraction process for the solution rather than statistical inaccuracies. The solution had to be kept clean, at constant temperature, and away from light and organic matter to obtain reproducible chemical extraction.

The absolute flux of neutrons at a depth of 940 g/cm^2 was found to be 2.6×10^{-2} n/cm$^2\cdot$sec. The number of neutrons produced in one gram of air per second at this depth was derived from this, assuming the neutrons were produced with the Maxwell distribution discussed earlier, and was found to be 9.2×10^{-5}.

4. Discussion of Results

Størmer[11]) has dicussed in detail the deflection of primary cosmic rays by the earth's magnetic field, which prevents the entry into the earth's atmosphere of lower energy primary cosmic rays at lower latitudes. The majority of cosmic-ray neutrons are produced by low-energy primaries and secondaries, and might be expected to show a similar latitude effect to these. Such an effect was investigated by Simpson [12]) who showed that the neutron flux remained constant from the poles to about latitude 50° and decreased to a minimum at the equator. Further, the change in energy spectrum of the incoming particles caused the exponent for the altitude dependence of neutron density to depend on latitude because the more energetic primaries at the equator travelled further through the atmosphere. Simpson found an absorption length for neutrons of 212 g/cm^2 at the magnetic equator, 181 g/cm^2 at 40°N geomagnetic, and 157 g/cm^2 at 53°N geomagnetic. None of these effects was found to be exactly symmetrical about the geomagnetic equator, as Størmer originally predicted, and in confirmation of this our result (together with other cosmic-ray results obtained in the vicinity [13])) would indicate a rather higher geomagnetic latitude at Canberra than the 44° found from magnetic measurements at ground level. As mentioned earlier, account must be taken of these effects in comparing results at different latitudes and altitudes. The discrepancy in absolute measurements was remarked in the same place. However, the most recent results of Yuan[14, 15]) and Simpson [12]) using BF_3 counters seem to be in reasonable agreement with this experiment, and better agreement should be obtained with improved knowledge of the generating function for neutrons in the atmosphere.

5. The slow Cosmic-Ray Neutron Flux below a Water Surface

The interaction of cosmic-ray neutrons with a water surface was first discussed by Bethe, Korff and Placzek [3]). They made approximate calculations of the slow neutron flux below a water surface of large area. Swetnick [16]) attempted to measure the slow neutron flux at shallow depths in Echo Lake, Colorado, using BF_3 counters. However, the B^{10} in the counters acted as a very strong neutron absorber, so that the measurement he made was not of the true flux but of the flux modified by the B^{10} counter. Although it might be expected that at large depths, where the neutron flux is changing slowly with depth, his relative measurements would be correct, the modifying influence of the B^{10} leads to inaccurate results for the flux close to the surface.

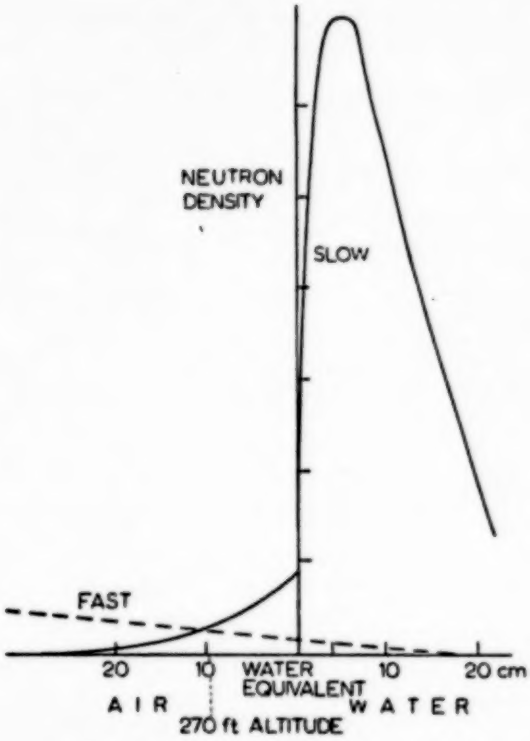

Fig. 3. Approximate neutron density near a water surface (Bethe *et al.* [3])).

5.1. METHOD

The Szilard-Chalmers reaction provides about the only convenient method of studying slow cosmic-ray neutrons in the vicinity of a water surface. By spreading a sufficiently dilute solution as a thin layer over a large area, one can make the detector very sensitive without its appreciably affecting the neutron moderating properties of water. In this experiment, a thin-walled aluminium box of area 2 500 cm² and depth 1 cm was used. This was filled with sodium permanganate solution and placed at various depths in a water tank, the activity being extracted from the solution and counted in a standard manner. Calibration runs with a Ra-Be source placed over the surface were also performed, and the results are shown in fig. 4.

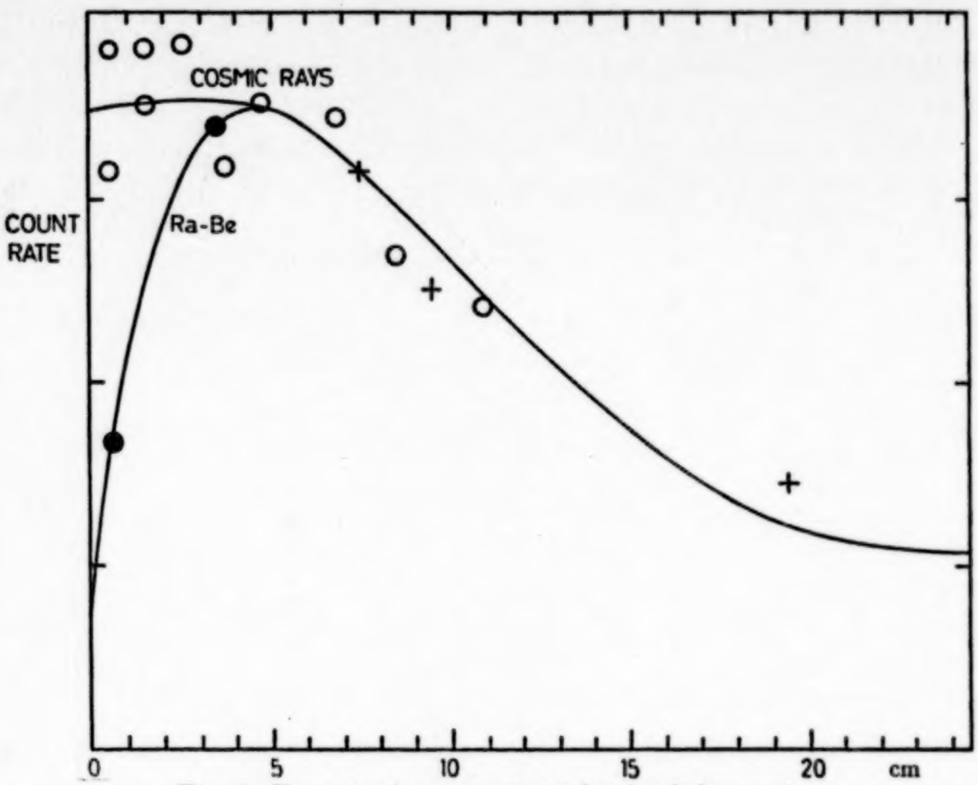

Fig. 4. Slow cosmic-ray neutron density below water.
○ Slow cosmic ray neutron density (Edge [6])) + Cosmic ray neutron density (Swetnick [16]))
● Ra-Be results

5.2. DISCUSSION OF RESULTS

The Ra-Be results may be fitted by a curve obtained assuming that there are no slow neutrons impinging on the water, whereas the cosmic-ray results indicate a large slow neutron flux at the interface. In comparing these results with the calculations of Bethe, allowance must be made for the fact that in the experiment only a small water tank (8 ft in diameter by 4 ft deep) was used, whereas the calculations apply to a surface of infinite area and depth. Bethe's curve was corrected for the local surroundings using known data on the composition of the earth and other matter, and cross-sections obtained from Hughes [2]). It will be seen that a fairly close fit to the results may be obtained. These results show a slight decrease as the water surface is approached, whereas the results of Swetnick show a continuous rise, confirming that his counters did not give a true reading of the slow neutron flux just under the surface.

5.3. FAST AND SLOW COSMIC-RAY NEUTRON FLUX IN AIR

The known slowing-down properties of neutrons in water [17]) were employed to discover that the slow neutron flux was approximately 0.27 of the fast flux of the cosmic-ray neutrons impinging on the water surface. Using the Ra-Be calibration, the neutron production rate in air calculated from these results was estimated to be approximately 7.7×10^{-5} n/g · sec at Canberra.

The author is indebted to Professor E. W. Titterton, who suggested the experiment and arranged with the Royal Australian Air Force for the aircraft which was used; and to Mr. M. Vernon for his assistance with the experiments.

References

1) H. v. Halban, L. Kowarski and M. Magat, C.R. **208** (1939) 572
2) D. J. Hughes *et al.*, A.E.C.U. 2040 (1952)
3) H. A. Bethe, S. A. Korff and G. Placzek, Phys. Rev. **57** (1940) 573
4) S. Flügge, Cosmic Radiation (Dover, 1946)
5) J. M. Blatt and V. F. Weisskopf, Theoretical Nuclear Physics (Wiley, 1952)
6) R. D. Edge, Aust. J. Phys. **34** (1957) 288
7) P. R. Wallace and J. Le Caine, N.R.C. no. 1480
8) J. S. Geiger, Can. Jour. Phys. **34** (1956) 288
9) W. C. G. Ortel, Phys. Rev. **93** (1954) 561
10) N. Adams, Phil. Mag. **41** (1951) 503
11) C. Størmer, The Polar Aurora (Oxf. Univ. Press, 1955)
12) J. A. Simpson, Phys. Rev. **83** (1951) 1175
13) Hopper, private communication
14) L. C. L. Yuan, Phys. Rev. **81** (1951) 175
15) H. J. Kouts and L. C. L. Yuan, Phys. Rev. **86** (1952) 128
16) M. Swetnick, Phys. Rev. **95** (1954) 793
17) R. E. Marshak, Revs. Mod. Phys. **19** (1947) 185
18) H. M. Agnew, W. C. Bright and D. Froman, Phys. Rev. **72** (1947) 203
19) S. A. Korff and A. Cobas, Phys. Rev. **73** (1948) 1010
20) S. A. Korff and B. Hamermesh, Phys. Rev. **69** (1946) 155
21) W. O. Davis, Phys. Rev. **80** (1950) 150
22) L. C. L. Yuan, Phys. Rev. **74** (1948) 804
23) S. Lattimore, Phil. Mag. **42** (1951) 334
24) M. Galli, Nuovo Cimento **10** (1953) 1187
25) C. G. Montgomery and A. R. Tobey, Phys. Rev. **76** (1949) 1478

8.C Nuclear Physics 12 (1959) 190—203; ©North-Holland Publishing Co., Amsterdam

Not to be reproduced by photoprint or microfilm without written permission from the publisher

AN EXAMPLE OF A FIELD THEORY WITH INDEFINITE METRIC IN HILBERT SPACE II

A. A. KOMAR
P. N. Lebedev Institute, Moscow
and
M. A. MARKOV
Joint Institute for Nuclear Research, Dubna

Received 29 December 1958

Abstract: A Lagrangian formalism is set up for the field equations proposed in ref. [1]). Energy-momentum tensors and current vectors are derived for boson and fermion fields and the corresponding conservation laws are considered. In space-time regions close to the light cone and hyperboloid the energy density of the boson field and charge density of the fermion field are not positive definite. The integrals of these quantities over the whole volume (energy and charge) are definite. The appearance of negative densities is interpreted in accord with the modification of the concept of a particle coordinate proposed in ref. [1]).

8. Boson Field

8.1. "QUASI-FREE" FIELD

Employing the technique presented in ref.[1]), one can rewrite in x coordinates eq. (48), i.e. the analogue of the d'Alembert equation ($\Box'\varphi = 0$), as follows (see appendix 2):

$$\frac{s^2}{s'^2}\Box\varphi + \frac{a^2(s^2+s'^2)}{s^4 s'^2}\left(x_\mu x_\nu \frac{\partial^2}{\partial x_\mu \partial x_\nu}\right)\varphi + \frac{a^2}{s^2}\left(\frac{3}{s'^2}-\frac{1}{s^2}\right)\left(x_\mu \frac{\partial}{\partial x_\mu}\right)\varphi = 0, \tag{52}$$
$$s^2 = -x_\mu^2, \quad s'^2 = s^2 - a^2.$$

As before, we shall denote the operator acting on function φ in (52) by $\Box'$. The corresponding "quasi-free" field equation for a meson with a characteristic mass m and zero spin can then be written briefly as

$$(\Box' - m^2)\varphi = 0. \tag{53}$$

Here the term "quasi-free" is understood to mean the following. In the usual theory the field source (scatterer) distorts the mode of propagation of the free field and its spectral composition (inelastic scattering) by means of specific charge (e, g, etc). We shall call this usual type of interaction "dynamic interaction". In the theory under consideration the source (scatterer, test body) is specified not only by its charge but also by a second constant, a characteristic length a. Owing to this new constant the field source distorts in a peculiar manner the mode of propagation of the free field. We shall call this peculiar effect of the source on propagation of the free field "metric interaction." It is assumed here that the constant a and charge constants (e, g, etc) are independent. In the usual sense, equation (52) pertains to a "free field" as it does not contain charge constants. However, equation (52) contains a second characteristic of the source ($a \neq 0$) and in this sense it describes a "quasi-free" field.

From the following it will be seen that metric interaction does not affect the energy state of the quasi-free field but does modify the propagation function.

Eq. (52) can be viewed as a type of approximate equation in which only a number of terms which account for the existence of the source are retained; thus, terms involving the constant a are retained, whereas terms containing the charge constant are neglected.

Eq. (53) can be obtained in the usual manner from the Lagrangian, which can be written in the form

$$\mathscr{L} = -\tfrac{1}{2}\left[\frac{\partial\varphi}{\partial x_\rho}\frac{\partial\varphi}{\partial x_\rho} + a^2\frac{s^2+s'^2}{s^6}\left(x_\mu\frac{\partial\varphi}{\partial x_\mu}\right)\left(x_\rho\frac{\partial\varphi}{\partial x_\rho}\right) + \frac{s'^2}{s^2}m^2\varphi^2\right]. \tag{54}$$

There is one circumstance which deserves special attention: although eq. (53) does follow from the Lagrangian (54) its left hand side turns out to be multiplied by the factor

$$f = \left(\frac{s'}{s}\right)^2. \tag{55}$$

To be more precise, Lagrangian (54) yields an Euler equation in the form

$$\left(\frac{s'}{s}\right)^2(\Box' - m^2)\varphi = 0. \tag{56}$$

The function $f = (s'/s)^2$ vanishes on the hyperboloid ($s'^2 = 0$) and has a pole on the cone ($s^2 = 0$).

Solutions of eq. (53) in these cases require special study.

It should be emphasized that no Lagrangian can be found which leads to eq. (56) without factor f.

The presence of the factor function f may not be important as far as the type of the solution of eq. (56) is concerned (excluding, possibly, points at which $s^2 = 0$, $s'^2 = 0$), but for the densities of physical quantities (energy, charge density) derived from the Lagrangian, the existence in the latter of multipliers responsible for the appearance of factor f may be quite important inasmuch as they structurally enter the expressions for the physical quantity densities. A consequence of this is that at points for which

$s^2 = 0$ singularities appear in the latter expressions which require a special treatment (see below).

In distinction to the usual theory the present one involves two invariants s'^2 and s^2. Thus, generally speaking, the dimensionless invariant $\Phi(s'^2/s^2)$ may enter various relations as in the case of eq. (56).

Since $\lim_{a\to 0} f = 1$, these possibilities are not encountered in the usual theory.

8.2. ENERGY-MOMENTUM TENSOR

Following the usual rule we can obtain the following energy-momentum tensor from Lagrangian (54):

$$T_{\mu\nu} = -\frac{\partial\varphi}{\partial x_\nu}\frac{\partial\mathscr{L}}{\partial\left(\dfrac{\partial\varphi}{\partial x_\mu}\right)} + \mathscr{L}\delta_{\mu\nu}, \tag{57}$$

or explicitly:

$$T_{\mu\nu} = \frac{\partial\varphi}{\partial x_\nu}\frac{\partial\varphi}{\partial x_\mu} + \frac{a^2(s^2+s'^2)}{s^6}\left(x_\rho\frac{\partial\varphi}{\partial x_\rho}\right)x_\mu\frac{\partial\varphi}{\partial x_\nu} + \mathscr{L}\delta_{\mu\nu}. \tag{58}$$

It is not difficult to obtain the Lagrangian and energy-momentum tensor for a complex field. In this case,

$$\mathscr{L} = -\left[\frac{\partial\varphi}{\partial x_\rho}\frac{\partial\varphi^*}{\partial x_\rho} + \frac{a^2(s^2+s'^2)}{s^6}\left(x_\mu\frac{\partial\varphi}{\partial x_\mu}\right)\left(x_\rho\frac{\partial\varphi^*}{\partial x_\rho}\right) + m^2\frac{s'^2}{s^2}\varphi\varphi^*\right], \tag{54'}$$

$$\begin{aligned} T_{\mu\nu} = {} & \frac{\partial\varphi}{\partial x_\nu}\frac{\partial\varphi^*}{\partial x_\mu} + \frac{\partial\varphi}{\partial x_\mu}\frac{\partial\varphi^*}{\partial x_\nu} + \frac{a^2(s^2+s'^2)}{s^6}\left[\left(x_\rho\frac{\partial\varphi}{\partial x_\rho}\right)x_\mu\frac{\partial\varphi^*}{\partial x_\nu}\right. \\ & \left. + \left(x_\rho\frac{\partial\varphi^*}{\partial x_\rho}\right)x_\mu\frac{\partial\varphi}{\partial x_\nu}\right] + \mathscr{L}\delta_{\mu\nu}. \end{aligned} \tag{58'}$$

Since the Lagrangian (54') for a quasi-free field depends explicitly on the space-time coordinates, the four-dimensional divergence of the energy-momentum tensor in general will not vanish[†]:

$$\frac{\partial T_{\mu\nu}}{\partial x_\mu} = \frac{\partial\mathscr{L}}{\partial(x_\nu)} \neq 0,$$

or

$$\begin{aligned} \frac{\partial T_{\mu\nu}}{\partial x_\mu} = -\Bigg\{ & \frac{2a^2}{s^6}\left(1+3\frac{s'^2}{s^2}\right)\left(x_\rho\frac{\partial\varphi}{\partial x_\rho}\right)\left(x_\mu\frac{\partial\varphi^*}{\partial x_\mu}\right)x_\nu \\ & + \frac{a^2(s^2+s'^2)}{s^6}\left[\frac{\partial\varphi}{\partial x_\nu}\left(x_\mu\frac{\partial\varphi^*}{\partial x_\mu}\right) + \frac{\partial\varphi^*}{\partial x_\nu}\left(x_\rho\frac{\partial\varphi}{\partial x_\rho}\right)\right] - \frac{2a^2x_\nu}{s^4}m^2\varphi\varphi^*\Bigg\}. \end{aligned} \tag{59}$$

Nevertheless, the conservation laws in integral form remain valid and this permits one to introduce the concept of conservative momentum and energy quantities. Indeed, consider a concrete solution of eq. (53) in the form of a quasi-plane wave (see (50)):

[†] $\partial\mathscr{L}/(\partial(x_\nu)$ denotes differentiation with respect to the explicit dependence of $\mathscr{L}$ on x_ν.

$$\varphi = B\mathrm{e}^{i(k,x)\frac{s'}{s}}. \tag{60}$$

Here B is a normalization constant $B = 1/(2k_0V)^{-\frac{1}{2}}$. For $a \to 0$ this solution goes over into the usual solution for a free field. Inserting this solution in (59) we obtain

$$\frac{\partial T_{\mu\nu}}{\partial x_\mu} = -2a^2B^2\left[\frac{x_\nu(k,x)^2}{s^8}(3s^2+s'^2)+\frac{s^2+s'^2}{s^6}(k,x)k_\nu-\frac{x_\nu m^2}{s^4}\right]. \tag{61}$$

Integrating over complete space we get (see appendix 3)

$$\int\frac{\partial T_{\mu\nu}}{\partial x_\mu}\,\mathrm{dv} = 0. \tag{62}$$

It should be noted that in integrating over the volume in (62) the poles in the integrand which lie on the light cone were circumvented in accord with a certain rule (see appendix 3). In the future this rule will be used whenever singularities of the pole type are encountered during integration.

Expressions for total momentum and energy can be written on the basis of eq. (62) in the usual manner:

$$P_i = \frac{1}{i}\int T_{4i}\mathrm{dv}, \tag{63}$$

$$E = -\int T_{44}\mathrm{dv}. \tag{64}$$

Thus, with some justification $(1/i)T_{4i}$ and $-T_{44}$ can be viewed respectively as momentum and energy densities in the given theory.

For a charged field the energy density has the following form:

$$\begin{aligned}-T_{44} = \Bigg\{&\sum_{i=1}^{3}\frac{\partial\varphi}{\partial x_i}\frac{\partial\varphi^*}{\partial x_i}+\frac{\partial\varphi}{\partial x_0}\frac{\partial\varphi^*}{\partial x_0}+\frac{a^2(s^2+s'^2)}{s^6}\left[\sum_{i=1}^{3}\left(x_i\frac{\partial\varphi}{\partial x_i}\right)\left(x_i\frac{\partial\varphi^*}{\partial x_i}\right)\right.\\ &\left.-\left(x_0\frac{\partial\varphi}{\partial x_0}\right)\left(x_0\frac{\partial\varphi^*}{\partial x_0}\right)\right]+\frac{s'^2}{s^2}m^2\varphi\varphi^*\Bigg\}.\end{aligned} \tag{65}$$

Expression (65) is not positive definite. A more detailed investigation shows that in the present theory the nature of this indefiniteness is quite peculiar. It is found that the energy density in the theory can assume negative values only in regions lying approximately between the light cone and hyperboloid characteristic of the given theory.

This region is due to the presence of the boson field source. For $a \to 0$

(free field) the energy-momentum tensor is positive definite. To prove the above statements, let us insert function (60) in (65); this yields an expression for $-T_{44}$ in the form

$$-T_{44} = B^2 \left\{ 2k_0^2 \frac{s'^2}{s^2} - \frac{2a^4}{s^8} \left[(\bar{k}\bar{x})^2 x_0^2 + k_0^2 x_0^2 r^2 - (\bar{k}\bar{x}) k_0 x_0 (x_0^2 + r^2) \right] \right\}. \quad (66)$$

For $s^2 \approx a^2$ the expression for $-T_{44}$ is obviously negative. On the other hand, in space-time regions for which $s^2 \gg a^2$ expression (63) goes over to the usual positive definite expression for the energy density of a free field

$$-T_{44} = B^2 2k_0^2. \quad (67)$$

An analysis of expression (66) yields more detailed information regarding the size of the indefiniteness region and the behaviour of the energy density. At a given point ($\mathbf{r}$) of space the energy density is a function of time and with increase of time tends to the classical expression (67) since at a given point $\mathbf{r}$ the interval $s^2 = x_0^2 - r^2$ increases with time. In other words the specific perturbation of the free field energy density due to the source decreases with time.

However, the most significant point here is that the integral of the energy density over the whole space (total energy) is positive definite and is identical to the corresponding classical expression (see appendix 4)

$$E = -\int T_{44} \mathrm{dv} = k_0. \quad (68)$$

In a similar manner (see appendix IV) one gets

$$P_i = \frac{1}{i} \int T_{4i} \mathrm{dv} = k_i. \quad (69)$$

Thus, in the given theory just as in the usual one, k_0 and $\mathbf{k}$ have the meaning of total energy and momentum. It should be noted that upon integration over the volume the time dependence of the energy and momentum drops out, which is just what should be expected according to (62).

Tensor (58′) is not symmetric ($T_{\mu\nu} \neq T_{\nu\mu}$). One might thus suspect that angular momentum is not conserved in the proposed theory. However, this is not the case. Consider as usual, the quantity

$$M_{\mu\nu\rho} = T_{\mu\nu} x_\rho - T_{\mu\rho} x_\nu \quad (70)$$

which is related to the angular momentum:

$$\frac{\partial M_{\mu\nu\rho}}{\partial x_\mu} = \frac{\partial T_{\mu\nu}}{\partial x_\mu} x_\rho - \frac{\partial T_{\mu\rho}}{\partial x_\mu} x_\nu + T_{\rho\nu} - T_{\nu\rho}. \quad (71)$$

According to (58′) and (59)

$$\frac{\partial M_{\mu\nu\rho}}{\partial x_\mu} = \frac{a^2(s^2+s'^2)}{s^6}\Big[-\Big(x_\mu \frac{\partial \varphi^*}{\partial x_\mu}\Big) x_\rho \frac{\partial \varphi}{\partial x_\nu} - \Big(x_\rho \frac{\partial \varphi}{\partial x_\mu}\Big) x_\rho \frac{\partial \varphi^*}{\partial x_\nu} - \Big(x_\rho \frac{\partial \varphi}{\partial x_\mu}\Big) x_\rho \frac{\partial \varphi^*}{\partial x_\nu}$$
$$+ \Big(x_\mu \frac{\partial \varphi^*}{\partial x_\mu}\Big) x_\nu \frac{\partial \varphi}{\partial x_\rho} + \Big(x_\mu \frac{\partial \varphi}{\partial x_\mu}\Big) x_\mu \frac{\partial \varphi^*}{\partial x_\rho} + \Big(x_\mu \frac{\partial \varphi}{\partial x_\mu}\Big) x_\rho \frac{\partial \varphi}{\partial x_\nu}$$
$$+ \Big(x_\mu \frac{\partial \varphi^*}{\partial x_\mu}\Big) x_\rho \frac{\partial \varphi}{\partial x_\nu} - \Big(x_\mu \frac{\partial \varphi}{\partial x_\mu}\Big) x_\nu \frac{\partial \varphi^*}{\partial x_\rho} - \Big(x_\mu \frac{\partial \varphi^*}{\partial x_\mu}\Big) x_\nu \frac{\partial \varphi}{\partial x_\rho}\Big] = 0.$$

Thus the law of conservation of angular momentum holds even in the differential form. The components of the total angular momentum are

$$M_l = \frac{1}{i}\int M_{4ik}\mathrm{dv} = \frac{1}{i}\int (T_{4i}x_k - T_{4k}x_i)\mathrm{dv} \qquad (72)$$
$$(i, k, l \text{ cyclic permutations}).$$

It should be of interest to compare the field theory investigated in the present paper with the non-local fields with an indefinite metric previously studied by Pais and Uhlenbeck [2]). We have in view here equations of the type

$$\prod_{i=1}^{N} (\Box - m_i^2)\varphi = \rho. \qquad (73)$$

In the case of eq. (73) the free field energy is a superposition of the energies of N fields possessing characteristic mass constants m_i and signs:

$$E = \sum_{i=1}^{N} k_i^0(-1)^{i-1}. \qquad (74)$$

Besides the fact that free boson states with negative energy contradict the experiments, transitions to negative energy states should be energetically favoured when the interaction is included.

These difficulties do not exist in the present theory. The reason is that the field obeys a very different equation (52), (53), which contains a single mass constant. Of course the solution of this equation can formally be expanded into solutions of the d'Alembert equation with a continuous mass spectrum (see for example (41)) but each of these solutions separately does not satisfy the equation (53) and thus cannot be ascribed to a real quantum of the free field.

As stated above, the boson field energy remains positive in the given theory, that is, the appearance of negative energy densities in a limited space-time region does not change the positive value of the integral of the energy density over complete space.

An inhomogeneity of the space-time continuum of this type appears only in the presence of the source (scatterer) of the given field.

8.3. CURRENT VECTOR

From the invariance of the Lagrangian (54′) under transformations of the type

$$\varphi \to \varphi e^{i\alpha}, \qquad \varphi^* \to \varphi^* e^{-i\alpha},$$

we find, according to the general rule, the expression for the four-dimensional current density vector; in our case it is

$$j_\nu = ie\left\{\frac{\partial\varphi^*}{\partial x_\nu}\varphi - \frac{\partial\varphi}{\partial x_\nu}\varphi^* + \frac{a^2(s^2+s'^2)}{s^6}x_\nu\left[\varphi\left(x_\mu\frac{\partial\varphi^*}{\partial x_\mu}\right) - \left(x_\rho\frac{\partial\varphi}{\partial x_\rho}\right)\varphi^*\right]\right\}. \tag{75}$$

It can be verified directly that the four-dimensional vector (75) satisfies the equation

$$\frac{\partial j_\nu}{\partial x_\nu} = 0. \tag{76}$$

The following expression is obtained for the charge density:

$$j_0 = -ie\left\{\frac{\partial\varphi^*}{\partial x_0}\varphi - \frac{\partial\varphi}{\partial x_0}\varphi^* - \frac{a^2(s^2+s'^2)}{s^6}x_0\left[\varphi\left(x_\mu\frac{\partial\varphi^*}{\partial x_\mu}\right) - \left(x_\rho\frac{\partial\varphi}{\partial x_\rho}\right)\varphi^*\right]\right\}. \tag{77}$$

In accord with (76), $\int j_0 \mathrm{dv}$ turns out to be constant and equal to e. Indeed, substitution of quasi-plane waves reduces the expression under consideration to

$$\begin{aligned}\int j_0 \mathrm{dv} &= 2B^2 e\int\frac{s'}{s}\left[k_0 + \frac{(k, x)a^2 x_0}{s^4}\right]\mathrm{dv}\\ &= 8\pi k_0 e\lim_{R\to\infty}\left(B^2\int_0^R\frac{s'}{s}\left(1 - \frac{a^2 x_0^2}{s^4}\right)r^2\,\mathrm{d}r\right).\end{aligned} \tag{78}$$

The corresponding integral is computed in appendix 5, the result $\int j_0 \mathrm{dv} = e$ being obtained.

9. Fermion Field

9.1. FIELD EQUATION AND ENERGY-MOMENTUM

The Lagrangian for a fermion field can be written down in the form

$$\begin{aligned}\mathscr{L} = -\tfrac{1}{2}\Bigg\{&\frac{s'}{s}\left[\bar\psi\gamma_\mu\frac{\partial\psi}{\partial x_\mu} - \frac{\partial\bar\psi}{\partial x_\mu}\gamma_\mu\psi\right] + 2\left(\frac{s'}{s}\right)^2 m\bar\psi\psi\\ &+ \frac{a^2 s'}{s^5}\left[\bar\psi(\gamma_\nu x_\nu)\left(x_\mu\frac{\partial\psi}{\partial x_\mu}\right) - \left(\frac{\partial\bar\psi}{\partial x_\mu}x_\mu\right)(\gamma_\nu x_\nu)\psi\right]\Bigg\}.\end{aligned} \tag{79}$$

The equation of motion which this Lagrangian yields has the form of (49) multiplied by the same factor $f = (s'/s)^2$:

$$\frac{s'}{s}\left[\gamma_\mu\frac{\partial\psi}{\partial x_\mu} + \frac{a^2}{s^4}(\gamma_\nu x_\nu)\left(x_\mu\frac{\partial\psi}{\partial x_\mu}\right)\right] + \frac{s'^2}{s^2}m\psi = 0. \tag{80}$$

Its solution is an analogue of a plane wave

$$\psi = B' u(p) e^{i(p,x)\frac{s'}{s}} \tag{81}$$

where $u(p)$ is a spinor which obeys the usual equation

$$(i\gamma p + m) u(p) = 0; \tag{82}$$

B' is a normalization constant $B' = V^{-\frac{1}{2}}$. The expression for the energy-momentum tensor assumes the form

$$T_{\mu\nu} = \frac{1}{2}\frac{s'}{s}\left[\bar{\psi}\gamma_\mu \frac{\partial\psi}{\partial x_\nu} - \frac{\partial\bar{\psi}}{\partial x_\nu}\gamma_\mu\psi + \frac{a^2}{s^4}x_\mu\left(\bar{\psi}(\gamma_\rho x_\rho)\frac{\partial\psi}{\partial x_\nu} - \frac{\partial\bar{\psi}}{\partial x_\nu}(\gamma_\rho x_\rho)\psi\right)\right]. \tag{83}$$

As in the case of a boson field,

$$\frac{\partial T_{\mu\nu}}{\partial x_\mu} = \frac{\partial \mathscr{L}}{\partial (x_\nu)} \neq 0,$$

but

$$\int \frac{\partial T_{\mu\nu}}{\partial x_\mu} \mathrm{dv} = 0,$$

and the conservative quantities, momentum and energy, can be determined.

We shall not investigate in detail the tensor (83) since an analysis of the expression for the fermion current vector seems to be of greater interest from the viewpoint of bringing out the characteristic features of the theory under consideration.

9.2. CURRENT DENSITY

In our theory the four-dimensional current vector assumes the form

$$j_\nu = ie\frac{s'}{s}\bar{\psi}\left(\gamma_\nu + \frac{a^2(\gamma_\rho x_\rho)}{s^4}x_\nu\right)\psi. \tag{84}$$

It can also be verified that the vector (84) satisfies the condition

$$\frac{\partial j_\nu}{\partial x_\nu} = 0. \tag{85}$$

The analogue of the charge density can be written as

$$j_0 = e\frac{s'}{s}\bar{\psi}\left(\gamma_4 + \frac{ia^2(\gamma_\rho x_\rho)}{s^4}x_0\right)\psi. \tag{86}$$

It should be noted that in regions lying between the light cone and hyperboloid, specified by the inequality $r^2 + a^2 > x_0^2 > r^2$, the factor

$$\frac{s'}{s} = \left(\frac{r^2 + a^2 - x_0^2}{r^2 - x_0^2}\right)^{\frac{1}{2}}$$

is purely imaginary and the charge density is in general complex.

In connection with the origin of the constant a in the present theory [1]) one might propose the following interpretation of complex values of the charge density. The complex charge density is a consequence of the circumstance that a region, which in a certain sense is "non-physical", exists between the light cone and hyperboloid, or in other words, there is a "time gap" in the interaction. The electron wave disappears (is "absorbed") at the instant $t = -a/c$ and appears again at $t = +a/c$. At times τ for which $-a/c < \tau < +a/c$, it is impossible to detect experimentally an electron which is incident on the source † with which it interacts. Therefore, neither the charge density nor the probability related to it can assume real values at the instants mentioned above. For space-time regions close to the hyperboloid, the charge density is negative. This can readily be seen if one takes

$$x_0{}^2 = r^2+a^2+\varepsilon, \qquad \varepsilon \to 0.$$

Then

$$j_0 = e\left(\frac{\varepsilon}{a^2+\varepsilon}\right)^{\frac{1}{2}} \bar{\psi}\left[\gamma_4\left(1-\frac{a^2(r^2+a^2+\varepsilon)}{(a^2+\varepsilon)^2}\right)+\frac{ia^2(\bar{\gamma}\bar{x})}{(a^2+\varepsilon)^2}(r^2+a^2+\varepsilon)^{\frac{1}{2}}\right]\psi,$$

$$1-\frac{a^2(r^2+a^2+\varepsilon)}{(a^2+\varepsilon)^2} = \frac{a^2(\varepsilon-r^2)}{(a^2+\varepsilon)^2} < 0,$$

and $\bar{\psi}\gamma_4\psi = \psi^*\psi > 0$ (at any rate, for solutions of the form (81)). The first term in the expression for j_0 is thus negative, and since the second term can have any sign, the whole expression may be negative in the indicated region. For $s^2 \gg a^2$, the charge density j_0 assumes the usual form $j_0 = e\psi^*\psi$. In other words, in the present theory the charge possesses a complex structure.

The peculiar situation encountered here is a consequence of the new interpretation of the concept of a particle coordinate proposed in ref.[1]), and also of the averaging over "internal" particle coordinates, a phenomenological expression of which is the occurrence of the new constant a in the theory.

Upon integration of the charge density over the whole space the time drops out and the charge density integral is normalized to unity (see appendix 5). It is interesting to note that the problem of computing of $\int j_0 \mathrm{dv}$ (at any rate when solutions of the type (81) are employed) reduces, after integration over the angles, to computation of the same integral as in the case of a boson field (see (78)). Indeed,

$$\begin{aligned}\int j_0 \mathrm{dv} &= eB'^2\int\frac{s'}{s}\bar{u}(p)\left(\gamma_4+\frac{ia^2(\gamma_\rho x_\rho)}{s^4}x_0\right)u(p)\mathrm{dv} \\ &= 4\pi e\lim_{R\to\infty}\left(B'^2\int_0^R\frac{s'}{s}\left(1-\frac{a^2x_0{}^2}{s^4}\right)r^2\right)\mathrm{dv};\end{aligned} \tag{87}$$

$\bar{u}(p)\gamma_4 u(p) = u^*(p)u(p) = 1$ in virtue of the normalization of the spinors.

---

† The term "source" should be understood in the sense of the right hand part of eq. (80) which appears as a result of the interaction.

The expression for the charge density (86) automatically yields the weight function employed to normalize function (81). It may be more advantageous to relate expression (86), not to the probability density but to the charge density or, in general, to the particle and antiparticle density. Thus, at the given state of analysis of the problem, there are at least no difficulties connected with the meaning of negative probabilities.

The validity of this viewpoint can be extended somewhat if the fermion field is treated as the fundamental field and boson fields as derivatives of fermion fields.³)

In following papers an attempt will be made to analyse the interaction problem, secondary quantization and also the general properties of the S matrix apparatus of the present theory.

The authors are thankful to Yu. Ysachov for helpful discussions.

Appendix 2

We shall write down the equation $\Box'\varphi = 0$ in the usual x coordinates. Recalling that

$$x_\mu = x'_\mu \frac{s'}{s} = x'_\mu \sqrt{1+\frac{a^2}{s'^2}}, \quad s'^2 = -x'^2_\mu,$$

we get

$$\frac{\partial}{\partial x'_\nu} = \frac{\partial x_\mu}{\partial x'_\nu}\frac{\partial}{\partial x_\mu} = \left(\delta_{\mu\nu}\sqrt{1+\frac{a^2}{s'^2}} + \frac{\frac{a^2}{s'^4}x'_\mu x'_\nu}{\sqrt{1+\frac{a^2}{s'^2}}}\right)\frac{\partial}{\partial x_\mu},$$

$$\Box' = \frac{\partial^2}{\partial x'^2_\nu} = \left[\frac{6\frac{a^4}{s'^4}x'_\mu}{\sqrt{1+\frac{a^2}{s'^2}}} + \frac{4\frac{a^2}{s'^6}x'_\mu x'^2_\nu}{\sqrt{1+\frac{a^2}{s'^2}}} - \frac{\frac{a^4}{s'^8}x'_\mu x'^2_\nu}{\left(\sqrt{1+\frac{a^2}{s'^2}}\right)^3}\right]\frac{\partial}{\partial x_\mu}$$

$$+\left(\delta_{\mu\nu}\sqrt{1+\frac{a^2}{s'^2}} + \frac{\frac{a^2}{s'^4}x'_\mu x'_\nu}{\sqrt{1+\frac{a^2}{s'^2}}}\right)\left(\delta_{\mu\nu}\sqrt{1+\frac{a^2}{s'^2}} + \frac{\frac{a^2}{s'^4}x'_\rho x'_\nu}{\sqrt{1+\frac{a^2}{s'^2}}}\right)\frac{\partial^2}{\partial x_\rho\,\partial x_\mu}$$

$$= \left(\frac{2a^2}{s^2 s'^2} + \frac{a^4}{s'^2 s^4}\right)\left(x_\mu\frac{\partial}{\partial x_\mu}\right) + \left[\delta_{\mu\rho}\frac{s^2}{s'^2} + \frac{a^2(s^2+s'^2)}{s'^2 s^4}x_\rho x_\mu\right]\frac{\partial^2}{\partial x_\rho\,\partial x_\mu}$$

$$= \frac{s^2}{s'^2}\Box + \frac{a^2(s^2+s'^2)}{s'^2 s^4}\left(x_\rho x_\mu\frac{\partial^2}{\partial x_\rho\,\partial x_\mu}\right) + \frac{a^2}{s^2}\left(\frac{3}{s'^2} - \frac{1}{s^2}\right)\left(x_\mu\frac{\partial}{\partial x_\mu}\right).$$

Thus $\Box'\varphi = 0$ assumes the form given in the paper (eq. (52)).

Appendix 3

In calculating $\int(\partial T_{\mu\nu}/\partial x_\mu)\mathrm{dv}$ we shall consider separately the cases $\nu = 1, 2, 3$ and $\nu = 4$. In the first case (see (61))

$$\int\frac{\partial T_{\mu i}}{\partial x_\mu}\mathrm{dv} = -2a^2B^2\int\left(\frac{x_i(k,x)^2}{s^8}(3s^2+s'^2)+\frac{s^2+s'^2}{s^6}(k,x)k_i-\frac{x_i m^2}{s^4}\right)\mathrm{dv},$$

which after integration over the angles yields

$$8\pi a^2\lim_{R\to\infty}(x_0k_0k_iB^2\int_0^R\left[\frac{2r^2(3s^2+s'^2)}{3s^8}+\frac{s^2+s'^2}{s^6}\right]r^2\mathrm{d}r. \qquad \text{(A1)}$$

In the second case we obtain similarly

$$\int\frac{\partial T_{\mu 4}}{\partial x_\mu}\mathrm{dv}=-8\pi a^2 i\lim_{R\to 0}\left(B^2x_0\int_0^\infty\left[\frac{k^2r^2+3k_0{}^2x_0{}^2}{3s^8}(3s^2+s'^2)\right.\right.$$
$$\left.\left.-\frac{m^4}{s^4}-\frac{k_0{}^2(s^2+s'^2)}{s^6}\right]r^2\mathrm{d}r\right). \qquad \text{(A2)}$$

The integrands in expressions (A1) and (A2) have singularities on the light cone ($r = x_0$) of the multiple pole type. It is suggested that such integrals be evaluated by passing the poles from above or below (Feynman or anti-Feynman procedure). In this manner the integrals assume finite values whose signs depend upon the way the integrals are evaluated. Indeed, consider an integral of the form

$$\int_0^R\frac{1}{s^{2n}}\mathrm{d}r = \tfrac{1}{2}\int_{-R}^R\frac{1}{(x_0{}^2-r^2)^n}\mathrm{d}r.$$

We shall pass the poles of the integrand in the manner indicated in fig. 1, a) and b). Closing the integration path in the upper semi-plane and taking

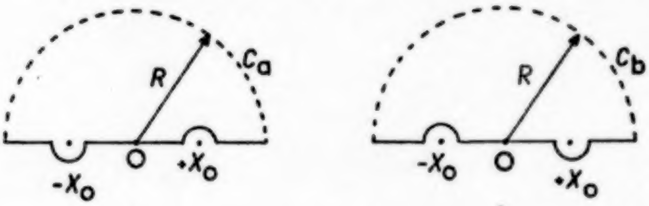

a b

Fig. 1

the residue for the corresponding pole we find

$$\tfrac{1}{2}\int_{C_a(C_b)}\frac{1}{(x_0{}^2-r^2)^n}\mathrm{d}r = \pi i\frac{(-1)^n}{(n-1)!}\left[\frac{\mathrm{d}^{n-1}}{\mathrm{d}r^{n-1}}\frac{1}{(r\mp x_0)^n}\right]_{r=\mp x_0}$$
$$= \pm\pi i\frac{n(n+1)\ldots(2n-2)}{(n-1)!}\frac{1}{(2x_0)^{2n-1}}. \qquad \text{(A3)}$$

The sign + refers to the contour c_a and the sign − to the contour c_b. The calculated value differs from that of the integral of interest for us by a quantity equal to the integral along the arc of the semi-circle. In the limit for $R \to \infty$ both values are equal.

Employing the rule indicated above for evaluation of the integrals we obtain finite expressions for the integrals in (A1) and (A2). However, there is a factor $B^2 \approx V^{-1} = (\frac{4}{3}\pi R^3)^{-1}$ before each integral, and hence they vanish for $R \to \infty$.

Appendix 4

The total energy of a boson field in the form of quasi-plane waves (60) can be expressed as (see (66))

$$E = -\int T_{44}\,\mathrm{dv} = 2B^2 \int \Big[k_0{}^2 \frac{s'^2}{s^2} - \frac{a^4}{s^8} \big((\bar{k}\bar{x})^2 x_0{}^2 + k_0{}^2 x_0{}^2 r^2$$

$$- (\bar{k}\bar{x}) k_0 x_0 (x_0{}^2 + r^2) \big) \Big]\,\mathrm{dv}.$$

Integrating over the angles we obtain

$$8\pi \lim_{R\to\infty} \left(B^2 \int_0^R \left[k_0{}^2 \frac{s'^2}{s^2} - \frac{a^4}{s^8} r^2 x_0{}^2 (\tfrac{1}{3}k^2 + k_0{}^2) \right] r^2\,\mathrm{d}r \right).$$

Evaluating the integrals in accord with the rule mentioned in appendix 3 we get

$$-\int T_{44}\,\mathrm{dv} = \lim_{R\to\infty} \left\{ \frac{3}{k_0 R^3} \Big[k_0{}^2 (\tfrac{1}{3}R^3 + a^2 R \mp \pi i \tfrac{1}{2} a^2 x_0)\right.$$

$$\left. \mp \frac{1a^4}{32 x_0} \pi i (\tfrac{1}{3}k^2 + k_0{}^2) \Big] \right\} = k_0.$$

The total momentum (also for the case of quasi-plane waves) is

$$P_i = \frac{1}{i} \int T_{44}\,\mathrm{dv} = 2B^2 \int \Big[k_0 k_i \frac{s'^2}{s^2} + \frac{a^2 (k, x)}{s^6} (s'^2 x_0 k_i - s^2 k_0 x_i)$$

$$- \frac{a^4 (k, x)^2 x_0 x_k}{s^8} \Big]\,\mathrm{dv}.$$

After integration over the angles this yields the expression

$$8\pi \lim_{R\to\infty} \left(k_0 k_i B^2 \int_0^R \left[\frac{s'^2}{s^2} - a^2 \left(\frac{s'^2}{s^6} x_0{}^2 + \frac{r^2}{3s^4} \right) + \frac{2a^4 x_0{}^2 r^2}{s^8} \right] r^2\,\mathrm{d}r \right).$$

Evaluating with the aid of the above mentioned rule, we get $p_i = k_i$. All other terms vanish for $R \to \infty$.

Appendix 5

The following expressions appear when the integrals of the fermion or boson field charge densities are evaluated (see (78) and (87)):

$$\lim_{R\to\infty}\left(\frac{3}{R^3}\int_0^R \frac{s'}{s}\left(1-\frac{a^2x_0^2}{s^4}\right)r^2\,\mathrm{d}r\right).$$

The integrand in this expression possesses a singularity at the point $r = x_0$ (light cone) and the function is branched at this point. Suppose a cut is made along the real axis in accord with fig. 2 and suppose that that branch

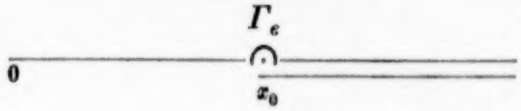

Fig. 2.

of the function is taken which corresponds to the first sheet of the Riemann surface.

If we pass the singularity from above our integral will assume the form

$$\lim_{\substack{R\to\infty\\ \varepsilon\to 0}}\left\{\frac{3}{R^3}\left[\int_0^{x_0-\varepsilon}+\int_{x_0+\varepsilon}^R+\int_{\Gamma_\varepsilon}\right]\right\}.$$

It is not difficult to see that the integrand

$$\frac{s'}{s}\left(1-\frac{a^2x_0^2}{s^4}\right)r^2=\sqrt{r^2+\frac{a^2r^2}{r^2-x_0^2}}\left(1-\frac{a^2x_0^2}{(r^2-x_0^2)^2}\right)r$$

is a complete derivative of the function

$$\tfrac{1}{3}\left(r^2+\frac{a^2r^2}{r^2-x_0^2}\right)^{\frac{3}{2}},$$

and hence

$$\int_0^{x_0-\varepsilon}+\int_{x_0+\varepsilon}^R$$

$$=\tfrac{1}{3}\left\{(x_0-\varepsilon)^3\left(1+\frac{a^2}{\varepsilon^2-2x_0\varepsilon}\right)^{\frac{3}{2}}-(x_0+\varepsilon)^3\left(1+\frac{a^2}{\varepsilon^2+2x_0\varepsilon}\right)^{\frac{3}{2}}+R^3\left(1+\frac{a^2}{R^2-x_0^2}\right)^{\frac{3}{2}}\right\}$$

$$\approx\tfrac{1}{3}\left\{\frac{a^3x_0^{\frac{3}{2}}}{i^3(2\varepsilon)^{\frac{3}{2}}}\left(1-\frac{3\varepsilon}{x_0}\right)\left(1-\frac{\varepsilon}{2x_0}\right)^{-\frac{3}{2}}\left(1-\frac{2x_0\varepsilon}{a^2}\right)^{\frac{3}{2}}\right.$$

$$\left.-\frac{a^3x_0^{\frac{3}{2}}}{(2\varepsilon)^{\frac{3}{2}}}\left(1+\frac{3\varepsilon}{x_0}\right)\left(1+\frac{\varepsilon}{2x_0}\right)^{-\frac{3}{2}}\left(1+\frac{2x_0\varepsilon}{a^2}\right)^{\frac{3}{2}}+R^3\right\}$$

$$\approx\tfrac{1}{3}\left\{\frac{ia^3x_0^{\frac{3}{2}}}{(2\varepsilon)^{\frac{3}{2}}}\left(1-\tfrac{9}{4}\frac{\varepsilon}{x_0}-\frac{3x_0\varepsilon}{a^2}\right)-\frac{a^3x_0^{\frac{3}{2}}}{(2\varepsilon)^{\frac{3}{2}}}\left(1+\tfrac{9}{4}\frac{\varepsilon}{x_0}+\frac{3x_0\varepsilon}{a^2}\right)+R^3\right\}.$$

Furthermore $r - x_0 = \varepsilon e^{i\varphi}$ on contour Γ_ε

$$\int_{\Gamma_\varepsilon} = \int_\pi^0 \sqrt{1+\frac{a^2}{\varepsilon e^{i\varphi}(2x_0+\varepsilon e^{i\varphi})}}\left(1-\frac{a^2x_0^{\,2}}{\varepsilon^2 e^{2i\varphi}(2x_0+\varepsilon e^{i\varphi})^2}\right)(x_0+\varepsilon e^{i\varphi})^2\varepsilon e^{i\varphi} i\,d\varphi$$

$$\approx -\frac{ia^3x_0^{\,\frac{3}{2}}}{4\sqrt{2}\varepsilon^{\frac{3}{2}}}\int_\pi^0\left(1+\frac{2x_0\,\varepsilon e^{i\varphi}}{a^2}\right)^{\frac{1}{2}}\left(1+\frac{\varepsilon e^{i\varphi}}{2x_0}\right)^{-\frac{1}{2}}\left(1+\frac{\varepsilon e^{i\varphi}}{2x_0}\right)^{-2}\left(1+\frac{\varepsilon e^{i\varphi}}{x_0}\right)^2 e^{-i\frac{3}{2}\varphi}\,d\varphi$$

$$\approx -\frac{ia^3x_0^{\,\frac{3}{2}}}{4\sqrt{2}\varepsilon^{\frac{3}{2}}}\int_\pi^0\left(1+\tfrac{3}{4}\frac{\varepsilon e^{i\varphi}}{x_0}+\frac{x_0\,\varepsilon e^{i\varphi}}{a^2}\right)e^{-i\frac{3}{2}\varphi}\,d\varphi$$

$$=\frac{a^3x_0^{\,\frac{3}{2}}}{4\sqrt{2}\varepsilon^{\frac{3}{2}}}\left[\tfrac{2}{3}(1-i)+\left(\tfrac{3}{2}\frac{\varepsilon}{x_0}+\frac{2\varepsilon x_0}{a^2}\right)(1+i)\right]$$

$$=\frac{a^3x_0^{\,\frac{3}{2}}}{3(2\varepsilon)^{\frac{3}{2}}}\left[\left(1+\tfrac{9}{4}\frac{\varepsilon}{x_0}+\frac{3\varepsilon x_0}{a^2}\right)-i\left(1-\tfrac{9}{4}\frac{\varepsilon}{x_0}-\frac{3x_0\varepsilon}{a^2}\right)\right].$$

The expression thus obtained exactly compensates the infinite terms which previously appeared, so that we finally get

$$\lim_{R\to\infty}\left(\frac{3}{R^3}\int_0^R\frac{s'}{s}\left(1-\frac{a^2x_0^{\,2}}{s^4}\right)r^2\,dr\right)=1.$$

As a result we find that for boson and fermion fields $\int j_0 dv = e$, which is just what one would expect.

References

1) M. Markov, Nuclear Physics **10** (1959) 140
2) A. Pais and G. E. Uhlenbeck, Phys. Rev. **79** (1950) 145
3) M. Markov, Sixth Rochester Conference on High Energies (1956)

1.E.1:
3.A

Nuclear Physics **12** (1959) 204—217; © *North-Holland Publishing Co., Amsterdam*

Not to be reproduced by photoprint or microfilm without written permission from the publisher

THE LEVEL SCHEME of ^{136}Ba

R. K. GIRGIS † and R. VAN LIESHOUT

Instituut voor kernphysisch Onderzoek, Amsterdam

Received 15 April 1959

Abstract: The gamma radiation following the decay of ^{136}Cs was investigated using a scintillation spectrometer. The energies of the various gamma rays are in good agreement with the values reported by Olsen and O'Kelley [2]); the relative intensities were also determined (table 1). Gamma-gamma coincidences were performed using a conventional fast-slow coincidence set-up; they were also studied by the summing technique. A decay scheme consistent with these results is proposed (fig. 9); it consists of levels at 830, 1900, 2090, 2170, 2240, 2330, 2430 and 2490 keV. The decay of ^{136}La, which also leads to levels in ^{136}Ba, was investigated. Only one gamma ray of 830 keV was found with certainty, thus confirming that the first 2+ level in ^{136}Ba has this energy.

1. Introduction

Brooksbank [1]) examined the gamma ray spectrum of ^{136}Cs using the scintillation technique and reported gamma rays of 830 keV and 1060 keV. A more detailed investigation on this nucleide was undertaken by Olsen and O'Kelley [2]) who used beta spectrometers, scintillation spectrometers and a proportional counter; gamma-gamma coincidences were also performed. These last authors proposed a decay scheme on the basis of gamma ray intensities and gamma-gamma coincidences. A striking feature of that decay scheme was the adoption of the 1040 keV gamma ray as corresponding to the transition from the first excited state in ^{136}Ba. An examination of the systematics of the energies of the first excited states of even-even barium isotopes (fig. 1) gives a value of $\approx$ 800 keV for ^{136}Ba, in strong disagreement with the one mentioned above. For the two even isotopes ^{134}Xe and ^{138}Ce containing 80 neutrons (the same number as for ^{136}Ba), the energy values for the first 2^+ state are 860 keV and 810 keV respectively. A value of $\approx$ 830 keV for the corresponding level in ^{136}Ba is thus interpolated from these two values in agreement with the one obtained from the systematics on the barium isotopes. In a private communication to the Nuclear Data Group, O'Kelley [3]) reported that the 820 keV peak is the strongest gamma ray, which led this group to reconstruct the level scheme of ^{136}Ba placing the first 2^+ level at 820 keV.

The present information [4]) about the decay of ^{136}La, which also leads to levels in ^{136}Ba, does not clear up this situation. No gamma rays were reported to follow this decay. It was therefore thought to be of interest to reexamine the gamma ray spectra of both nuclei, ^{136}Cs and ^{136}La.

---

† On leave of absence from the Faculty of Science, University of Cairo, Giza, Egypt, U.A.R.

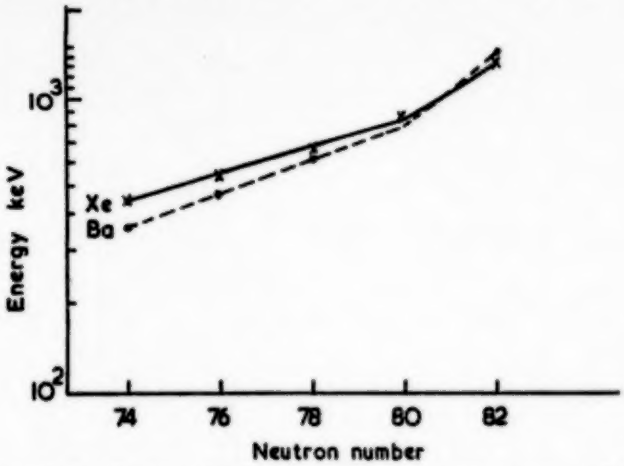

Fig. 1. Energy values of the first excited states in some even-even nucleides of Xe and Ba plotted against their neutron numbers.

2. Production and Chemical Procedure

The ^{136}Cs sources were prepared by bombarding barium oxide with $\approx$ 23-MeV deuterons from the synchro-cyclotron of this Institute. Two different sources were prepared by the (d, α) reaction (20 and 110 μAh respectively) for direct gamma spectrum and for coincidence studies. After decay of the short-lived activities ($\approx$ 1 week) the irradiated target was dissolved in nitric acid. Cesium and ferric ion holdback carriers were added and barium was precipitated as the sulfate. The filtrate was made basic with ammonia and the lanthanum and ferric ions were scavenged. This last step was repeated. The remaining solution was evaporated until only a small volume remained, after which 70 % perchloric acid was added to the chilled solution. The addition of alcohol causes the cesium to precipitate as the perchlorate. The final step consisted of a recrystallization and drying with absolute alcohol.

The ^{136}La sources were prepared by alpha bombardment of cesium chloride. The irradiations lasted for $\approx$ 10 minutes and the bombarding energy was chosen as $\approx$ 24 MeV in order to suppress the formation of the cumbersome 6 minute ^{134}La, which is formed by the (α, 3n) reaction. The irradiated target was dissolved in water and holdback carriers of divalent Cu-, Zn- and Ba-ions and of trivalent Fe- and La-ions were added in the form of nitrates in order to avoid the presence of excessive amounts of chloride ions. For the beta ray sources the amount of lanthanum added was reduced to 10 μg. Fe and La were coprecipitated by the addition of ammonia. This procedure was repeated twice; each time barium and cesium holdback carriers were added. Finally the precipitate was dried with alcohol and ether.

The complete lanthanum separation took approximately 10 minutes.

3. Measurements and Results

3.1. DIRECT SPECTRUM

The gamma ray spectra of ^{136}Cs and ^{136}La were examined using a cylindrical NaI(Tl) crystal of 2.5×2.5 cm, coupled to a 6292 DuMont photomultiplier. The spectra were displayed on a RIDL 100 channel analyzer. Care was taken to suppress summing effects by placing the sources at $\approx$ 8 cm; alternatively absorbers were used for the same purpose.

The spectrum of ^{136}Cs was examined in an energy region from 20 keV to 3000 keV. The various parts of the spectrum are shown in the figures 2, 3 and 4.

The analysis of the spectrum was performed in the usual way, applied before in several investigations [5]); it will be described in detail in a forthcoming article [6]). Table 1 gives the energies and relative intensities of the gamma rays analysed. The energy values are in good agreement with those reported by Olsen *et al.* [2]), except for the high energy gamma rays of 2.35 MeV and 2.49 MeV, which were not found in the present work. (The relative

TABLE 1

Energies and relative intensities of the gamma rays from the decay of ^{136}Cs.

^{136}Cs produced by $^{(138)}$Ba(25-MeV d, α)chem.

Energy (keV)	Intensity (% per disintegration)
KX-ray	22 ± 4
67 ± 3	13 ± 2
86 ± 3	7 ± 1.5
152 ± 5	19 ± 3
170 ± 5	23 ± 3
200 ± 10	3 ± 1
230 ± 10	3 ± 1
270 ± 5	22 ± 3
337 ± 5	59 ± 6
830 ± 5	100 ± 10
1065 ± 10	84 ± 8
1255 ± 10	21 ± 2

Doubtful peak at 110 ± 10 keV (1 ± 1 %)
No 1410 γ (<0.1 %)
No 1900 γ (<0.1 %)
No 2350 γ (<0.05 %)
No 2490 γ (<0.05 %)
No gamma with $350 < E < 820 (< 1\ \%)$

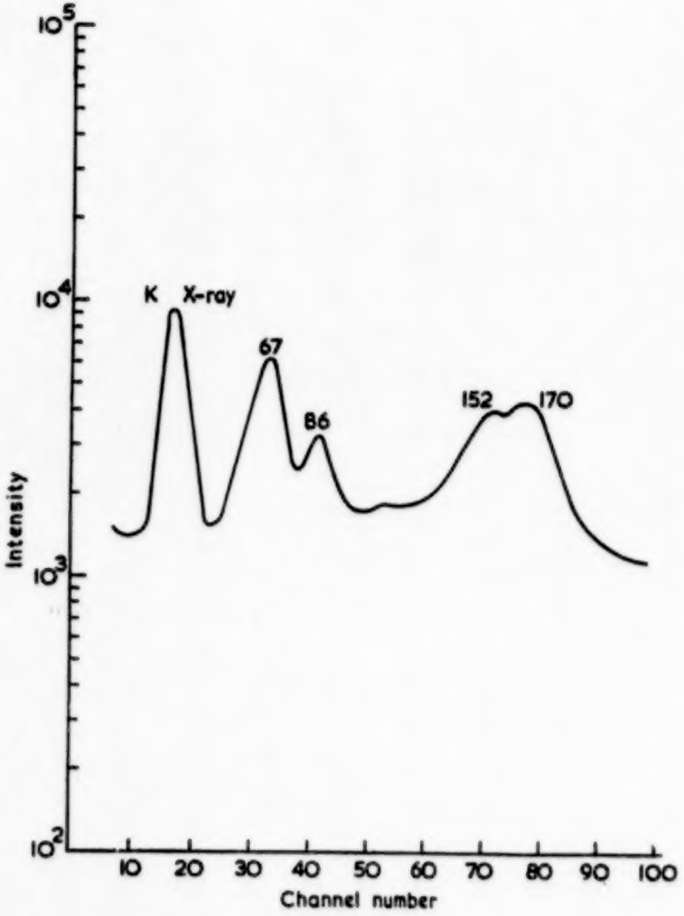

Fig. 2. Gamma ray spectrum of ^{136}Cs in the low energy region.

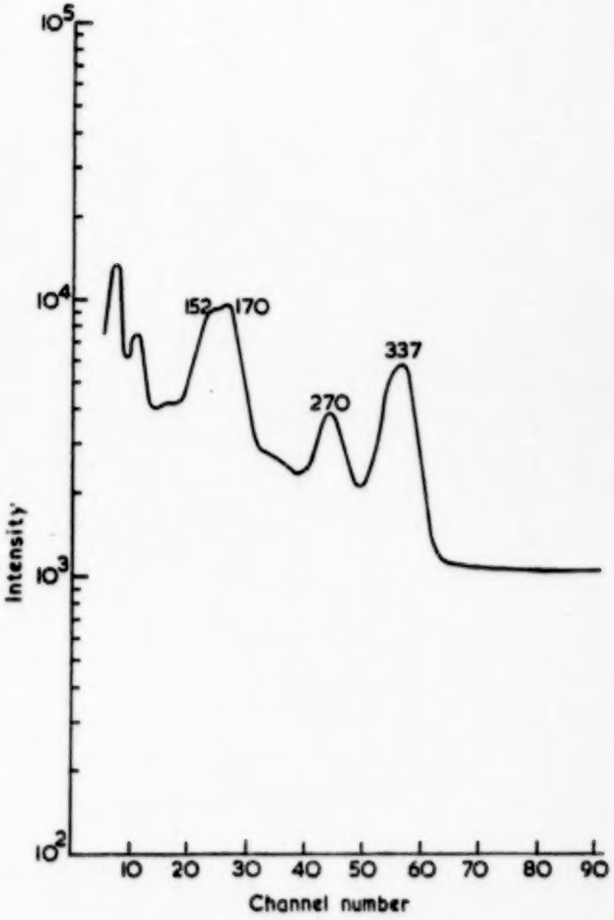

Fig. 3. Gamma ray spectrum of ^{136}Cs in an energy region between ≈ 60 keV and ≈ 500 keV.

intensities of the gamma rays found cannot be compared with those obtained by Olsen *et al.* [2]), since these were not quoted in ref. [2])). The peak at 1.41 reported in ref. [2]) was found to be due to summing. This was checked by measuring summing peaks of 2.50 MeV in ^{60}Co (1.17+1.33) and 1.79 MeV in ^{22}Na (0.511+1.28) measured under the same conditions of source size and source-crystal distance; corrections for crystal efficiency were applied. In addition a summing peak at 1.90 was found. In the energy region from 350 to 820 keV no gamma ray peaks were found (< 1 %), except for a line at 672 keV, which decayed with a half-life of 7 days and which was therefore assigned to ^{132}Cs.

The ^{136}La sources were examined under the same conditions as those for ^{136}Cs. Its half-life was determined to be 10.0 ± 0.5 minutes. The source was sandwiched between aluminium absorbers to ensure complete annihilation of positons at the source position. The decay of the source was followed over a period of a few days in order to subtract the contribution due to the long-lived activity of 19 hour ^{135}La produced in the accompanying (α, 2n) reaction. This contribution was found to be negligible at the beginning of the investigation.

Fig. 5 shows the relevant part of the spectrum. The pulse height distribution due to annihilation in flight of positons was also subtracted. This was obtained by interpolation between those found for various pure positon emitters measured with the same crystal and photomultiplier combination used in this investigation and reported in previous work [7]). The maximum energy reported below for the positon spectrum of ^{136}La was used. Only one gamma ray of 830 ± 5 keV was found with certainty in the spectrum of ^{136}La in addition to the annihilation peak; its intensity amounts to 3.8 % of the 511 keV peak, a correction for absorption in the annihilators having been applied. An upper limit of 0.4 % can be placed on the intensity of the 1065 keV gamma ray relative to the 511 keV peak. No gamma rays of energy below 511 keV were found, in particular a 337 keV gamma ray was shown to be absent (< 1 %). The 513 keV peak in the decay of ^{85}Sr examined under the same conditions as ^{136}La was found to fit exactly to the 511 keV peak in ^{136}La after peeling off the contribution due to the 830 keV peak.

3.2. GAMMA-GAMMA COINCIDENCES

Gamma-gamma coincidences were performed using a conventional fast-slow coincidence circuit having a resolving time of $2\tau = 17$ ns. Two NaI(Tl) crystals of 2.5×2.5 cm were employed.

To give an impression of the results, fig. 6 shows a typical coincidence spectrum obtained selecting the 1255 keV gamma ray as gating peak and examining the low energy part of the spectrum coincident with that peak,

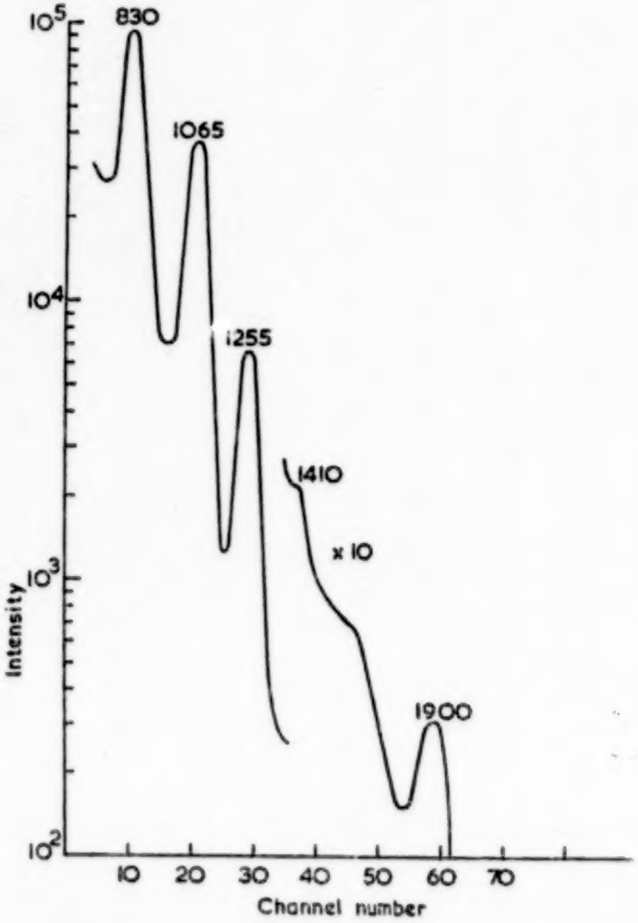

Fig. 4. Gamma ray spectrum of ^{136}Cs in the high energyregion. All peaks of energy higher than 1255 keV proved to be due to summing effects.

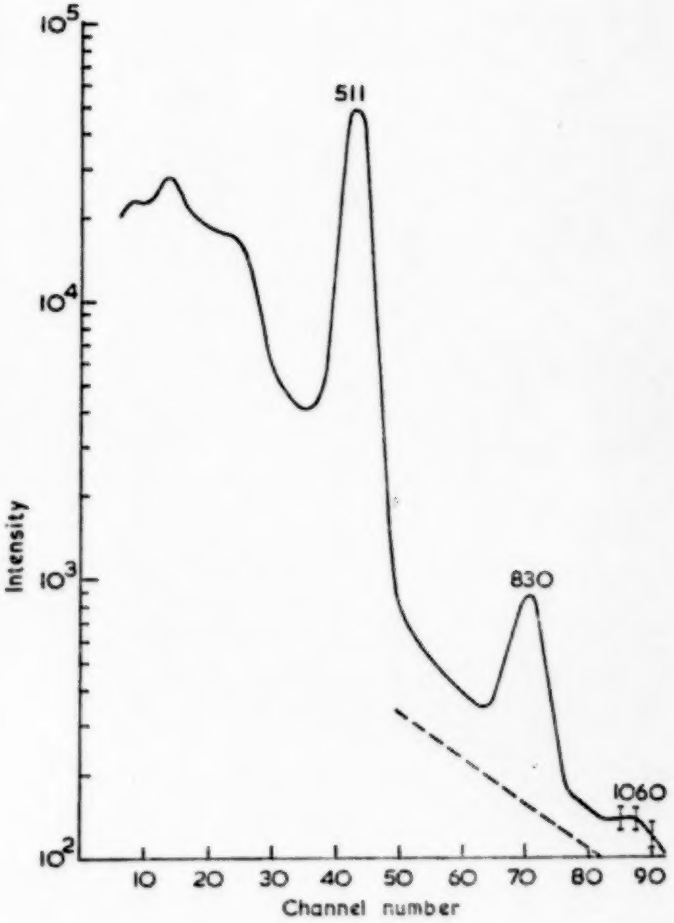

Fig. 5. Gamma ray spectrum of ^{136}La in an energy region between ≈ 200 keV and 1200 keV, the dashed line represents the contribution of annihilation in flight of the positons.

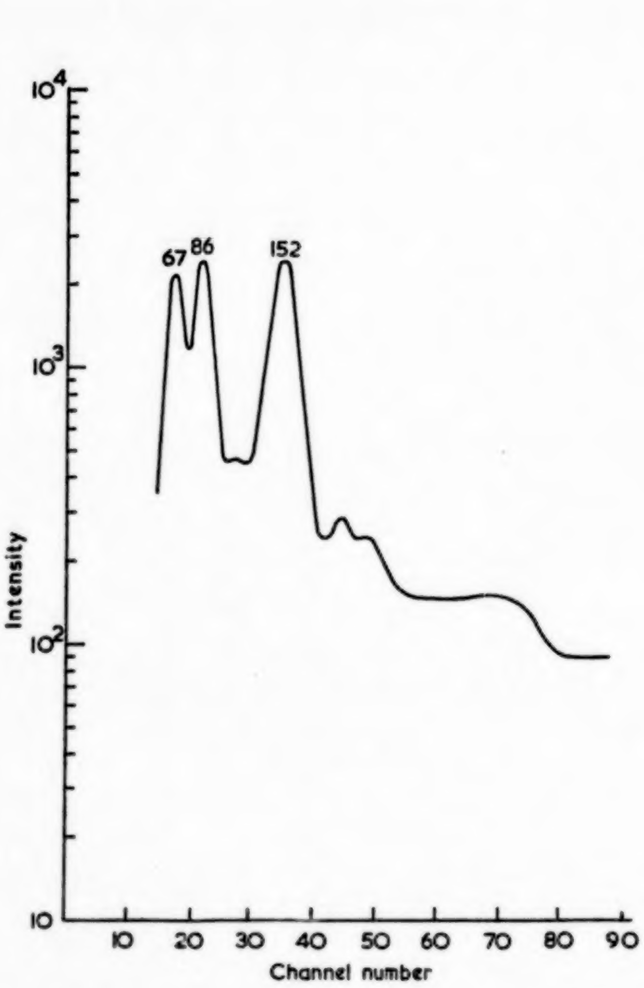

Fig. 6. Coincidence spectrum of ^{136}Cs in the energy region between ≈ 40 keV and ≈ 500 keV, with the 1255 keV gamma ray as the gating peak.

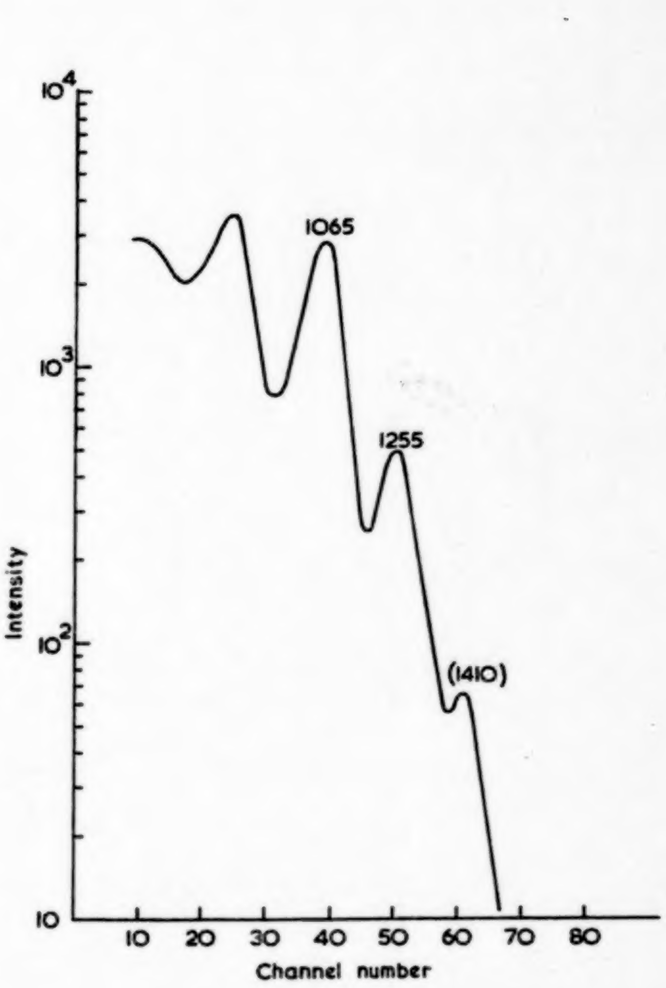

Fig. 7. Coincidence spectrum of ^{136}Cs in the high energy region with the 830 keV gamma ray as the gating peak. The 1410 keV peak is the sum of the 337 and 1065 keV gamma rays which are in cascade.

while fig. 7 shows the high energy part of the spectrum in coincidence with the 830 keV peak.

Selecting the 270 keV gamma ray and examining the low energy region yields a very strong peak at 67 keV and a very weak one at 170 keV. A weak indication for coincidences with the 86 keV line can be inferred. The gamma rays at 337 keV and 152 keV are not in coincidence with the 270 keV peak. Examination of the high energy part of the coincidence spectrum shows strong peaks of 830 and 1065 keV, whereas the 1255 keV peak is greatly reduced. The remaining part of the 1255 keV peak is completely due to coincidences with the flat Compton distribution under the 270 keV peak as shown by selecting part of the flat Compton distribution on the high energy side of the 337 keV peak with the same window width.

Using the 337 keV peak to gate the coincidences yields the same picture as selecting the 270 keV peak except that the 67 keV peak disappears. It should be mentioned that the relative intensities of the 830 and 1065 keV peaks are the same in the two cases, but the 830 keV line appears to be weaker than in the direct spectrum.

Coincidences with the 830 keV peak were also examined. All low energy gamma rays were found to be in coincidence with that peak, with approximately the same relative intensities as in the direct spectrum, except that the 170 keV peak is considerably suppressed; this probably means that it is in coincidence with the 830 keV peak only through delayed gamma ray transitions. No definite conclusions can be drawn with respect to the gamma rays of 200 and 230 keV, since they are hidden by the backscattering peaks of the high energy gamma rays. The peaks of 1065 and 1255 keV were found to be in coincidence with the 830 keV peak. Their relative intensities in the coincident spectrum are the same as in the direct spectrum.

TABLE 2

Summary of the results of gamma-gamma coincidence measurements

Energy (keV)	67	86	152	170	200	230	270	337	830	1065	1255
270	Yes	Yes	No	U			No	No	Yes	Yes	No
337	No	Yes	No	U			No	No	Yes	Yes	No
830	weak	weak	weak				Yes	Yes	No	Yes	Yes
1255	weak	Yes	Yes		weak	weak		No			

U: coincidences uncertain, but probable.
weak: corresponding gamma ray suppressed relative to the direct spectrum.

The vertical entry column represents the gating peaks, the horizontal row represents the gamma rays observed in the direct spectrum.

The coincidences with the 1255 keV peak were examined only in the low energy region, since it was already known from the above investigations to be in coincidence with the 830 keV peak. It must be parallel to the 1065 keV gamma ray since there is not enough decay energy to place all three gamma rays (830, 1065, 1255 keV) in cascade. The coincident spectrum showed a very strong 152 keV peak (fig. 6) and one at 86 keV. The intensity ratio of these two gamma rays coincident with the 1255 keV peak is approximately the same as in the direct spectrum.

No other gamma-gamma coincidences were performed since the information already obtained was sufficient for the construction of the main features of the decay scheme of ^{136}Cs. The various coincidence results are summarized in table 2.

The results mentioned above are qualitatively in agreement with those obtained by Olsen *et al.* ^{2}) as can be concluded from their proposed decay scheme, except for the 1255 keV gamma ray which proved to be in coincidence with the 830 keV gamma ray.

3.3. SUMMING SPECTRUM

A cylindrical well-type NaI(Tl) crystal of 6.2 cm × 6.2 cm external size having a hole of 9 mm diameter and 31 mm depth was used for summing studies. The summing spectrum due to ^{136}Cs was examined over the whole energy region with the source at various distances from the crystal and also inside the well. Copper absorbers were used to suppress the KX-ray from being summed to the various peaks; the 67 and 86 keV peaks also diminished somewhat in intensity by this device. Fig. 8 shows the summing spectrum inside the crystal for the high energy region, the spectrum for the source outside the crystal at a distance of $\approx$ 12 cm is shown by the dotted line for comparison. Additional peaks of 2.49 ± 0.02, 2.43 ± 0.02, 2.24 ± 0.02, and 2.09 ± 0.01 MeV can easily be seen. The peaks at 1.90 and 1.41 MeV, which are completely due to summing, considerably increased in height. Levels at 2.49, 2.43, 2.24 and 2.09 MeV must therefore exist, since the four gamma rays cannot be placed above the 830 keV level, the total decay energy as derived from beta systematics ^{8}) being only $\approx$ 2.8 MeV. The 1.90 MeV peak is very likely due to summing of the 830 and 1065 keV transitions which were found to be in coincidence. The 1.41 MeV peak is probably the sum of the strong gamma rays of 337 and 1065 keV.

The ^{136}La was examined on top of the summing crystal; a peak at 1.34 MeV was found, suggesting summing of the 511 keV annihilation peak to the 830 keV gamma ray.

3.4. ^{136}La POSITON SPECTRUM

The end point of the ^{136}La positon spectrum was determined by several authors ^{4,9,10}). The first two groups reported a value of 2.1 MeV, whereas the third group reported a value of 1.8 ± 0.1 MeV. The latter value agrees somewhat better with beta decay energy systematics ^{8}). The present authors measured the positon spectrum of ^{136}La with an anthracene crystal 1 cm

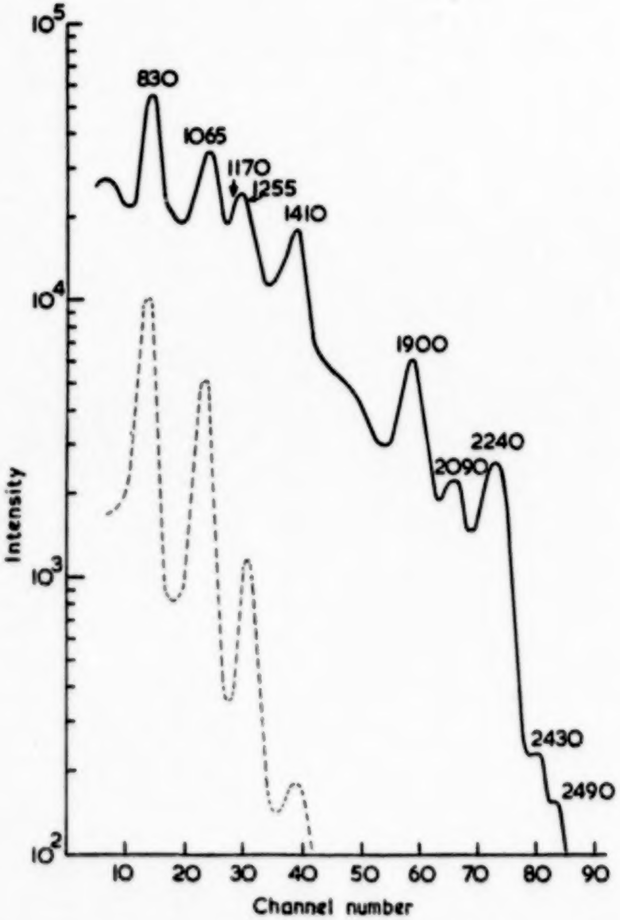

Fig. 8. Summing spectrum of ^{136}Cs in the high energy region. The direct spectrum for the source placed at $\approx$ 12 cm distance from the summing crystal is shown in dashed line. The peak at 1.410 MeV in the direct spectrum is due to residual summing. The peak at $\approx$ 1.2 MeV is probably composed of the 1255 keV peak and a summing peak of 1170 resulting from the coincident 830 and 337 keV gamma rays.

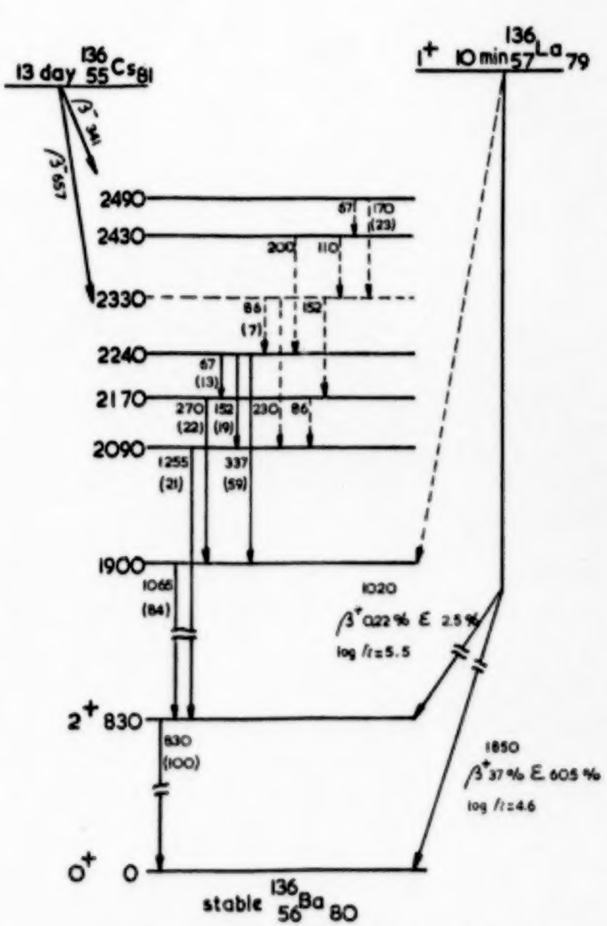
13 day $^{136}_{55}$Cs$_{81}$
β^- 341
β^- 657
1^+ 10 min $^{136}_{57}$La$_{79}$
2490
2430
2330
2240
2170
2090
1900
2^+ 830
0^+ 0
67
170 (23)
200
110
86 (7)
152
67 (13)
270 (22)
152 (19)
230
86
1255 (21)
337 (59)
1065 (84)
830 (100)
1020
β^+ 0.22 % E 2.5 %
log ft = 5.5
1850
β^+ 37 % E 60.5 %
log ft = 4.6
stable $^{136}_{56}$Ba$_{80}$

Fig. 9. Proposed level scheme of ^{136}Ba. The numbers in parentheses represent the intensity of the transitions in the decay of ^{136}Cs.

thick and 4 cm in diameter mounted on a 6292 DuMont photomultiplier. The crystal was calibrated for energy using ^{90}Sr+^{90}Y (2.25 MeV), ^{32}P (1.71 MeV) and ^{207}Bi(976 keV conversion peak). The end point was found to be 1.85±0.07 MeV, in agreement with that of Robertson *et al.*[10]). Table 3 gives the various characteristics of the decay of ^{136}La.

TABLE 3

Characteristics of the decay of ^{136}La

^{136}La produced by ^{133}Cs (25-MeV α, n) chem	
$T_{\frac{1}{2}} = 10.0 \pm 0.5$ min	
β^+ 1.85 ± 0.07 MeV scin	
Energy (keV)	Relative intensity
$\gamma^{\pm}$	2×100
830 ± 5	7.5
1065	<1
No gamma with $200 < E < 500$ (< 1)	

4. Discussion

A level scheme of ^{136}Ba constructed on the basis of gamma ray intensities and gamma-gamma coincidences found in this investigation is shown in fig. 9. The first excited state occurs at 830 keV since it explains the strongest gamma ray following the decay of ^{136}Cs, in agreement with O'Kelley's observations [3]). The fact that it is the only gamma ray found in the spectrum of ^{136}La makes this assignment certain. The energy value is in good agreement with the systematics of the first excited state for even mass Ba-nucleides.

The gamma-gamma coincidence and summing measurements suggest levels at 1.90 MeV and 2.09 MeV, which are the origin of gamma transitions of 1065 and 1255 keV. A spin of 2^+ could be assigned to the level at 1.90 MeV since its energy, being ≈ 2.3 times that of the first excited state, fits with the general trend for even mass nucleides in the medium weight range [11, 12]). However, the absence of a cross over transition to the ground state is not in favour of this assignment suggesting higher spin values, unless, for some reason, an E2 transition to the ground state from this second excited state is highly suppressed. The level at 1.90 MeV must have a spin 2, if the bump at 1065 keV in the gamma spectrum of ^{136}La corresponds to a real gamma ray. The sum of the intensities of the 1065 keV and 1255 keV gamma ray is in excellent agreement with that of the 830 keV gamma ray. This adds to the validity of the argument to place the 1065 keV and 1255 keV transitions directly on the top of the 830 keV level. The fact that these two gamma rays have the same relative heights in the coincidence spectrum with 830 keV as in the direct spectrum is also in accord with this interpretation.

The 337 keV gamma ray is placed above the 1.900 MeV level originating from a level at 2.240 MeV in agreement with a strong summing peak of that energy and also with the coincidence measurements with the high energy region. This explains the slightly reduced intensity of the 830 keV peak when measured in coincidence with the 337 keV transition relative to that found in the direct spectrum, since the coincidence takes place through the 1065 keV gamma ray only.

The transition of 152 keV fits between the 2.24 MeV level and the 2.09 MeV level and this interpretation is in agreement with the strong coincidence between the 152 keV and the 1255 keV gamma rays. The strong summing peak at 1410 keV can be explained as the sum of the strong 337 and 1065 keV gamma rays, which are in coincidence, whereas the 152 and 1255 keV also contribute.

The pair of gamma rays of 270 and 67 keV, which are in cascade, also fits between the levels at 1.900 and 2.240 MeV. The coincidence results involving the 67, 152, 270 and 337 keV transitions support this interpretation, but do not fix the order of the two gamma rays in the cascade. The energy relation between the 67, 86 and 152 keV lines suggests an intermediate level at 2.17 MeV. However, it is unlikely that the major part of the 86 keV transition occurs at this position, since the intensity balance between the 152 and 1255 keV transition is already satisfactory, leaving no room for other strong transitions to populate the 2.09 MeV level. (Of course this argument is invalid if the 152 keV transition proves to be double). Moreover the 86 keV peak is found to be in coincidence with both the 270 and the 337 keV peaks, indicating it should at least partly be placed above the 2.24 MeV level. The arguments for the position of the 270 keV transition are supported by the results of the coincidences between the 270 keV peak and the 830 and 1065 keV gamma rays, in particular by the fact that the relative intensity of these two latter gamma rays is the same in this coincidence run as in that with the 337 keV peak.

Up to the level at 2.24 MeV the various gamma rays can be accommodated with reasonable confidence. The intensity balance to and from the levels is very satisfactory, although the position of some of the weak gamma rays cannot be determined by this procedure. The high total intensity of the transitions originating at the 2.24 MeV level shows that the major part of the beta transitions must end at this or higher levels. The intensity of the summing spectrum drops off sharply above 2.24 MeV. This may be taken as an indication that the beta ray group of 341 keV, reported [2]) to constitute 93 % of all beta decays, goes directly to the level at 2.24 MeV. A total decay energy of 2.58 MeV is thus deduced for ^{136}Cs.

The existence of a delayed transition has been postulated to explain the coincidence results involving the 170 keV gamma ray. The 86 keV transition is the most likely candidate for this delayed one. In that case it cannot be excluded that the stronger beta ray group goes to the highest level at 2.49 MeV, yielding a total decay energy of 2.83 MeV.

Although the exact position of the gamma rays to be placed above the 2.24 MeV level is somewhat speculative, the existence of various levels seems well established from the summing results. These occur at 2.43 and 2.49 MeV and, together with a postulated level at 2.33 MeV, they can explain the 170, 86 and also the weak 200 and 230 keV transitions as well as some of the coincidence results involving the 86, 170, 200 and 230 keV peaks. For instance, both the 86 and 230 keV peaks can originate at the 2.33 MeV level. The position of the relatively strong gamma ray of 170 keV is not very certain, since it is only rather weakly in coincidence with the three gating peaks of 270, 337, and 830 keV. If it occurs between the 2.49 and the 2.33 MeV levels it must be concluded that the 86 keV transition is both delayed and highly converted, mainly in the L-shell. The intensity of the KX-ray peak (after corrections for fluorescence yield and for the escape peak) is namely too low to explain the amount of conversion needed for the balance, which probably indicates an appreciable amount of L-conversion. A remeasurement of the conversion spectrum would therefore greatly help in constructing a definite level scheme of ^{136}Ba in the region above 2.24 MeV excitation energy.

A number of possibilities for placing some of the remaining gamma transitions has been indicated in fig. 9 by dotted lines. The presence of a level at 1.4 MeV deduced [13]) from the capture gamma ray work cannot be confirmed in the present work since the peak of that energy found in the gamma spectrum proved to be entirely due to summing effects.

The authors wish to thank Prof. Dr. P. C. Gugelot for his interest in this work and Prof. Dr. A. H. W. Aten Jr. and Prof. Dr. A. H. Wapstra for valuable criticism. They are also indebted to Mrs. A. Funke-Klopper for performing the many chemical separations and to the staff of the cyclotron for the irradiations. This work is part of the research program of the "Stichting voor Fundamenteel Onderzoek der Materie (F.O.M.)", which is financially supported by the "Nederlandse Organisatie voor Zuiver-Wetenschappelijk Onderzoek (Z.W.O.)". One of the authors (R. K. G.) is indebted to the Egyptian Atomic Energy Commission for a grant.

References

1) W. A. Brooksbank, Oak Ridge National Laboratory Report —1474 (1953)
2) J. L. Olsen and G. D. O'Kelley, Phys. Rev. **95** (1954) 1539
3) G. D. O'Kelley, private communication to Nuclear Data Sheets, NRC **58**—8—53 (National Research Council, Washington, D.C.)

4) R. A. Naumann, F. L. Reynolds and I. Perlman, Phys. Rev. **77** (1950) 398
5) R. K. Girgis and R. van Lieshout, Physica **25** (1959) 133
6) R. K. Girgis, R. A. Ricci and R. van Lieshout, to be published
7) R. A. Ricci, R. K. Girgis and R. van Lieshout, Nuovo Cimento **11** (1959) 156
8) K. Way and M. Wood, Phys. Rev. **94** (1954) 119
9) W. Maurer, Z. Naturforsch, **2a** (1947) 586
10) B. E. Robertson, W. L. Carss and M. L. Pool, Phys. Rev. **77** (1950) 747A
11) G. Scharff-Goldhaber and J. Weneser, Phys. Rev. **98** (1955) 212
12) K. Way, D. N. Kundu, C. L. McGinnis and R. van Lieshout, Annual Review of Nuclear Science **6** (1956) 129
13) B. B. Kinsey and G. A. Bartholomew, Can. J. Phys. **31** (1953) 1051

10.A

Nuclear Physics **12 (1959) 218;** © *North-Holland Publishing Co., Amsterdam*

NEWS ITEMS

CERN COUNCIL MEETING IN GENEVA

(26 May 1959)

Apparatus:

The 25 GeV proton synchrotron will begin trial operations at the end of this year or early 1960, exactly in accordance with schedule. CERN's second particle accelerator, the 600 million electron-volt synchro-cyclotron, has been in operation at full capacity since the beginning of 1958.

Both particle accelerators will benefit from an increasingly extensive programme of instrumentation, now being prepared. This will include the construction of big bubble chambers, beam transport and shielding devices, nuclear data processing, high-speed electronic counters, photographic emulsion techniques and cloud chambers.

Budget:

A ceiling of 120 million Swiss francs was accepted by the Council for contribution for 1959 and 1960. This sum will cover estimated expenditure for the completion and operation of the accelerators, research on new accelerating techniques, the experimental programme for both accelerators, as well as administration, general services and staff expenses.

Austria to become 13*th Member State:*

Following applications made in 1958 by the Austrian Government, the Council agreed unanimously to accept Austria as the 13th European Member State to participate in CERN.

New Appointments:

Professor C. Møller, formerlyDirector of CERN's Theoretical Study Division when the latter was still in Copenhagen and Professor of Theoretical Nuclear Physics at the University of Copenhagen, together with Professor C. F. Powell, of Bristol University, have been appointed members of the Scientific Policy Committee, headed by Professor E. Amaldi of Italy.

INSTITUTE OF PHYSICS "NOTES FOR AUTHORS"

The Institute of Physics has just published a 36-page revised edition of its booklet to assist less-experienced authors and to serve as a reference booklet for all those who wish to contribute to the Institute's publications. Under its new title "Notes for authors", it gives hints on the preparation of scripts and diagrams, on the layout of mathematics, the correction of proofs and so on. In addition to a bibliography of reference books and works on technical writing, the pamphlet also contains lists of the spellings, symbols and abbreviations used by the Institute.

Copies of this booklet are obtainable from The Institute of Physics, 47 Belgrave Square, London, S.W.1, price 3s 6d, including postage.

Editor's Note: This booklet contains much useful information, but contributors to *Nuclear Physics* should be warned that the list of abbreviations for units (which is not free from internal contradictions) deviates in some respects from the SUN Commission recommendations, which are strictly adhered to in this journal. They are also advised not to adopt the British system of printers' marks for correcting proofs, given in the booklet, because it gives rise to ambiguities and obscurities.

10.D

Nuclear Physics **12** (1959) 219; © *North-Holland Publishing Co., Amsterdam*

BOOK REVIEWS

J. R. HARRISON, *Nuclear Reactor Shielding* (Nuclear Engineering Monographs. Temple Press, 1958. viii-68 pages. 10s 6d).

This small book has been written for students who require a certain amount of knowledge about shielding — and this purpose is fulfilled remarkably well in so few pages.

The explanation of the physical processes and of the approximations ordinarily used in broad beam calculations is excellent, but a student without training in shielding calculations may need some further discussion of the geometrical problems in the calculations of doses from a reactor core.

This shortcoming is perhaps due to the limitation of space inherent to this type of book. All in all it seems that the value of such books is doubtful, because they usually contain too little for anyone going to work with the problems, and if this is not the case, the book is too detailed.

B. Micheelsen

J. H. BOWEN and E. F. O. MASTERS, *Nuclear Reactor Control and Instrumentation* (Temple Press, 1959. x-78 pages. 12s 5d).

This book, which is volume IV in a series of monographs on nuclear engineering, contains a treatment of the kinetic, control, and instrumentation problems connected with graphite moderated, gas cooled reactors.

The greater part of the book is concerned with control problems such as the neutron kinetics of the nuclear chain reaction, the temperature kinetics of a temperature-stabilized reactor and control rod calculations. Only the last chapter gives a short account of instrumentation problems connected with reactors.

On the cover of the book it is stated that this book is intended for students, research assistants and qualified technicians who require a broad understanding of those topics of nuclear engineering outside their own field of study. Unfortunately this book cannot be said to fulfil this aim. On account of the condensed form of presentation, a considerable knowledge in the fields of mathematics and nuclear engineering is required in order to appreciate the contents of this book. In particular this is true as regards the chapter on neutron kinetics.

However, for senior students and scientists well acquainted with the topics of nuclear engineering, though not experts in the field of reactor control, this book contains much interesting information.

P. L. Ølgaard

International Atomic Energy Agency Bulletin (Public Information Division, I.A.E.A., Kärntnerring 11, Wien I)

The first issue of the Bulletin of the IAEA has just appeared (April, 1959). The purpose of this publication is set out as follows by Mr. L. J. Lind, Chief of the Division of Public Information:

"The purpose of this Bulletin is to disseminate information about IAEA, about what the Agency does and how it does it. It seeks to give an account in the layman's language of the major steps that are being taken at a truly international level 'to accelerate and enlarge the contribution of atomic energy to peace, health and prosperity throughout the world'.

"To realize this aim, IAEA must enlist the broadest possible interest and support and this Bulletin is intended to serve that purpose. The success of the Bulletin itself will depend on the co-operation of those who can ensure that its contents reach the widest possible reading public.

"Effective dissemination will depend on the extent to which the material contained in this Bulletin is suitably re-used. The Bulletin itself will not have a mass circulation, but its objective will be fulfilled if its contents are re-transmitted to a wider readership in different areas by those who are best qualified to judge local interests and requirements."

The Bulletin is available in English, French, Russian and Spanish, and will be issued on a quarterly basis.

The first issue comprises 24 pages of neat 2-column typescript, with illustrations. It is full of varied information of general interest about the activities of the IAEA. At the end, there is a 3-page calendar of events for the period May-August, 1959.

L.R.

K. Way (Editor), 1959 *nuclear data tables* (U.S. Government Printing Office, Washington 1959. viii–151 p. $ 1)

This is the first issue of a new periodical publication of the Nuclear Data Group, superseding the New Nuclear Data Cumulations which were published from 1952 to 1957. The current cumulation of data about individual nuclei being achieved by the Nuclear Data Sheets, it has now become possible to reserve for yearly publication systematic compilations referring to special nuclear properties. In the present volume there is, for example, a cumulative table of isotopic abundances and several tables of new information about nuclear moments, neutron cross-sections, etc.

Besides, a first supplement is given to the recent Directory to nuclear data tabulations (cf. this journal **9** (1958/59) 356), listing 60 new entries! In this connexion it is comforting to note that the Nuclear Data Group are inviting physicists who have been induced to work out compilations of specific data to offer their material to the Group for publication in a suitably unified style. It is to be hoped that this commendable initiative will find the general support it deserves. The volume under review already contains two valuable contributions from physicists outside the Group, the usefulness of which is clearly enhanced by their incorporation in a systematic context of uniform presentation.

The only note of regret is that the Group should still keep to the aberrant American usage regarding unit symbols (e.g. Mev instead of MeV, and — still worse — evb instead of eV · b or b · eV for integrated cross-sections). For a group so closely related to the same institution (the National Academy of Sciences) which gives its support to the work of the S.U.N. Commission, this is a bit paradoxical, the more so as the adoption of the S.U.N. Commission recommendations would not involve the least practical difficulty.

L. R.

L. Slack and K. Way, *Radiations from radioactive atoms in frequent use* (U.S. Atomic Energy Commission, Washington 1959. xii–75 p. $ 0.55)

Biological and medical workers using radioactive elements as sources of radiation have great difficulty in extracting the relevant data from the specialized physical publications. This critical work has now been done for them in authoritative fashion, and all useful information collected in tabular or graphical form in this handy compilation.

L. R.

Č. Šimáně, *Accelerators of ions and electrons* (Artia, Prague; Constable & Co., London. No date. 191 p. 16 s.)

This English edition of a Czech publication is not a success. The translation is exceedingly poor, and in addition the book has many misprints both in the text and in the accompanying illustrations. Most photographs are of inferior quality. The English adaptation gives the impression of being very carelessly done, as for instance when the title of an English book, in a footnote, is quoted in Russian with the mention „(translated from the English)"! It also seems somewhat confusing to write high frequency instead of high voltage and conversely. This, I imagine, is the fault of the translators.

Apart from the poor translation, one must admit that Šimáně gives a very clear general view of most of the methods used for acceleration of electrons and heavy particles. The types of accelerators are classified into two main groups: linear (divided into electrostatic and high-frequency) and circular (divided into induction, high-frequency and electron cyclotron). Unfortunately, there is no mention of the newest development of the van de Graaff generator, the so-called tandem van de Graaff. As there is no evidence as to when this translation, or even the original edition, was published, I dare not call this a neglect, but it certainly is unfortunate.

As to the circular accelerators the author has chosen to postpone the explanation of the classical cyclotron until the last, in the section on high-frequency circular accelerators. I myself believe that, pedagogically, this is not correct. The most natural order seems to be the classical succession, in which, from the knowledge of the classical cyclotron and its limitations, the new methods are developed.

There are eight appendices, which give a more detailed mathematical treatment of the individual problems. The text proper closes with a section called „conclusion"; though it only takes up one page, it could, in my opinion, have been omitted, especially the last sentence, expressing the idea that in the socialist countries „scientific work is likely to find the best appreciation and utilization for the benefit of mankind." This would seem out of place in a scientific book.

J. H. Bjerregaard

WOLFGANG RIEZLER and WILHELM WALCHER (Editors), with particular cooperation of WOLFGANG FINKELNBURG and HEINZ MAIER-LEIBNITZ, *Kerntechnik: Physik-Technologie-Reaktoren* (B. G. Teubner, Stuttgart, 1958. xx+1002 p. DM 150.—)

The utilization of nuclear energy and radiations for practical purposes is a task that requires the collaboration of specialists in a wide range of fields: physics, chemistry, metallurgy, biology as well as civil, mechanical and electrical engineering, not forgetting economics and law. A satisfactory result of such a cooperation depends to a great extent upon the mutual understanding that can be achieved between the different groups of experts.

This book is an attempt to further such cooperation and mutual understanding. About 40 outstanding experts from German universities, technical high schools, Max-Planck-institutes and industrial establishments have contributed to the work. That the presentation nevertheless is exemplarily uniform in style is an obvious demonstration of a thorough editorial effort. Particular (one might even be tempted to say pedantic) care has been exercised to avoid confusion with units and symbols in the numerous formulas and equations.

The work is divided into 5 sections and 28 subsections. The first section contains an introduction to nuclear physics, followed by subsections on nuclear fission, the penetration of radiation through matter and measuring technique in nuclear physics. The greater part of the book is made up by the sections 2 (special technological problems: reactor materials, radiochemistry, isotope separation, irradiation effects, radioactive waste, use of radioactive and stable nucleides, "hot" laboratories, radiation shielding and radiation damage) and 3 (reactors: reactor theory, measurements, heat problems, reactor control, research and power reactors, safety, analog computers and simulators). In section 4 is found a brief treatment of controlled fusion (fusion energy, thermonuclear reactions, plasma physics and fusion experiments). Finally, section 5 is devoted to the economical and juridical problems. The economy of nuclear power plants is considered from both an optimistic and a pessimistic point of view, representing the standpoints of plant producer and customer respectively. In addition to a thorough treatment of the various subjects the text is filled with a great number of references and further accompanied by several useful tables and copious name and subject indexes.

The work seems in every respect to be well suited to introduce the beginner and help the experienced to deeper understanding of the many problems that arise from the immense development of nuclear energy in the service of man.

Sven Holm

Bernard Kopelman (Editor), *Materials for nuclear reactors* (McGraw-Hill Book Company, New York, 1959. x–411 pages. Price 95 s.)

This book is an introduction to the field of nuclear materials and manufacturing, and it contains selective reviews of unclassified information related to these subjects. The editor, B. Kopelman, who has also contributed to several chapters of this book, was formerly chief engineer at the Atomic Energy Division, Sylvania Electric Products; the other contributors, about thirty, have all been attached to the same division.

This book introduces several topics, beginning with a discussion of the extractive metallurgy of special reactor materials (U, Th, Zr, Be), followed up by a characterization of these materials as well as uranium alloys, ceramic fuels and dispersion mixtures; in connection with these chapters a general description of the reprocessing of irradiated spent fuel elements is given.

Fuel element fabrication and testing techniques are briefly described; the reader might perhaps want here a survey of the different types of fuel elements. The assembly methods of plate type fuel elements are extensive and remarkably described.

Other topics covered by this book are radiation effects, fluid materials and materials for moderators, shielding and control rods. Among these sections, the survey of radiation effects must especially be emphasized; further, this chapter includes a very useful chart of irradiation covering the different radiations and their interactions with matter and influence on reactions.

This book gives, as above mentioned, a survey of this special nuclear field, and thus it is very useful for beginners and for those who want a general view of the subject. For those who are working in the field, this book is useful as a reference work, but an objection is that the latest references mentioned are from 1957; it is especially regrettable to miss the references from the second Geneva conference.

Niels Hansen

W. **Kunz** und J. **Schintlmeister**, *Tabellen der Atomkerne*, Teil I: Eigenschaften der Atomkerne, Bd. 1: Die Elemente Neutron bis Zinn (Akademie-Verlag, Berlin 1958. xliii–465 p. DM 105)

With this publication, the Berlin Academy of Sciences is helping to fruition an undertaking of systematic tabulation of nuclear properties as extensive in its scope as the current project of the American Nuclear Data Group. The present volume, sumptuously produced, in a style reminiscent of the Landolt-Bornstein tables, covers the elements from neutron to Sn, and gives for each nucleide the usual data: mass, isotopic abundance, decay characteristics, modes of production, spin, magnetic and electric moment, conversion coefficients; many diagrams of decay schemes, as well as a full bibliography, are also included. The table headings are in German, but the detailed explanation of the tables is presented in German, English and Russian. The closing date for the compilation of the data was the 1st January, 1958.

Considering how frequently such data still receive significant improvement, one cannot help questioning whether the traditional book form with rigid binding is the most judicious to adopt. It would seem that loose sheets, like those issued by the Nuclear Data Group, are a more flexible and serviceable mode of presentation in this case. It is perhaps not too late for the publishers to study the possibility of going over to this style. The problem of how to collect the loose pages would not be straightforward, since the interior margins do not seem to be wide enough to allow the punching of holes; but some other practical solution might yet be found.

Another, more serious, question is whether the wasteful duplication of highly skilled work implied by the co-existence of the two projects — the American and the German one — should really be allowed to go on without any attempt to turn it to better advantage. It would not seem so tremendously difficult for the two national academies sponsoring the respective projects to find ways and means of combining their efforts, thus transforming pointless competition into fruitful collaboration. Physicists, who like so much to talk about how good they are at generating a spirit of international co-operation, have here a splendid opportunity of demonstrating what they are actually capable of achieving in this line.

L.R.

G. J. **Neary**, R. J. **Munson** and R. H. **Mole**, *Chronic radiation hazards — An experimental study with fast neutrons* (Pergamon Press, London 1957. x—191 p. 45s.)

Nuclear physicists cannot afford to remain indifferent to the devastating results which their empirical findings may produce in organic tissue. And though it is true that a few theoretical physicists have occasionally discussed purely biological phenomena, their approach nevertheless suggested on the whole speculative conjectures rather than solid, scientific reasoning. It is therefore of decisive importance for experimental and theoretical physicists alike to gain an insight into a piece of sound quantitative research that deals with the biological effects of chronic irradiation.

The report under review describes the damage caused by fast neutrons (f.n.). The dose rates were kept close to the maximum permissible for human exposure. For almost 6 years a daily running nuclear reactor was adapted to the requirements of this experiment in radiotoxicology. However, since fast neutrons produced in a reactor are accompanied by slow neutrons and gamma rays, fission reaction in uranium suitably arranged outside the reactor was utilized in order to eliminate those 'disturbing' radiations as much as possible. The doses of f.n., gamma radiation and thermal neutrons were determined by means of 3 homogeneous chambers with differential sensitivities to the 3 types of radiation; these chambers contained acetylene, argon and boron trifluoride, so-called tissue-like gases. The f.n. doses were measured in rads: 1 rad corresponds to an energy absorption of 100 ergs in one gramme of tissue. The maximum dose rate actually used was about 1 rad/day.

CBA mice were chosen as the most suitable animals for this experiment. They were placed in batches of 100 in 4 continuously irradiated areas: the maximum, medium, minimum and control tanks; the weekly doses of f.n. ranged from 0.08 to 6.4 rads. As index of the likely damage caused by chronic irradiation by f.n. the authors decided upon the shortening of life span, but loss of weight, tumour production, effects on fertility, cataract, change in blood count and weights of organs were also recorded. The mice were 11 to 13½ weeks old when irradiation commenced. The mean energy of the f.n. reaching the animals amounted to 0.7 MeV. (A mouse of 30 g weight can be regarded as a cylinder of roughly 2½ cm diameter and 6 cm length.) To determine the ill-effects of neutron and gamma irradiations it was indicated to use a quantitative criterion, the so-called relative biological efficiency (r.b.e.).

It is obvious that an interpretation of many of the data submitted for scrutiny will, at present at least, remain a matter of conjecture. Still, the information contained in the report is of such tremendous relevancy, academically and practically, that it warrants to be widely communicated. The experiment showed that the mean survival time (m.s.t.) was shortened by a third in the maximum group (with a weekly dose of 6.4 rads of f.n.). In the medium tank the m.s.t. was decreased by less than 10 per cent. There was clear evidence that increasing radiation doses led to shorter m.s.t. (excess mortality), that deaths of irradiated mice occurred earlier than in a radiation-free environment.

Of immediate significance are, however, some of the pathological observations, perhaps even more so than the analysis of excess mortality, since the cause of death was hardly ever discovered *post mortem*. Apart from neoplasms (abnormal growth of cellular tissue, either benign or malignant), the commonest determined cause of death was intestinal obstruction. The increase of tumours of breast and nasopharynx in the maximum group provided indubitable support for the claim that chronic neutron irradiation is conducive to carcinogenesis; mammary tumours appeared even in male animals, and the m.s.t. of mice inflicted with such tumours was 419 days, i.e. 80 days shorter than the m.s.t. for the whole experimental group. (The m.s.ts. of CBA mice in the control groups were 743 days for males and 818 for females.) Yet there was no indication that chronic irradiation with f.n. was *generally* carcinogenic. Surprisingly, overweight mice lived longer than unirradiated obese mice.

Next, the measurable damage to gonads was one of the most striking characteristics revealing the greater radiation-sensitivity of the testis as compared with the ovary: male mice were more easily sterilized than female mice. On the whole, almost all radio-biological experiments so far suggest that testicular atrophy (and thus decrease of reproductive function) is the most dramatic result of chronic irradiation. This fact was also confirmed by observations on mice bred in an irradiated area: body weight and growth rate were distinctly affected, the m.s.t.

shortened, the testis weight considerably reduced, whereas the weight of other organs and glands was merely proportionally less than in mice irradiated when about 10½ weeks old. Moreover, the recovery of testis weight was very slow and still incomplete several months after removal from exposure to f.n. The damage to the gonads was undoubtedly earlier noticeable than any other ill-effect and therefore the most sensitive indication of radiation injury.

Considerable decrease in the white blood count shortened life span by more than 50 per cent.

Finally, the authors computed the relative biological efficiency (r.b.e.) of f.n. and gamma radiation from ^{60}Co for chronic exposure in a series of separate experiments; the ratio of the gamma dose to the f.n. dose for equal amounts of damage gives the exact magnitude of the r.b.e. One of the interesting results: within a certain range of exposure times (from 24 hours to 9 months) neither changes of exposure time nor of dose rate altered the r.b.e. It was found that there was no qualitative difference between f.n. and gamma radiation regarding their effects on testis, spleen and thymus, male and female fertility, and white blood cell count. The numerical values of the r.b.e. of f.n. and gamma radiation lay between 3 and 11; the mortality of irradiated mice suggested a likely r.b.e. of about 10; the r.b.e. reflecting the damage to the female gonad was significantly less than the corresponding r.b.e. for the male gonad.

Needless to say, the singularly relevant observations in this radio-biological report, though presented in an impassive, factual and scholarly manner, may easily lead to premature, unjustified conclusions. For instance, one has to bear in mind that the pathic effects occurring after irradiation might well be exaggerated or obscured by hitherto unknown causes. Likewise, will it ever be possible to determine — with a reasonable measure of exactitude — the relative radio-sensitivities of the different tissues of the experimental animal? The investigators are, of course, also aware of the fact that it would be poor scientific reasoning to attempt simple extrapolation to the human organism on the findings obtained for mice. For all we know, the data concerning mice may hardly be of any consequence concerning radiation damage in other mammals.

It is a trivial reflection that facts should not be defined but interpreted. Yet any attempt at a comprehensive analysis of the data so neatly stated in the report under discussion poses more and more problems of a physical, biological, statistical and even moral nature. To cite a few: the relation of dose level, rate and exposure time, the interaction of radiation and of ageing of a biological system, and the seemingly undecidable issue of whether increased liability to tumours or cataract or impairment of fertility is the most crucial defect.

Radio-toxicological experiments, rigidly controlled, of the kind undertaken by the authors, will become a vital necessity during the next few years. It is only on the basis of such academic studies that we shall be able to meet the imminent challenge of our time. Neary, Munson and Mole, i.e. the Medical Research Council Radiobiological Research Unit at Harwell, have succeeded in designing a series of cautious experiments whose results may become of staggering significance.

W. Yourgrau

Herbert Goldstein, *Fundamental aspects of reactor shielding* (Addison-WesleyPublishing Company, 1959. xvi—416 pages. $ 9.50)

This book is a revised edition of *The attenuation of gamma rays and neutrons in reactor shields*, which was reviewed in this journal (7 (1958) 690).

The new edition does not exhibit major changes compared with the original. The chapter on radiation sources, however, has been rewritten in order to include recently published information on this subject. Further, the list of references has been brought up to date and a number of appendices, containing valuable shielding calculation data, have been included.

The changes introduced have increased the practical value of the book considerably. To this can be added that the book is undoubtedly the best that has been published until now on the more basic aspects of reactor shielding.

P. L. Ølgaard

NORTH-HOLLAND BOOKS

ANALYTICAL and CANONICAL FORMALISM in PHYSICS

by ANDRÉ MERCIER

Head of the Department of Theoretical Physics University of Berne

6×9″ VIII + 222 pp. Guilders 20.00 (40s.)

CONTENTS

i. Lagrangian Formalism
ii. Lagrangian Density
iii. Canonical Formalism
iv. Canonical Form of Electrodynamics
v. Hamiltonian Densities
vi. Transformations
vii. Canonical Formalism with Vanishing Jacobian Determinant

Those who are not highly specialized in these matters but do want to get a fairly broad knowledge of the subject are not aware of the fact that the greater parts of this formalism, including many specific conclusions of physical concern, do not involve in the least quantum theory, i.e. "quantization" of the fields. To show this and to provide the reader with a fairly complete presentation of the *classical* (i.e. not yet quantized) theory of fields is one of the main aims of the book.

This formalism is presented with great generality. Some special topics have also been included when they are found to be of importance in connection with the problems raised; however, they are not elaborated with the same generality, but just formulated as far as is found necessary for the understanding of these connections; for instance we can name: tensorial formalism and spinorial formalism.

A special chapter has been devoted to transformations of several kinds including canonical transformations, reversibility and the like as well as their interrelations, so that the ground is prepared for an understanding of the CPT-Theorems.

A short chapter on Dirac's dynamics with vanishing Jacobian closes the book.

The work builds upon the well-known *Principles of Analytical Dynamics* by the same author (in French), where particular weight is laid upon the homogeneous formalism, but it can easily be read with profit without knowledge of the latter by any advanced students in physics, astronomy or mathematics as well as by research workers who want to get a thorough practice in the use of these methods.

Many examples and as many as 124 problems illustrate the formalism exposed.

Sole Agency for U.S.A.: Interscience Publishers Inc. - New York

NORTH-HOLLAND PUBLISHING COMPANY - AMSTERDAM

NORTH-HOLLAND BOOKS

TURNING POINTS IN PHYSICS

A series of lectures given at
OXFORD UNIVERSITY in TRINITY TERM 1958

5 × 8″ viii + 192 pages Guilders 10.50 (20s.)

THE CONTENTS

INTRODUCTION
by A. C. Crombie,
All Souls College, Oxford

i. THE END OF MECHANISTIC PHILOSOPHY AND THE RISE OF FIELD PHYSICS
by R. J. Blin-Stoyle,
Clarendon Laboratory, Oxford

ii. THE QUANTUM NATURE OF MATTER AND RADIATION
by D. ter Haar,
Clarendon Laboratory, Oxford

iii. PROBABILITY ENTERS PHYSICS
by K. Mendelssohn,
Clarendon Laboratory, Oxford

iv. FROM THE RELATIVE TO THE ABSOLUTE
by G. Temple,
Mathematical Institute, Oxford

v. THE DECLINE AND FALL OF CAUSALITY
by F. Waismann,
New College, Oxford

vi. TOWARDS NEW CONCEPTS: ELEMENTARY PARTICLES
by D. H. Wilkinson,
Clarendon Laboratory, Oxford

THIS VOLUME CONTAINS the text of a series of six lectures organised by the Reader in the Philosophy of Science and the Lecturer in the History of Science in the University of Oxford and given by senior members of the University to an audience composed mainly of philosophers and scientists, who were not physicists. As a consequence these lectures are non-technical and can be understood by laymen who are interested to read about the development of physics in the last hundred years.

The first lecture describes how the concept of fields was introduced by Faraday and Maxwell, the next two lectures and the fifth lecture describe the changes in outlook brought about by the advent of quantum mechanics. These changes incorporate a change in the concepts of probability, causality and determinism, as well as the introduction of the idea of quantisation. The fourth lecture deals with relativity and the last lecture describes the galaxy of so-called elementary particles which nowadays dominate such a large part of physics.

Sole Agency for U.S.A.: Interscience Publishers Inc. - New York

NORTH-HOLLAND PUBLISHING COMPANY - AMSTERDAM